

DIELECTRIC RECOVERY OF SHORT A-C ARCS

BETWEEN HIGH-BOILING-POINT ELECTRODES

Thesis by

Louis T. Rader

In Partial Fulfillment of the Requirements

For the Degree of Doctor of Philosophy

California Institute of Technology

Pasadena, California

1938

TABLE OF CONTENTS

	<u>Page</u>
Summary.	
I. Introduction .....	1
II. Theory .....	4
III. Experimental Procedure .....	5
IV. Results .....	9
A. Copper Electrodes .....	10
1. Data .....	10
2. Effect of Current .....	11
3. Effect of Pressure .....	12
4. Effect of Arc Length .....	13
B. Steel Electrodes .....	16
1. Data .....	17
2. Effect of Current .....	17
3. Effect of Pressure .....	18
4. Effect of Arc Length .....	20
C. General - Temperature .....	20
V. Conclusions .....	22
VI. Acknowledgment .....	24
Appendix A - Apparatus .....	25
Appendix B - Experimental Technique .....	28
Appendix C - Probable Accuracy of the Method	32
Appendix D - Temperature Calculation .....	34
Appendix E - Equations for Sparking in an Ionized Gas .....	35
Appendix F - Reignition-Voltage Time Equations	36
Appendix G - Arc Behavior .....	38

## SUMMARY

Continuing work done by an earlier investigator, the reignition characteristics of short arcs between copper and iron electrodes were studied in detail. Current, pressure, and arc length were varied to obtain curves of restriking voltage versus time at current zero. Data were obtained by making use of an oscillating circuit, varying the rate of rise of voltage across the arc terminals by varying the circuit constants, and observing and recording the voltage phenomena by the use of a cathode ray oscilloscope.

Results were obtained which check previous work on brass electrodes as to the kind of voltage recovery characteristic obtained for short arcs. The previously held theory that high melting point electrodes have a dielectric recovery directly proportional to arc length for short times, is shown to be false. An optimum arc length for dielectric strength for both copper and steel electrodes is seen to exist between 1.0 and 2.05 mm.. Temperatures calculated for the arc space agree in order of magnitude with results for earlier determinations.

The method used is held to be particularly appropriate, because average values were obtained in all cases, and results obtained with the apparatus were consistently checked over time intervals of more than two years.

The circuit used was the same as used by Dr. T. E. Browne, Jr.\* The same method of obtaining the data was used and his thesis should be consulted for a more detailed analysis of the circuit.

---

\* Browne, "Dielectric Recovery of Short A-C Arcs between Low-Boiling-Point Electrodes", Thesis for Ph.D. degree, C.I.T., (1936).

## I. INTRODUCTION

In a remarkable paper published in 1892,<sup>1</sup> Mr. A. J. Wurtz described his experimental discovery of the fact that metals fall into two main classes in their arc-supporting characteristics. Between electrodes of a metal of one group, he found that an arc burned freely with considerable noise, light, and movement. Metals of this group, including carbon, tin, and lead; iron, cobalt, and nickel; and copper and aluminum, all having boiling points between 1500°C. and 3600°C., he designated as "arcing" metals. Between electrodes of lower boiling point, such as zinc, cadmium, and mercury, he found that an arc was maintained with difficulty, and that if it did burn, there was little noise or light. These, he designated as the "non-arcing" metals and used their arc-quenching properties in a multigap type of lightning arrester. Mr. Wurtz was also the first to discover the almost paradoxical fact that as the electrode separation decreased, a higher voltage was required to maintain an arc between zinc or antimony electrodes.

Many workers have since studied this effect in more detail<sup>2,3</sup>, showing some dependence on electrode boiling point and electrode separation. However, a satisfactory and complete theory of short-

---

1. Wurtz, "Lightning Arresters", Trans. A.I.E.E. 9, p. 102 (1892).
2. Browne, "Extinction of Short A-C Arcs", Trans. A.I.E.E., 50, p. 1461, (1931).
3. Slepian and Strom, "Arc in Low-Voltage A-C Networks", Trans. A.I.E.E., 50, p. 847, (1931).

arc performance has not yet been proposed. As pointed out by Darrow<sup>4</sup>, the work of many researchers in conduction in gases is of little or no use for purposes of correlation, because their data were taken under such varying conditions, and results often given with the omission of some necessary parameter information, that it cannot be correlated into a theory of arc performance. For example, much data have been taken on arcs between cylindrical electrodes as in the common carbon arc. In such cases the arc is usually bowed out at an edge so that no true figure can be used for arc length and actual separation of electrodes has little meaning.

Browne<sup>5</sup> with an exhaustive set of tests started a very systematic study on brass electrodes. Using the same apparatus built by Browne, the same set of tests was made by the author on copper and steel, two high boiling point metals, in an attempt to obtain further data on the subject. Current, electrode separation, and pressure were varied to obtain their effect on the restriking voltage of an arc. All results are given in the form of curves between arc reignition voltage and time after current zero. When the current goes through zero in an A-C arc, it does not immediately start flowing in the opposite direction. Instead a quite considerable voltage of the order of hundreds of volts is usually required to initiate current flow through the arc in the new direction.

---

4. Darrow, "Electrical Phenomena in Gases", (a book)  
Williams & Wilkins Co. (1932).

5. Browne, "Dielectric Recovery of Short A-C Arcs between Low-Boiling-Point Electrodes", Thesis for Ph.D. degree, C.I.T., (1936).

This is the voltage known as the reignition restriking, or recovery voltage. The rise of this voltage across the arc space is, of course, a function of the circuit parameters and time. The ability of an arc space to withstand breakdown; i.e., its dielectric strength, is also a function of time so that by varying the circuit constants, the time of breakdown of the arc space was varied, thus giving a measure of dielectric recovery with time.

This subject is of vital importance in electrical engineering. Short arcs are found in all circuit breakers, such as knife and snap switches used on low voltages and in fuses. In modern secondary networks the fault must burn clear. Present day industrial welding is a field intimately bound up with short-arc behavior. The deion circuit breaker and the autovalve lightning arrester are excellent examples of the use of the extinction characteristics of short arcs.

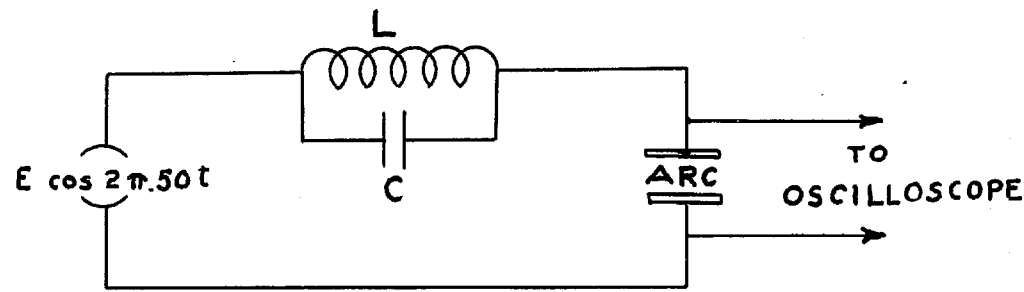


Fig. 1.

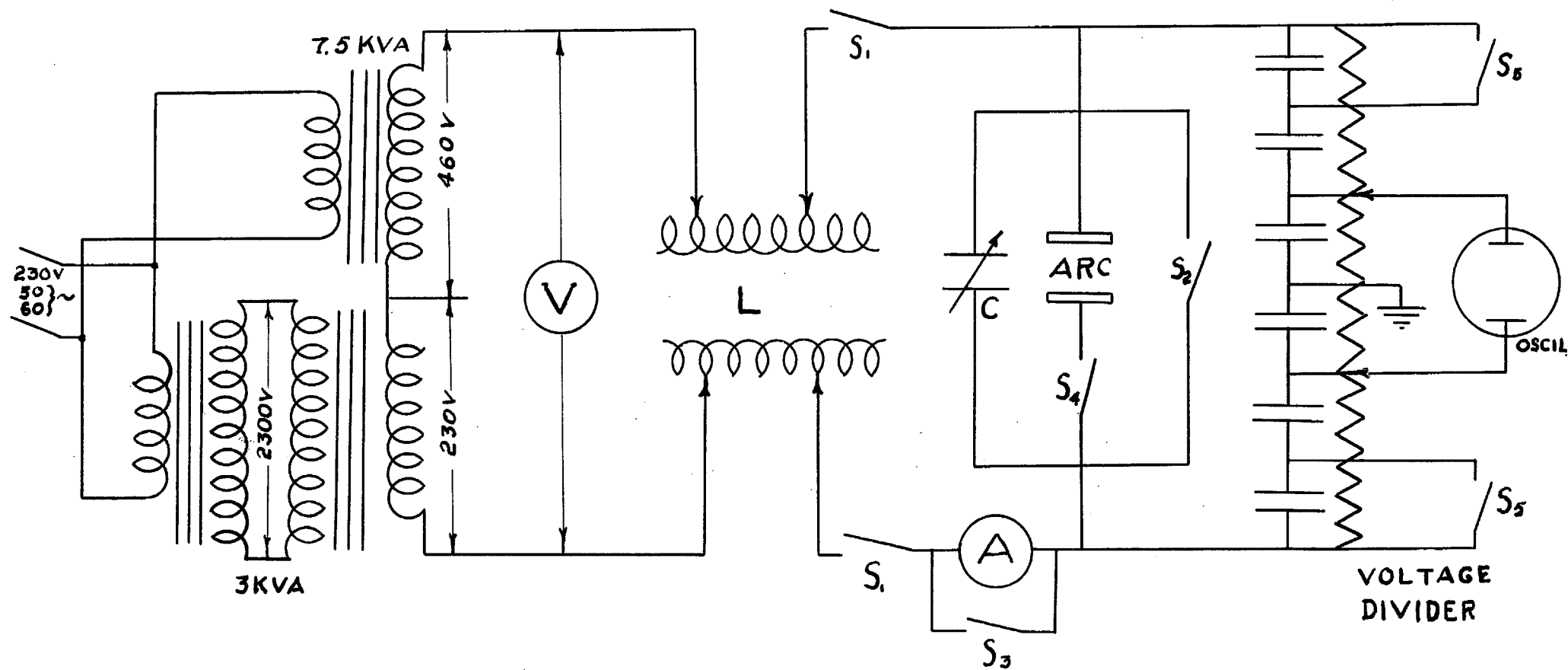


Fig. 4.

## II. THEORY

A most complete summary of the theories underlying and explaining short arc phenomena is to be found in Browne's thesis<sup>5</sup>. He has made use of seven principal references on the subject from 1923 to 1936 to give a comprehensive discussion and summary under the following heads:

1. Arc Reignition.
2. Space Charge Formation.
3. Dielectric Strength of Space Charge Sheath.
4. Conditions Affecting Dielectric Strength.
5. Rate of Dielectric Recovery.
6. Phenomena at the Anode.
7. Ionizing Activity.

There has been no departure in theory from those presented since 1936, so that it is felt unnecessary to reproduce this phase of the subject in this thesis.

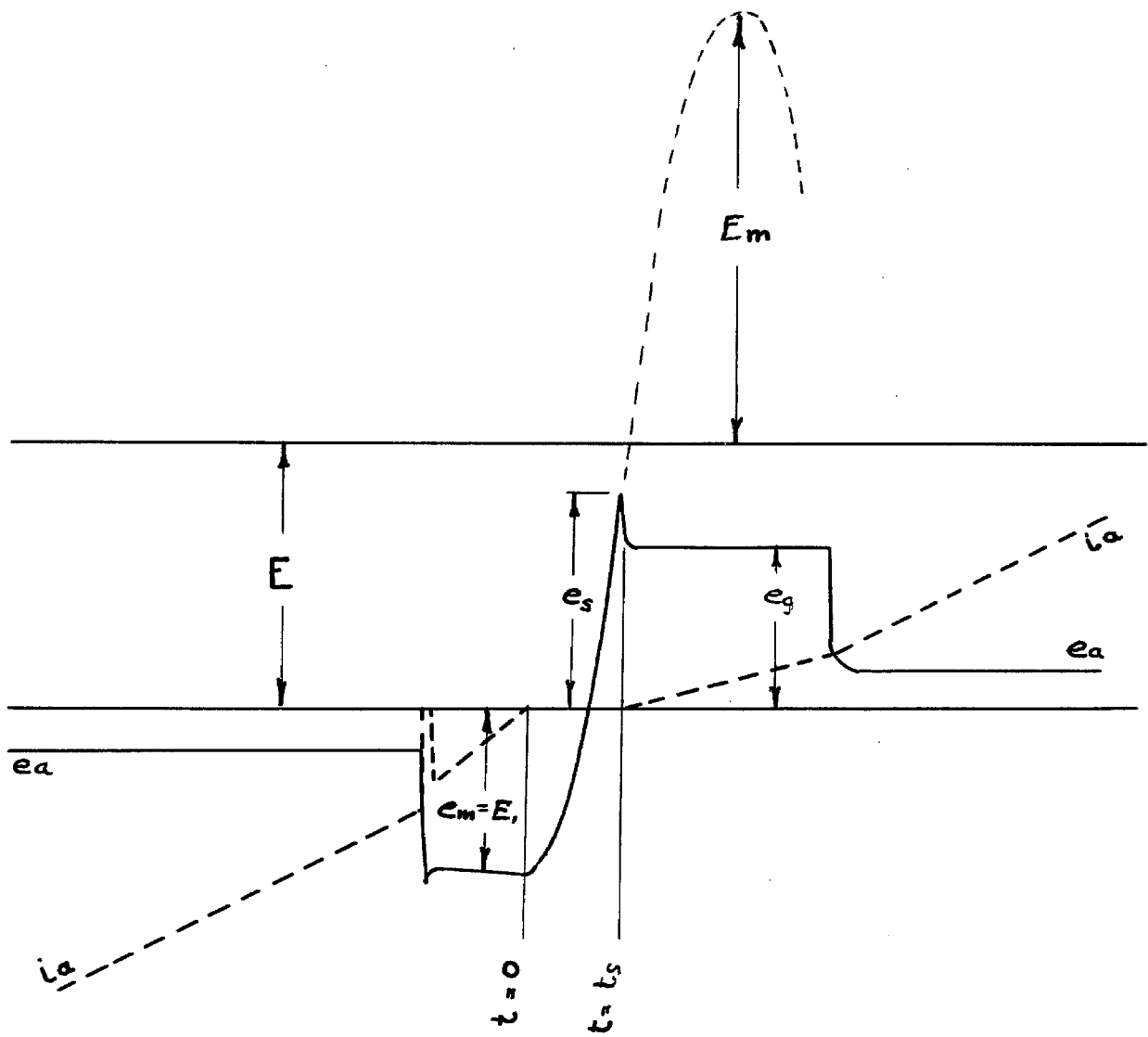


Fig. 2.

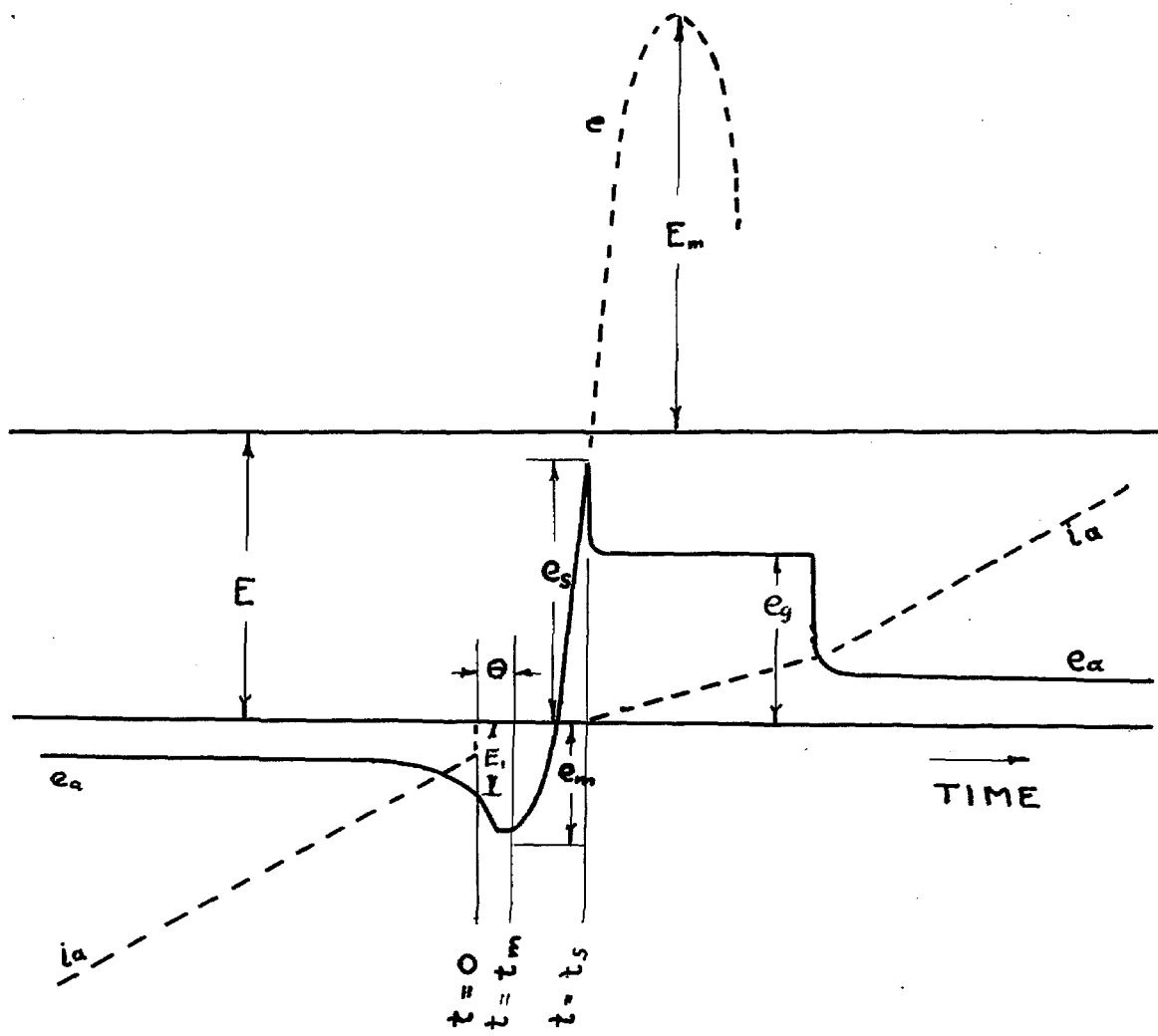


Fig. 3.

### III. EXPERIMENTAL PROCEDURE

The apparatus used for the taking of data was the same as that used by Browne<sup>5</sup>. As shown in Fig. 1, current from a 690 volt circuit was limited by almost pure reactance,  $L$ , placed in series with the arc. All readings were taken in air on continuously-burning arcs between plane parallel metal electrodes. The metals were copper and steel; the currents 12.5, 25, and 50 amps.; the electrode separations 0.45, 1.0, 2.05, and 4.13 millimeters, and the pressures 1/4, 1/2, and 1 atmosphere. Condensance,  $C$ , (Fig. 4) was placed across the arc to vary the natural frequency of the circuit, and so give varying rates of voltage rise across the arc. A cathode ray oscilloscope of the Braun type (R.C. 104) with fluorescent screen was connected across the arc and gave a visual picture of the voltage wave at the time of current zero from which AVERAGE amplitude readings were taken.

The time relationships existing between supply voltage  $e_s$ , of maximum value  $E$ , arc voltage  $e_a$ , and arc current  $i_a$ , are shown in Fig. 2. Due to the very expanded scale of the figure, (the interval  $t = 0$  to  $t = t_s$ , representing a maximum time of about 250 micro-seconds) the applied voltage which is at its maximum, appears as a horizontal straight line. Except near current zero, the current wave is a pure sine wave lagging the applied voltage by ninety degrees. As the arc current, approaching zero sinusoidally,

reaches a small value of the order of 0.1 amps., it suddenly fails, falling immediately to zero, where it remains until a reignition voltage is reached so that at  $t = t_s$  it starts to flow in the opposite sense.

The current in the inductance cannot drop instantly when the arc current fails and it surges into the capacity in the circuit, the reactors' distributed capacity which is in parallel with the capacity across the arc. Due to oscillations, then, the voltage across the inductance and capacity in parallel, rises from the value it had at  $t = 0$ , to  $e_m$  at  $t = t_m$  and  $e_s$  at  $t = t_s$ . The boundary conditions obtaining at  $t = 0$  are the values of  $E$ , the arc voltage and  $I$ , the arc current. The former is quite constant but the latter is subject to fairly large random variations with consequent variations in  $e_m$ .

At  $t = t_s$  reignition occurs, the voltage across the arc falls to the glow voltage, and a glow discharge characterized by low current density and high cathode drop occurs. As the current increases, the glow turns into an arc the current then follows a sine wave and the arc voltage remains substantially constant for the next half cycle.

From  $t = 0$  to  $t = t_s$  the arc voltage can be computed quite simply by the circuit equations since the current is zero. This has been done by Attwood, Dow and Krausnick<sup>6</sup>. See Appendix A.

---

6. Attwood, Dow and Krausnick, "Reignition of Metallic A-C Arcs in Air", Trans. A.I.E.E., 50, p. 949, (1931).

$$e_a = E - E_m \cos (\omega t + \theta)$$

where  $e_a$  = the arc voltage during the period of  $t = 0$  to  $t = t_1$ .

$E$  = maximum value of the applied A-C wave.

$E_m = E - e_m$  = amplitude of the voltage oscillation about  $E$ .

$\omega = 2\pi \frac{1}{\sqrt{LC}}$  =  $2\pi$  times the natural frequency of the circuit.

$e_m$  = the negative maximum of the oscillation.

$\theta = \tan^{-1} \frac{I_1/wC}{E - E_1}$  = the phase angle by which the negative maximum lags behind the time  $t = 0$ .

The above equation can be solved for  $t_s$  by substituting  $e_s$  for  $e$  and obtain:-

$$t_s = \sqrt{LC} \cos^{-1} \frac{E - e_s}{E - e_m} + \tan^{-1} \sqrt{\frac{E - e_m}{E - E_1} - 1}$$

With  $L$  in henries,  $C$  in microfarads,  $-t$  is given in microseconds.

Two kinds of negative maxima occur; viz., the negative glow, and the no-glow cases. The former is shown in Fig. 2 and occurs when the current fails earlier in the cycle and so drops from a larger negative value to zero. The negative electrode voltage falls very sharply to a sufficient value to produce a negative glow which lasts for a few microseconds. The same effect occurs for low values of  $C$ , as may be seen from the equations:

$$|e_m| = |E_m| - |E|$$

and

$$E_m = \sqrt{(E - E_1)^2 + \left(\frac{I_1}{wC}\right)^2}$$

so that an increase in  $I_1$  or a decrease in  $C$  both tend to increase  $E_m$  and  $e_m$ . For this negative glow case, the initial voltage  $E_1$  is identical with the negative maximum  $e_m$ , so that the inverse tangent term disappears in the expression for  $t_s$  and

$$t_s = \sqrt{LC} \quad \cos^{-1} \frac{E - e_s}{E - e_m} .$$

For each value of arc current and gap spacing, readings were taken, with values of capacity across the arc from zero to the highest possible at which the arc was stable. For each of these readings  $t_s$  was calculated and plotted against  $e_s$  giving a curve of reignition voltage versus time after current zero.

The method used for obtaining the data plotted on the accompanying curves was to adjust the gap spacing and current to the desired values. The value of the condenser,  $C$ , (Fig. 4) was then varied. This change in the value of the condenser changed the time required for the voltage to reach its reignition potential. This is the time  $t_s$ . Knowing the value of the condenser and of the inductance, the time  $t_s$  was calculated from the equation alone.

IV. RESULTS.

Results are given for copper electrodes under the following Figure numbers:-

COPPER ELECTRODES

	Separation	Pressure in Atmos.			Fig. Nos.
Effect of Current	4.13 mm.	1	1/2	1/4	5,6,7
	2.05 mm.	1	1/2	1/4	8,9,10
	1.0 mm.	1	1/2	1/4	11,12,13
	0.45 mm.	1	1/2	1/4	14,15,16
	Separation	Current			Fig. Nos.
Effect of Pressure	4.13 mm.	50,	25,	12.5	17,18,19
	2.05 mm.	50,	25,	12.5	20,21,22
	1.00 mm.	50,	25,	12.5	23,24,25
	0.45 mm.	50,	25,	12.5	26,27,28
	Pressure	Current			Fig. Nos.
Effect of Arc Length	1 atmosphere	50,	25,	12.5	29,30,31
	1/2 "	50,	25,	12.5	32,33,34
	1/4 "	50,	25,	12.5	35,36,37

Figures 38 and 39 are representative curves which are given to show the correlation between the actual data and the curves drawn through them.

## A. Copper Electrodes

### 1. Data

Figures 5 to 38 show 34 sets of curves. In all, 589 readings were taken on copper, - about 15 points making up one curve. About 90 of these readings were made to re-check data in order to make certain that the apparatus gave consistent results and to check probable mistakes.

Data were taken for all possible combinations of 50, 25, and 12.5 amps.; 4.13, 2.05, 1.0, and 0.45 mm.; and pressures of 1, 1/2, and 1/4 atmosphere. It was impossible to get consistent results with 50 amps. at 1 atmos. and 0.45 mm. separation, though a portion of the curve is shown.

The number of curves is too large to include them all on separate sheets, so that the results are given under three main heads:-

- (1) Figures 5 to 16 show the effect of current on dielectric recovery;
- (2) Figures 17 to 28 show the effect of pressure, and;
- (3) Figures 29 to 37 show the effect of arc length.

Figures 38 and 39 are submitted to show how, in general, calculated points agree with the final curve drawn through them. They are representative examples. In all cases the curves drawn follow the data points very closely.

## EFFECT OF CURRENT ON DIELECTRIC RECOVERY

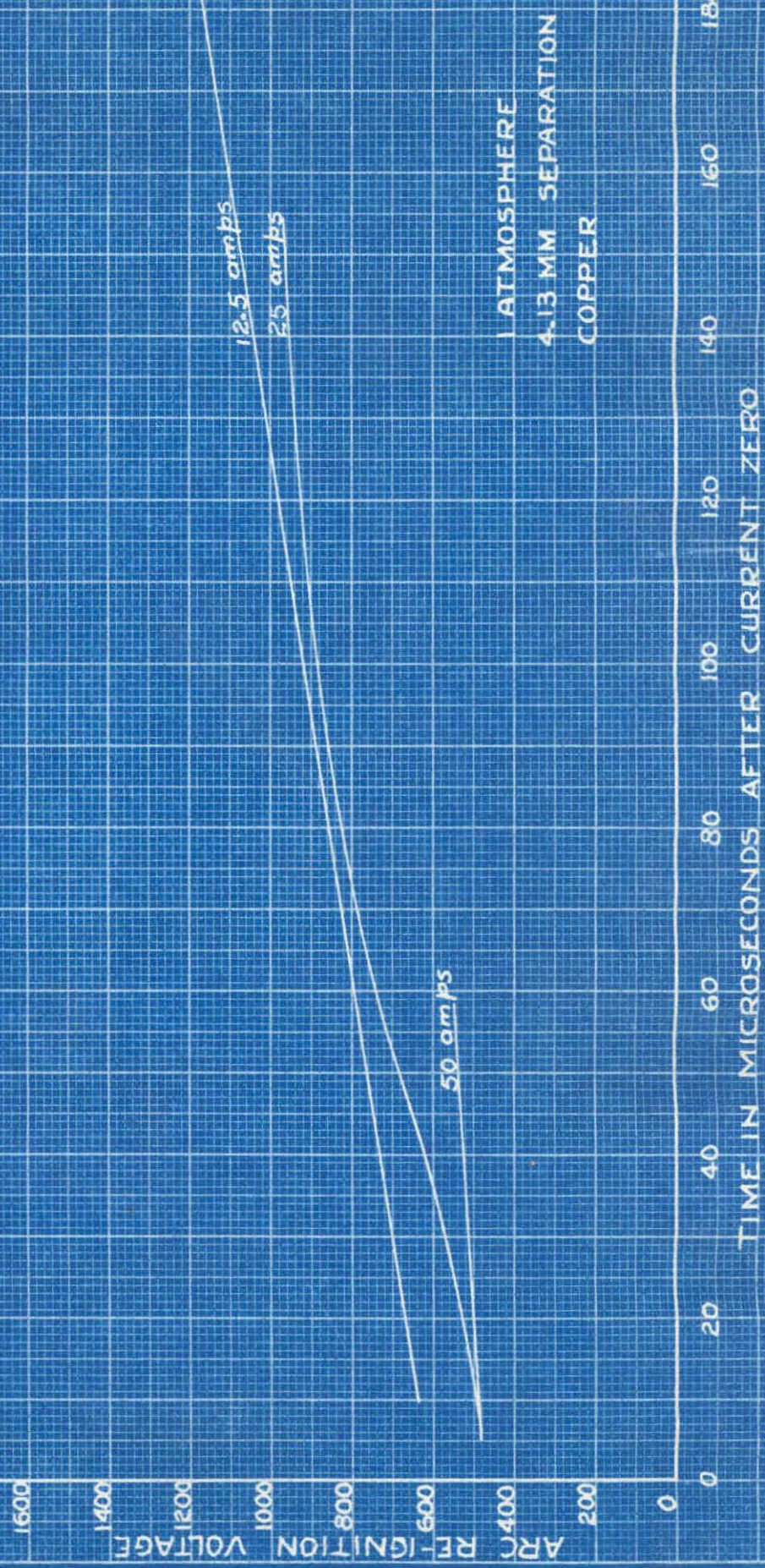


FIG. 5.

## EFFECT OF CURRENT ON DIELECTRIC RECOVERY

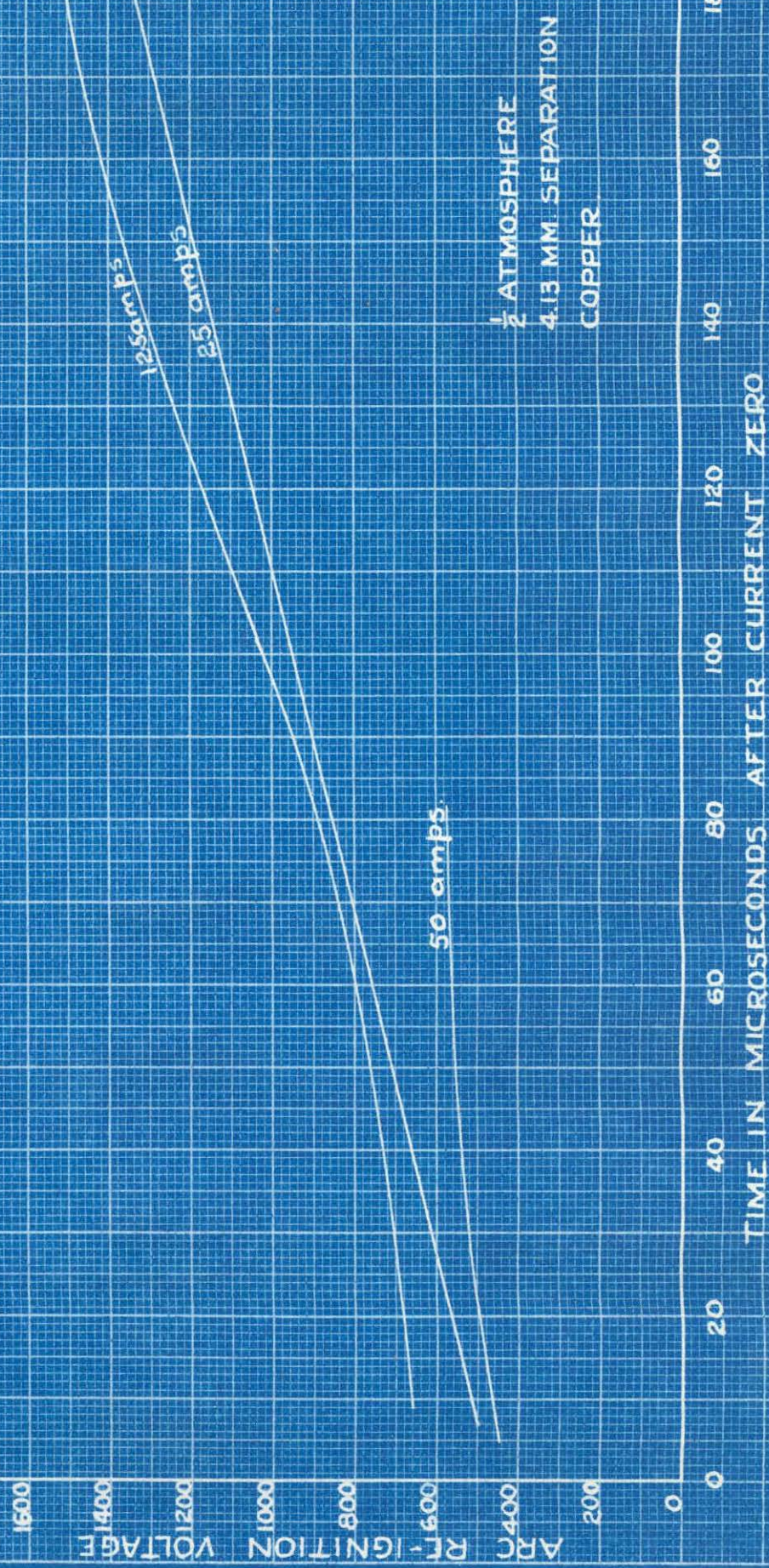


FIG. 6.

# EFFECT OF CURRENT ON DIELECTRIC RECOVERY

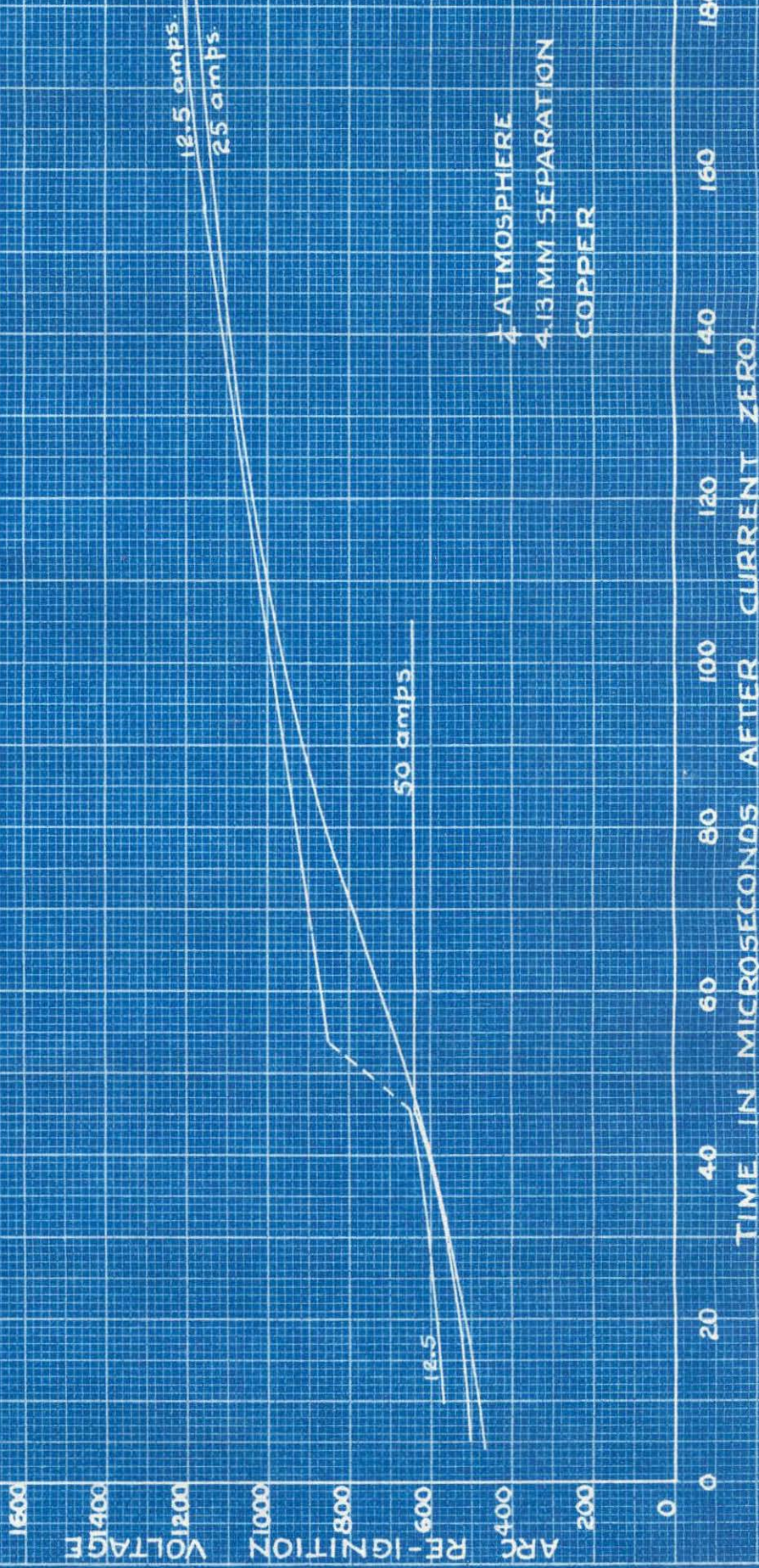
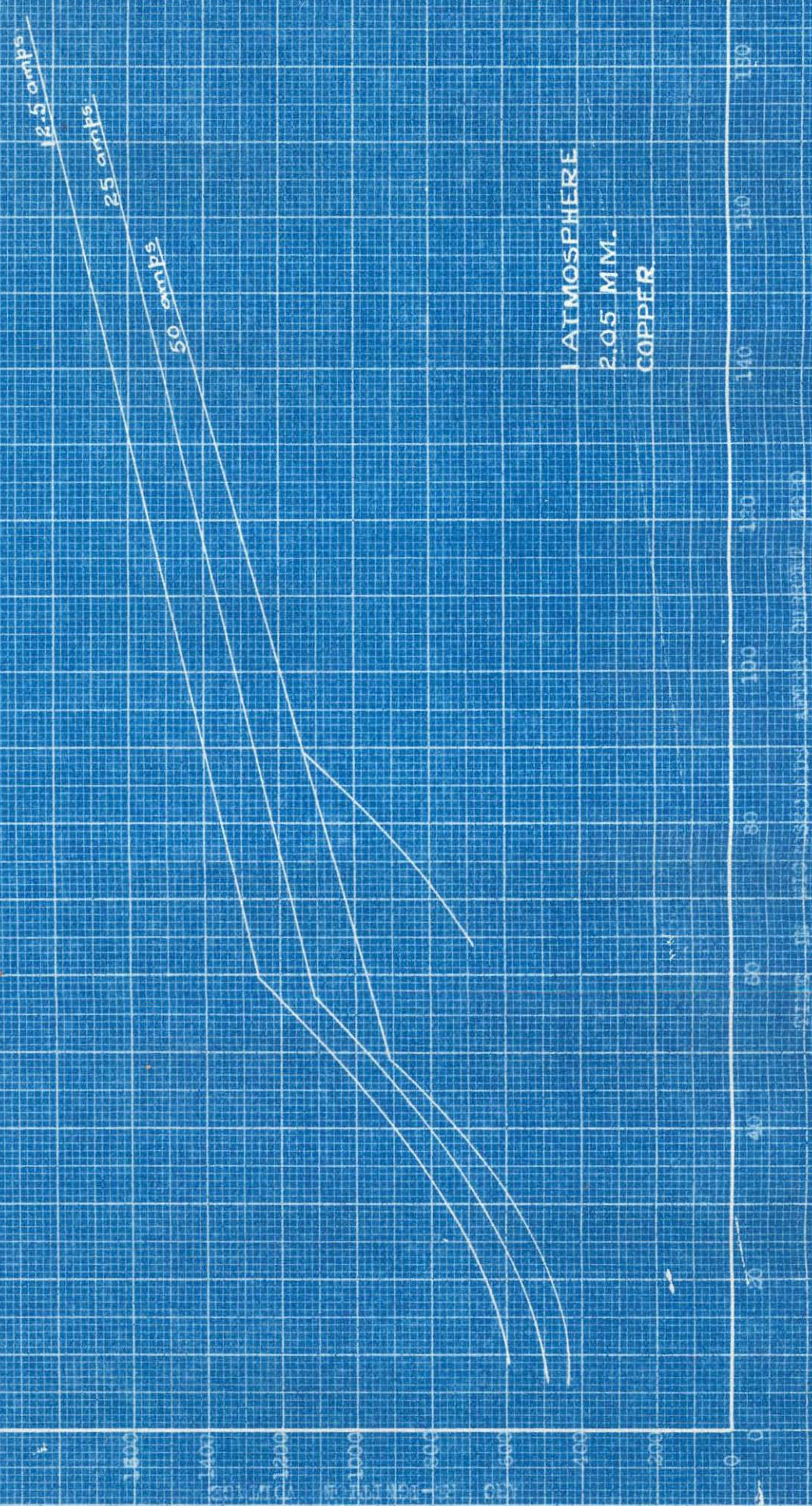


FIG. 7.

EFFECT OF CURRENT ON DIELECTRIC RECOVERY



四

## EFFECT OF CURRENT ON DIELECTRIC RECOVERY

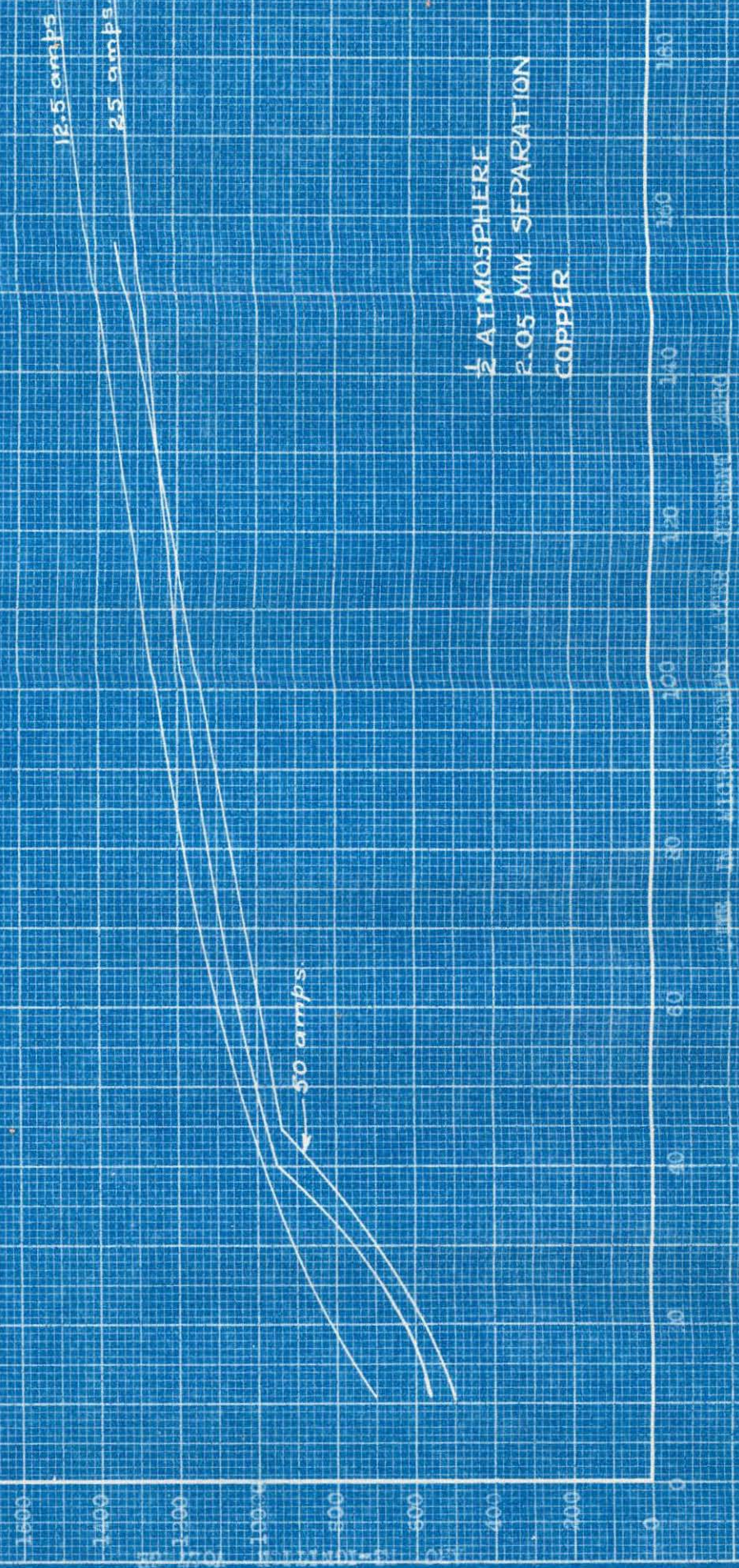


Fig. 6

## EFFECT OF CURRENT ON DIELECTRIC RECOVERY

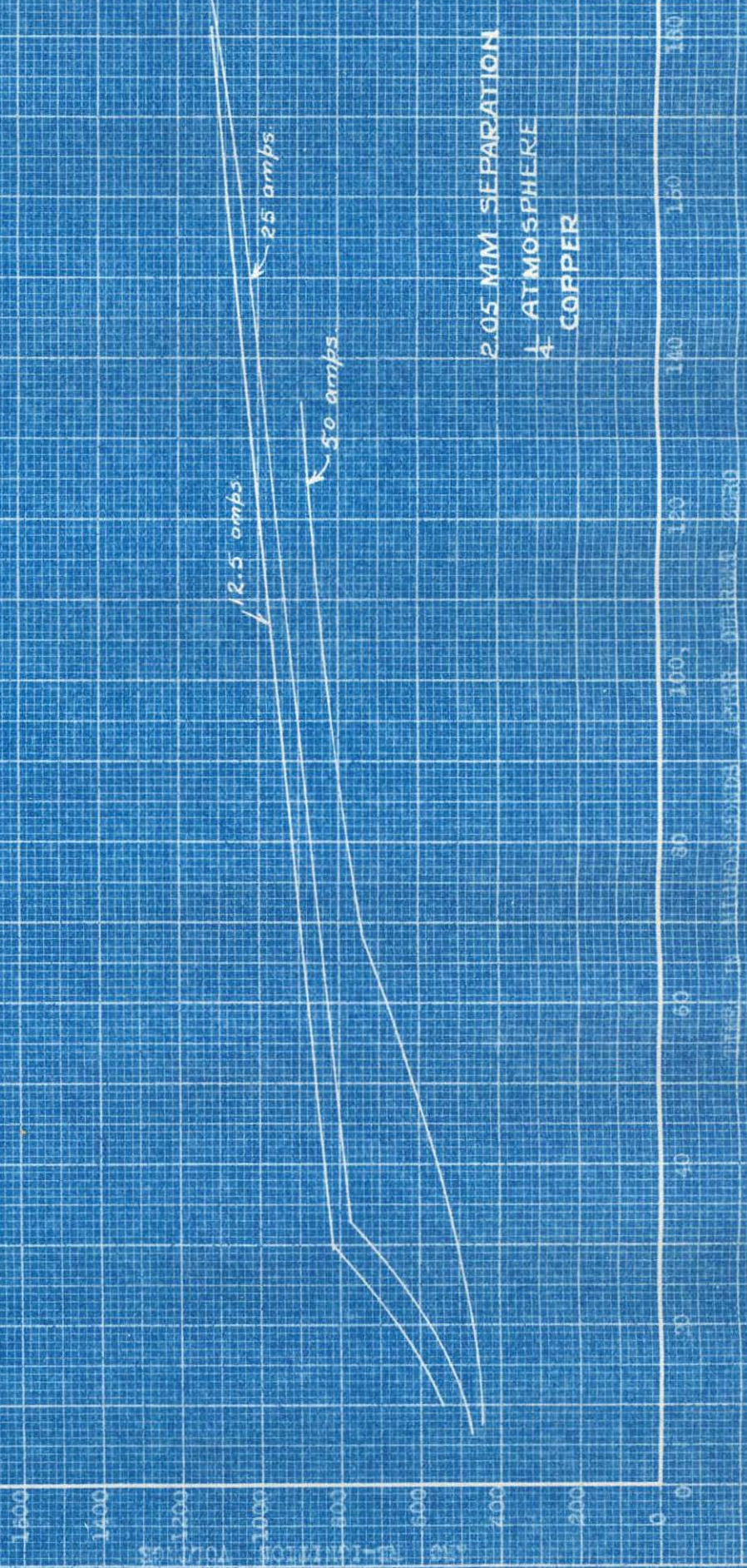
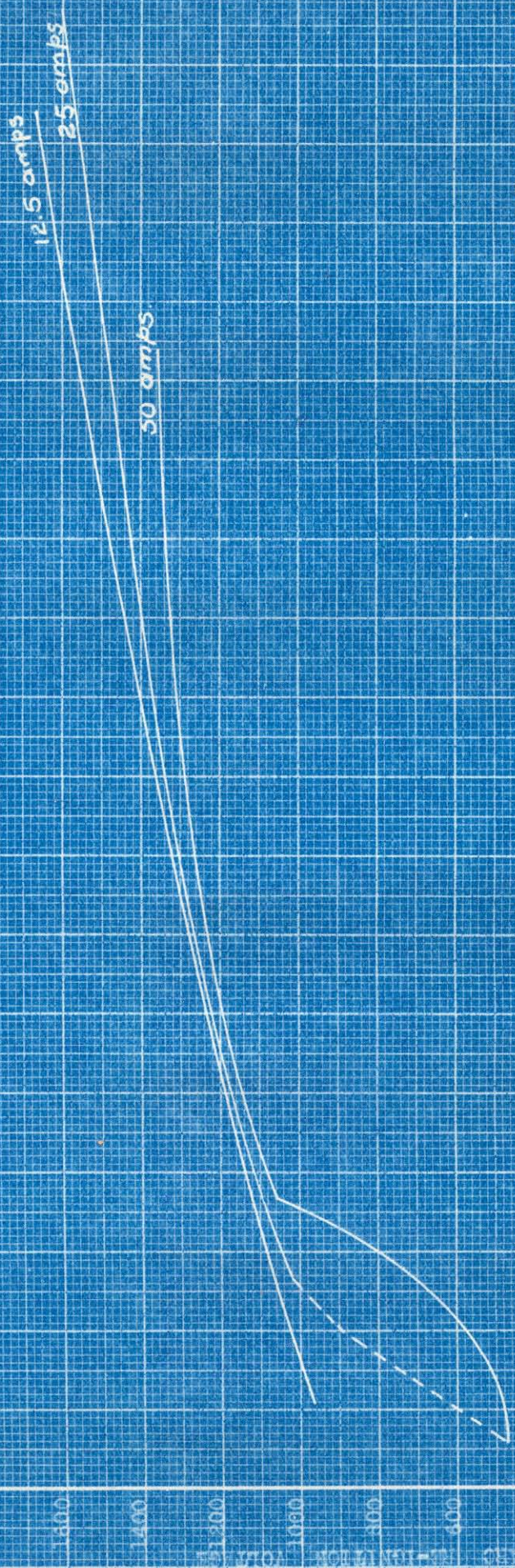


FIG. 10.

## EFFECT OF CURRENT ON DIELECTRIC RECOVERY



ATMOSPHERE PRESSURE  
1 MM. SEPARATION  
COPPER

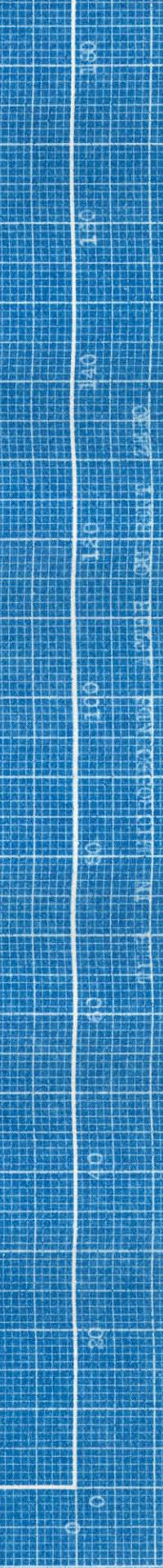
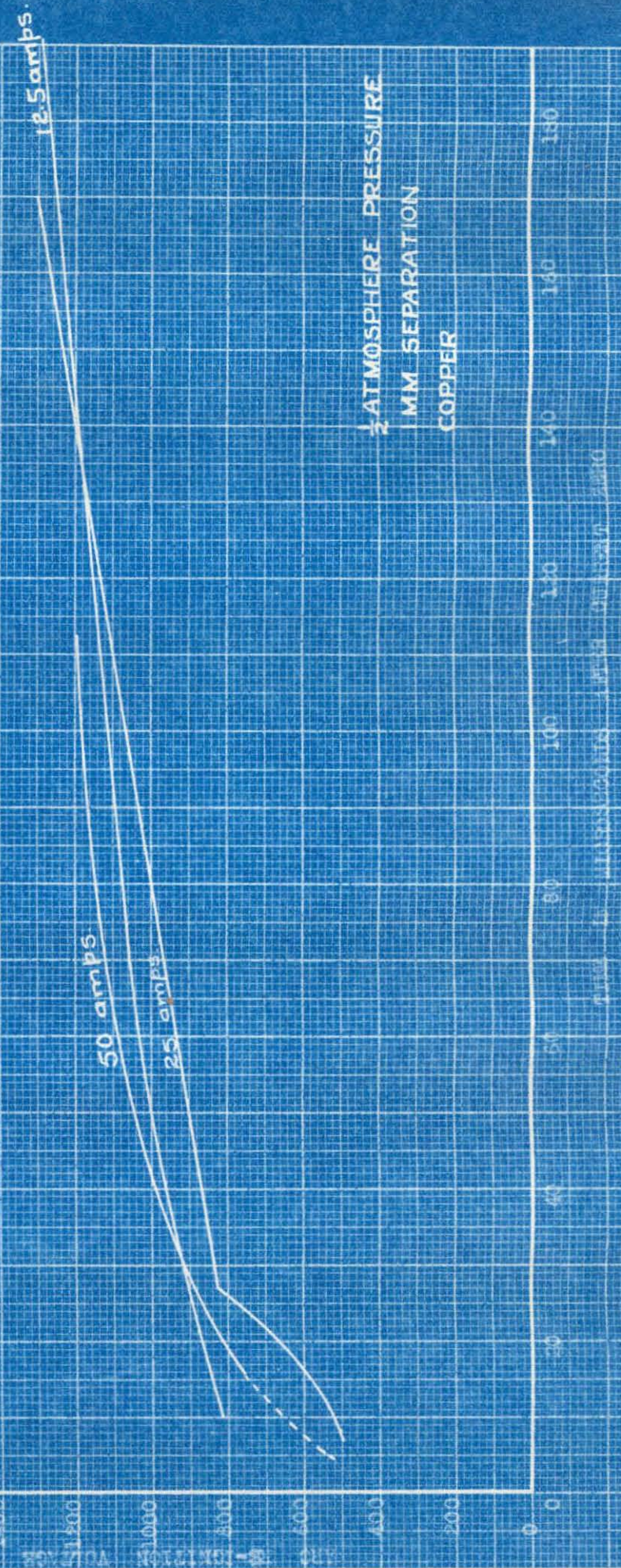


FIG. 11.

EFFECT OF CURRENT ON DIELECTRIC RECOVERY



## EFFECT OF CURRENT ON DIELECTRIC RECOVERY

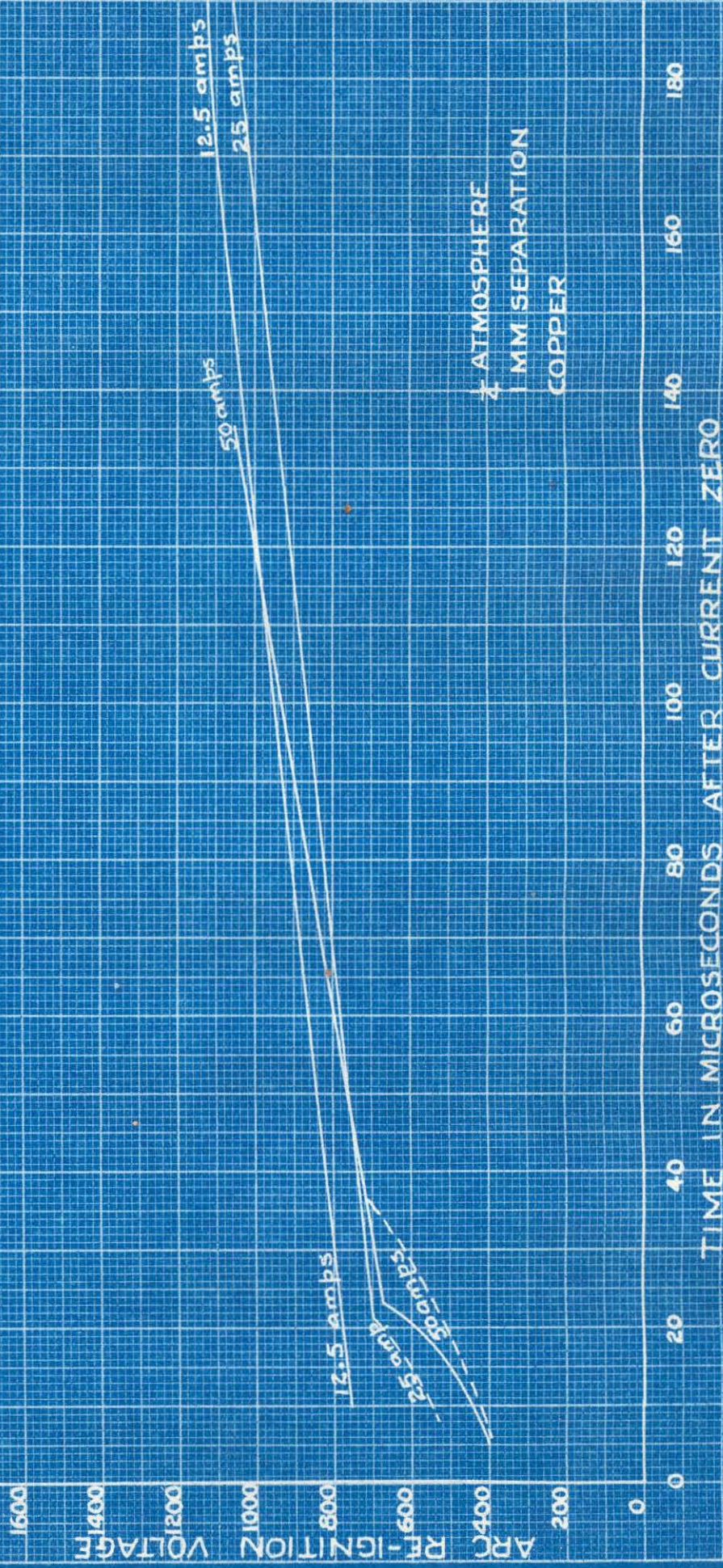


FIG. 13

# EFFECT OF CURRENT ON DIELECTRIC RECOVERY

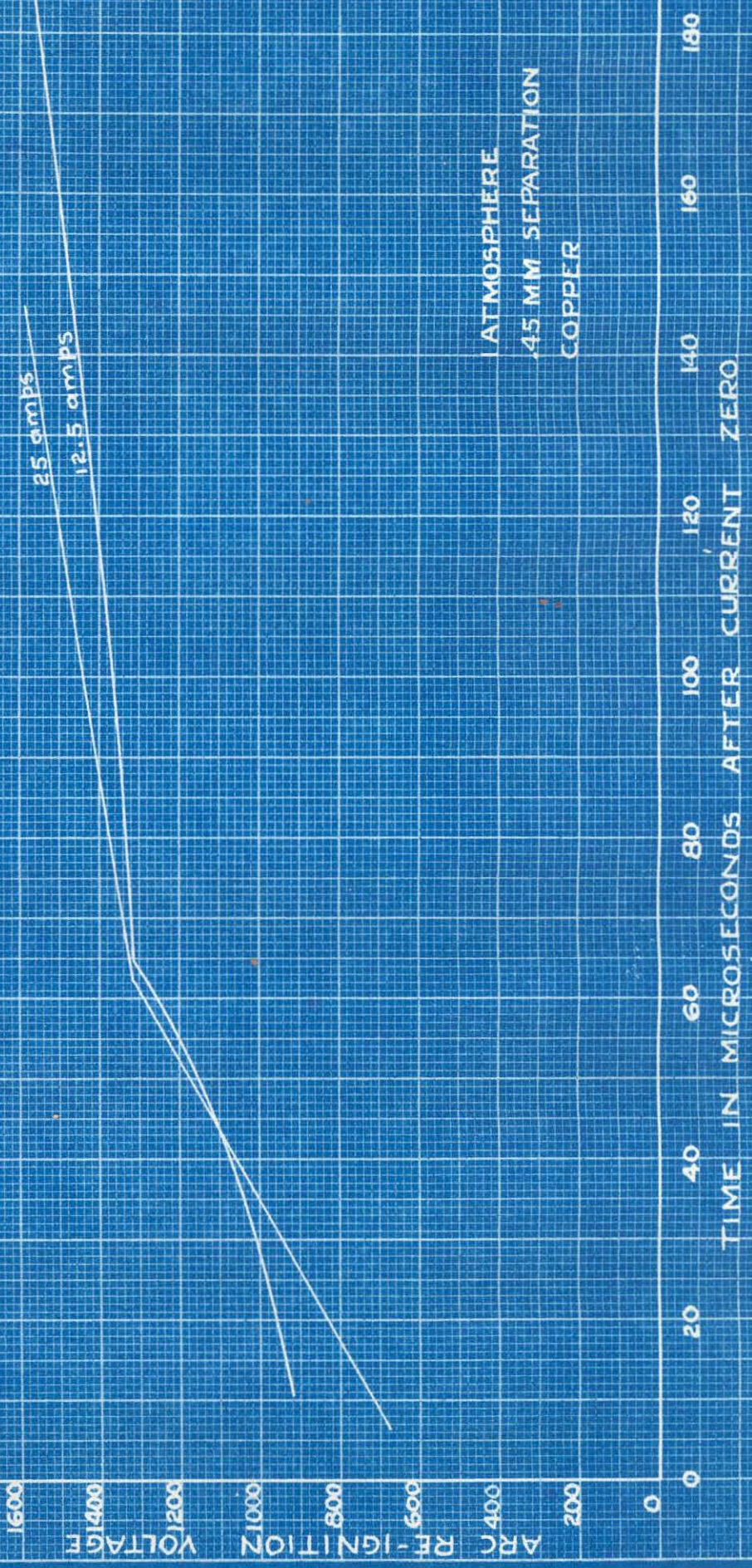


FIG. 4.

## EFFECT OF CURRENT ON DIELECTRIC RECOVERY

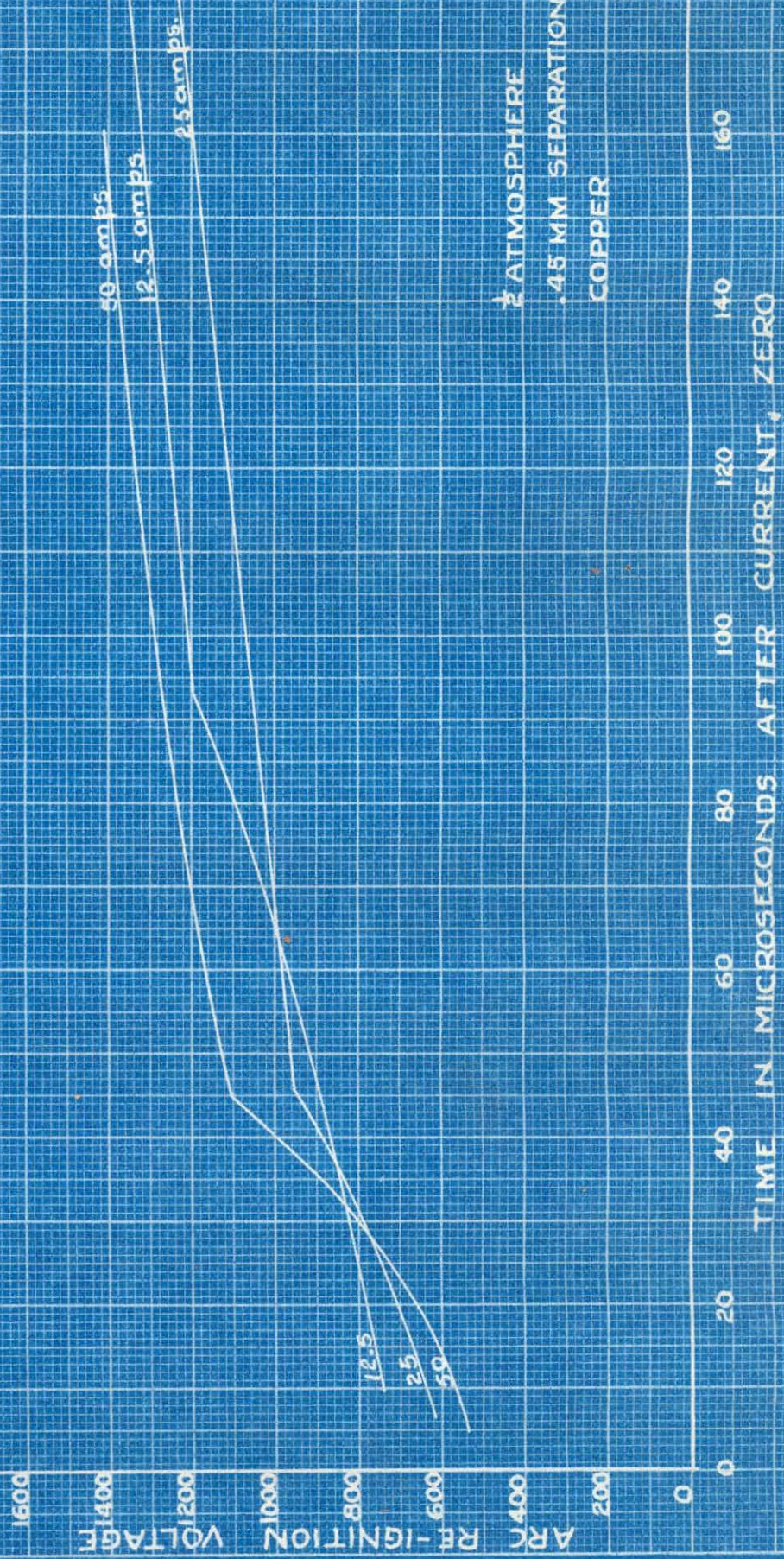
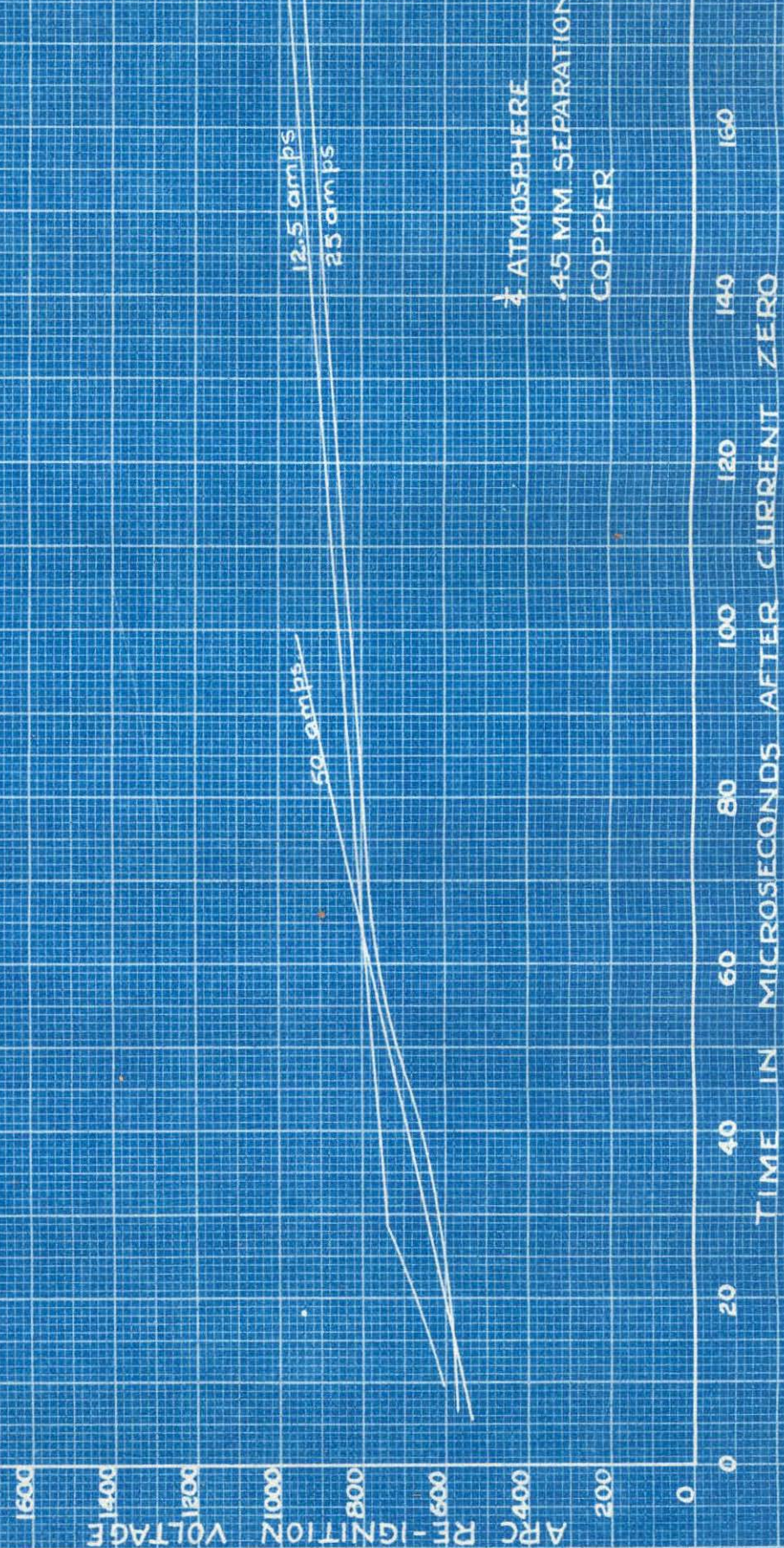


FIG. 5.

## EFFECT OF CURRENT ON DIELECTRIC RECOVERY



## FIG. 1G.

## EFFECT OF PRESSURE ON ELECTRIC RECOVERY

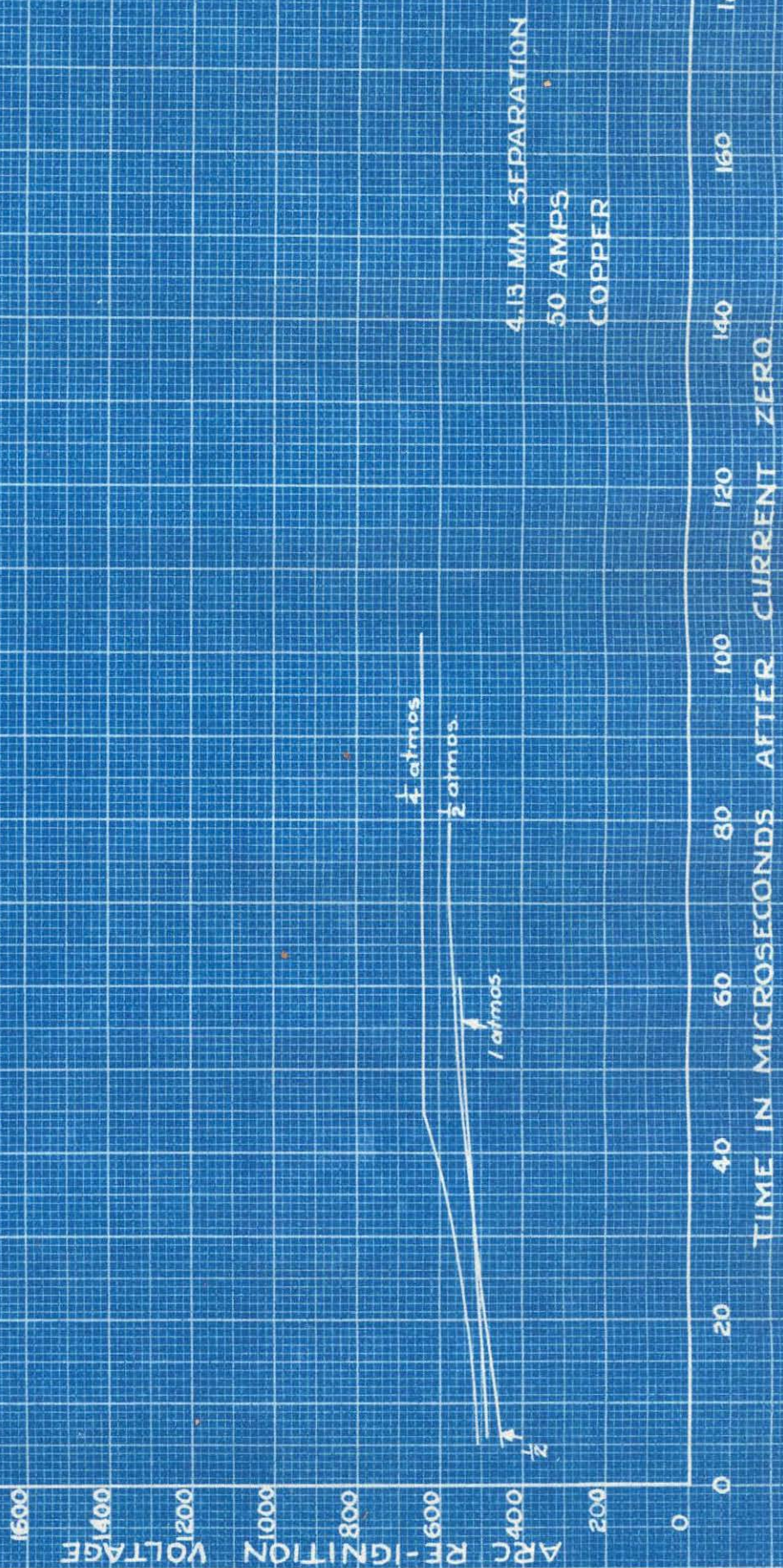


FIG. 17

## EFFECT OF PRESSURE ON DIELECTRIC RECOVERY

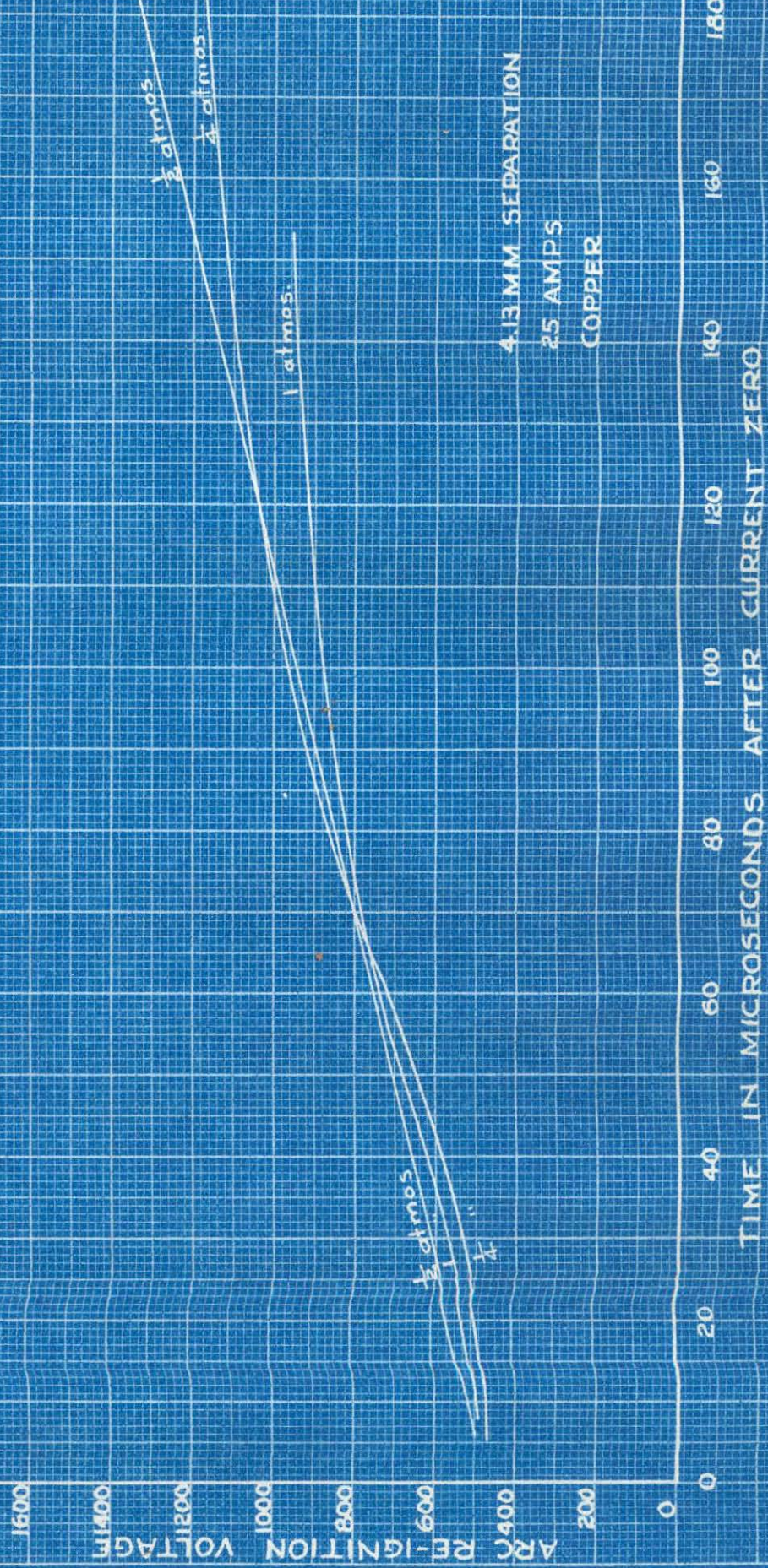


FIG. 18.

## EFFECT OF PRESSURE ON ELECTRIC RECOVERY

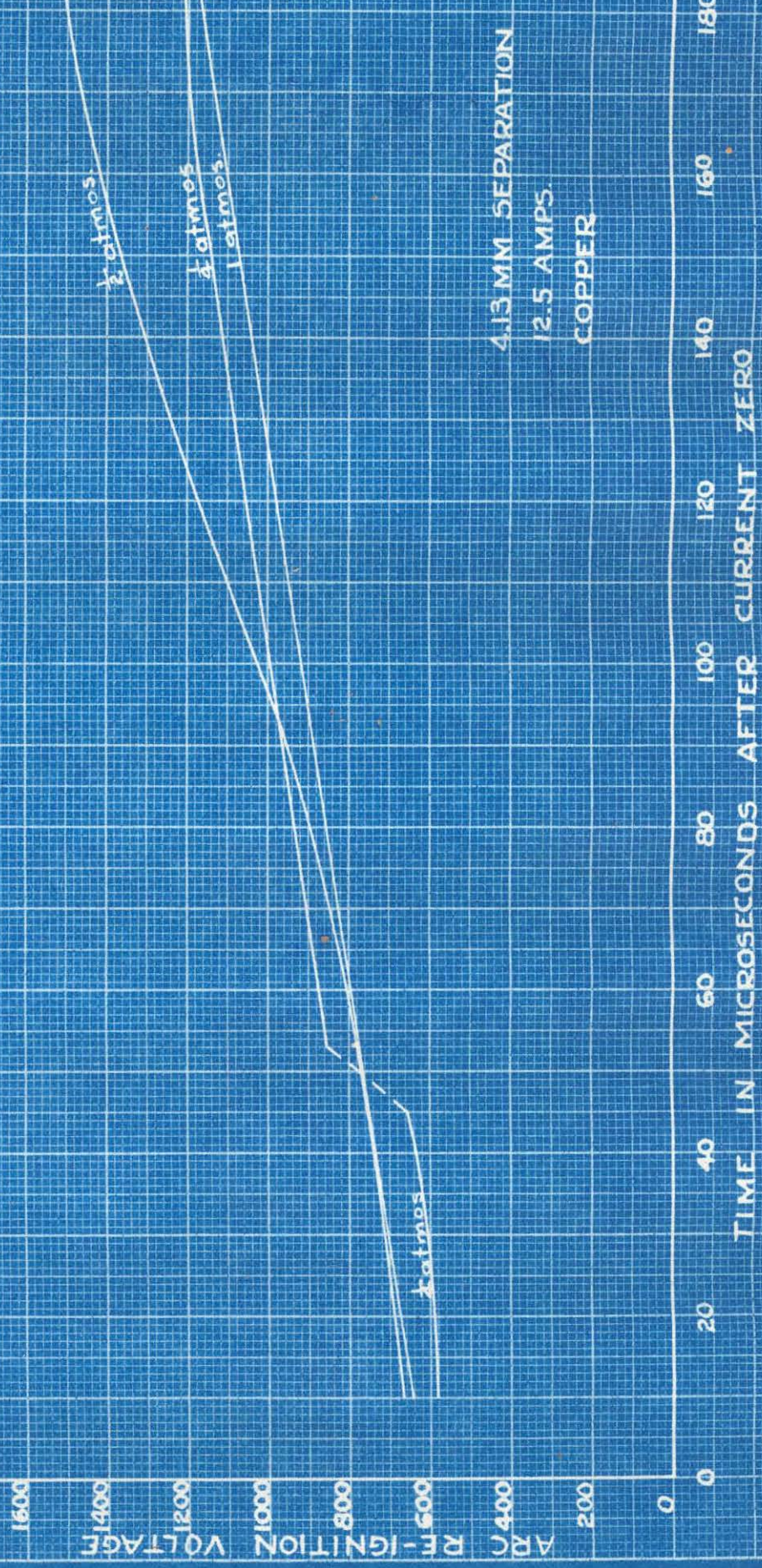


FIG. 19.

## EFFECT OF PRESSURE ON DIELECTRIC RECOVERY

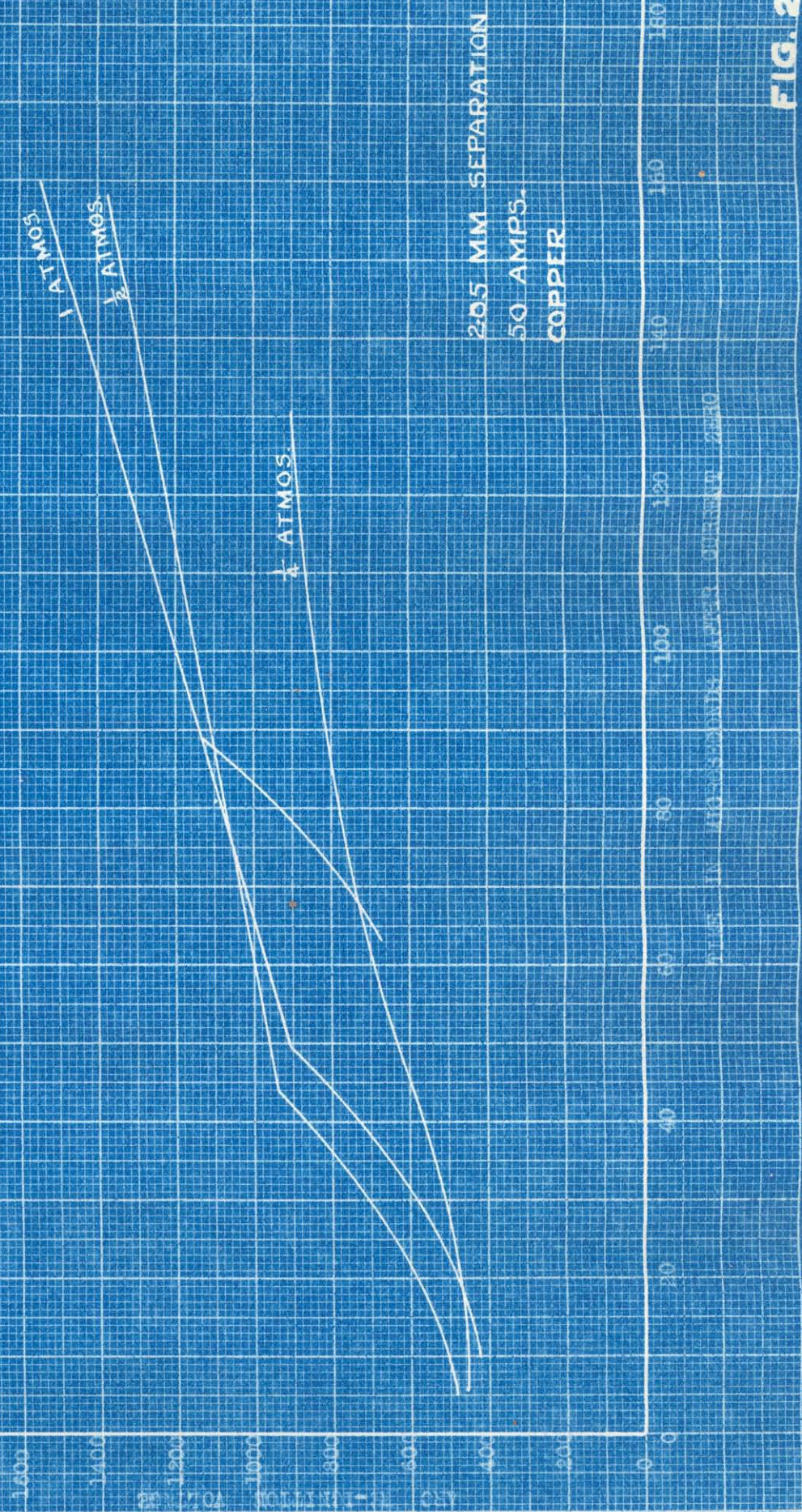


FIG. 20.

## EFFECT OF PRESSURE ON DIELECTRIC RECOVERY

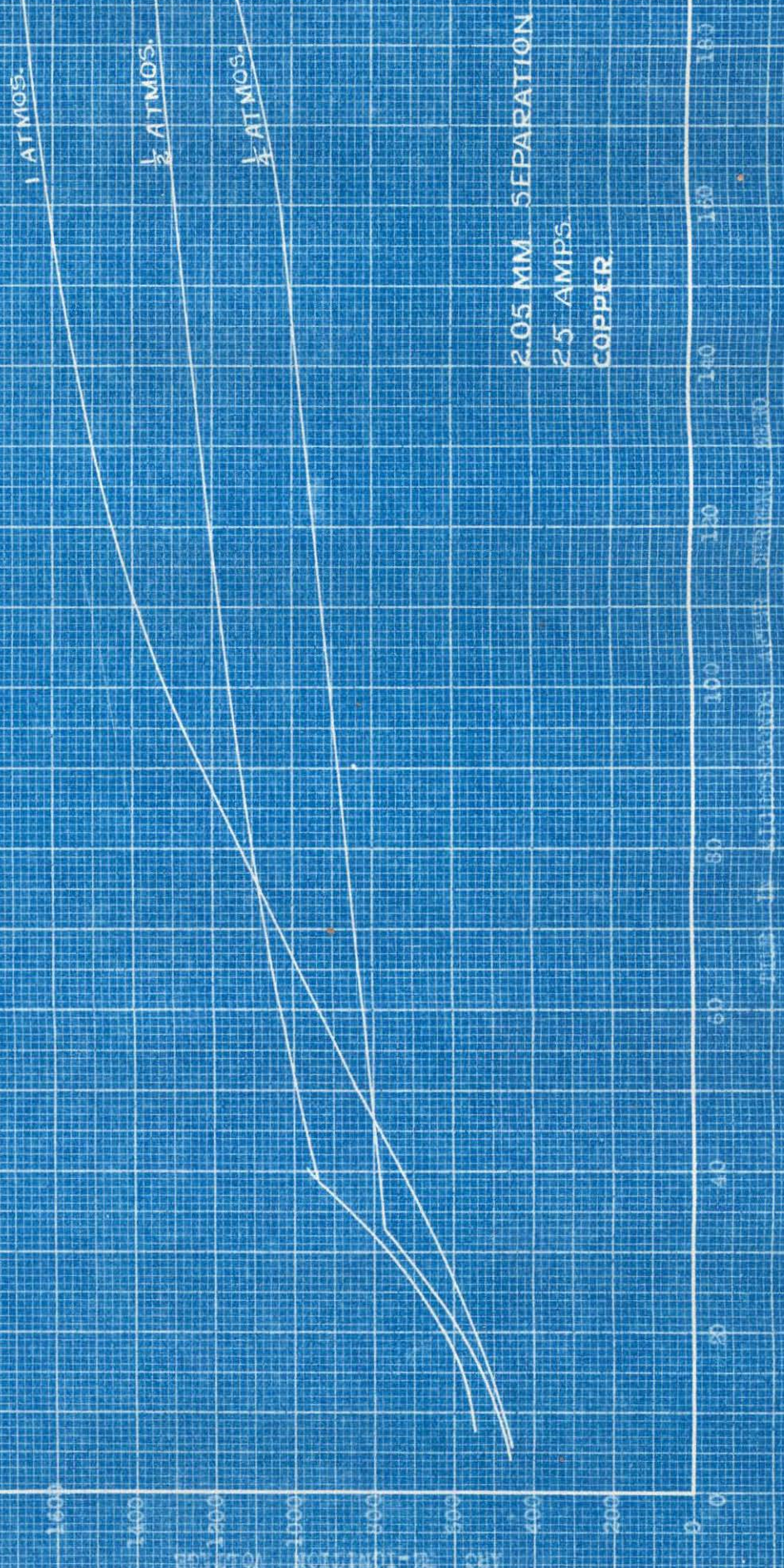


FIG. 21

## EFFECT OF PRESSURE ON DIELECTRIC RECOVERY

1 ATMOS

$\frac{1}{2}$  ATMOS

$\frac{1}{4}$  ATMOS

2.05 MM. SEPARATION

12.5 AMPS

COPPER

180

160

140

120

100

80

60

40

20

0

1000  
1200  
1300  
1400  
1500  
1600  
1700  
1800  
1900  
2000  
2100  
2200  
2300  
2400  
2500  
2600  
2700  
2800  
2900  
3000  
3100  
3200  
3300  
3400  
3500  
3600  
3700  
3800  
3900  
4000  
4100  
4200  
4300  
4400  
4500  
4600  
4700  
4800  
4900  
5000  
5100  
5200  
5300  
5400  
5500  
5600  
5700  
5800  
5900  
6000  
6100  
6200  
6300  
6400  
6500  
6600  
6700  
6800  
6900  
7000  
7100  
7200  
7300  
7400  
7500  
7600  
7700  
7800  
7900  
8000  
8100  
8200  
8300  
8400  
8500  
8600  
8700  
8800  
8900  
9000  
9100  
9200  
9300  
9400  
9500  
9600  
9700  
9800  
9900  
10000  
10100  
10200  
10300  
10400  
10500  
10600  
10700  
10800  
10900  
11000  
11100  
11200  
11300  
11400  
11500  
11600  
11700  
11800  
11900  
12000  
12100  
12200  
12300  
12400  
12500  
12600  
12700  
12800  
12900  
13000  
13100  
13200  
13300  
13400  
13500  
13600  
13700  
13800  
13900  
14000  
14100  
14200  
14300  
14400  
14500  
14600  
14700  
14800  
14900  
15000  
15100  
15200  
15300  
15400  
15500  
15600  
15700  
15800  
15900  
16000  
16100  
16200  
16300  
16400  
16500  
16600  
16700  
16800  
16900  
17000  
17100  
17200  
17300  
17400  
17500  
17600  
17700  
17800  
17900  
18000  
18100  
18200  
18300  
18400  
18500  
18600  
18700  
18800  
18900  
19000  
19100  
19200  
19300  
19400  
19500  
19600  
19700  
19800  
19900  
20000  
20100  
20200  
20300  
20400  
20500  
20600  
20700  
20800  
20900  
21000  
21100  
21200  
21300  
21400  
21500  
21600  
21700  
21800  
21900  
22000  
22100  
22200  
22300  
22400  
22500  
22600  
22700  
22800  
22900  
23000  
23100  
23200  
23300  
23400  
23500  
23600  
23700  
23800  
23900  
24000  
24100  
24200  
24300  
24400  
24500  
24600  
24700  
24800  
24900  
25000  
25100  
25200  
25300  
25400  
25500  
25600  
25700  
25800  
25900  
26000  
26100  
26200  
26300  
26400  
26500  
26600  
26700  
26800  
26900  
27000  
27100  
27200  
27300  
27400  
27500  
27600  
27700  
27800  
27900  
28000  
28100  
28200  
28300  
28400  
28500  
28600  
28700  
28800  
28900  
29000  
29100  
29200  
29300  
29400  
29500  
29600  
29700  
29800  
29900  
30000  
30100  
30200  
30300  
30400  
30500  
30600  
30700  
30800  
30900  
31000  
31100  
31200  
31300  
31400  
31500  
31600  
31700  
31800  
31900  
32000  
32100  
32200  
32300  
32400  
32500  
32600  
32700  
32800  
32900  
33000  
33100  
33200  
33300  
33400  
33500  
33600  
33700  
33800  
33900  
34000  
34100  
34200  
34300  
34400  
34500  
34600  
34700  
34800  
34900  
35000  
35100  
35200  
35300  
35400  
35500  
35600  
35700  
35800  
35900  
36000  
36100  
36200  
36300  
36400  
36500  
36600  
36700  
36800  
36900  
37000  
37100  
37200  
37300  
37400  
37500  
37600  
37700  
37800  
37900  
38000  
38100  
38200  
38300  
38400  
38500  
38600  
38700  
38800  
38900  
39000  
39100  
39200  
39300  
39400  
39500  
39600  
39700  
39800  
39900  
40000  
40100  
40200  
40300  
40400  
40500  
40600  
40700  
40800  
40900  
41000  
41100  
41200  
41300  
41400  
41500  
41600  
41700  
41800  
41900  
42000  
42100  
42200  
42300  
42400  
42500  
42600  
42700  
42800  
42900  
43000  
43100  
43200  
43300  
43400  
43500  
43600  
43700  
43800  
43900  
44000  
44100  
44200  
44300  
44400  
44500  
44600  
44700  
44800  
44900  
45000  
45100  
45200  
45300  
45400  
45500  
45600  
45700  
45800  
45900  
46000  
46100  
46200  
46300  
46400  
46500  
46600  
46700  
46800  
46900  
47000  
47100  
47200  
47300  
47400  
47500  
47600  
47700  
47800  
47900  
48000  
48100  
48200  
48300  
48400  
48500  
48600  
48700  
48800  
48900  
49000  
49100  
49200  
49300  
49400  
49500  
49600  
49700  
49800  
49900  
50000  
50100  
50200  
50300  
50400  
50500  
50600  
50700  
50800  
50900  
51000  
51100  
51200  
51300  
51400  
51500  
51600  
51700  
51800  
51900  
52000  
52100  
52200  
52300  
52400  
52500  
52600  
52700  
52800  
52900  
53000  
53100  
53200  
53300  
53400  
53500  
53600  
53700  
53800  
53900  
54000  
54100  
54200  
54300  
54400  
54500  
54600  
54700  
54800  
54900  
55000  
55100  
55200  
55300  
55400  
55500  
55600  
55700  
55800  
55900  
56000  
56100  
56200  
56300  
56400  
56500  
56600  
56700  
56800  
56900  
57000  
57100  
57200  
57300  
57400  
57500  
57600  
57700  
57800  
57900  
58000  
58100  
58200  
58300  
58400  
58500  
58600  
58700  
58800  
58900  
59000  
59100  
59200  
59300  
59400  
59500  
59600  
59700  
59800  
59900  
60000  
60100  
60200  
60300  
60400  
60500  
60600  
60700  
60800  
60900  
61000  
61100  
61200  
61300  
61400  
61500  
61600  
61700  
61800  
61900  
62000  
62100  
62200  
62300  
62400  
62500  
62600  
62700  
62800  
62900  
63000  
63100  
63200  
63300  
63400  
63500  
63600  
63700  
63800  
63900  
64000  
64100  
64200  
64300  
64400  
64500  
64600  
64700  
64800  
64900  
65000  
65100  
65200  
65300  
65400  
65500  
65600  
65700  
65800  
65900  
66000  
66100  
66200  
66300  
66400  
66500  
66600  
66700  
66800  
66900  
67000  
67100  
67200  
67300  
67400  
67500  
67600  
67700  
67800  
67900  
68000  
68100  
68200  
68300  
68400  
68500  
68600  
68700  
68800  
68900  
69000  
69100  
69200  
69300  
69400  
69500  
69600  
69700  
69800  
69900  
70000  
70100  
70200  
70300  
70400  
70500  
70600  
70700  
70800  
70900  
71000  
71100  
71200  
71300  
71400  
71500  
71600  
71700  
71800  
71900  
72000  
72100  
72200  
72300  
72400  
72500  
72600  
72700  
72800  
72900  
73000  
73100  
73200  
73300  
73400  
73500  
73600  
73700  
73800  
73900  
74000  
74100  
74200  
74300  
74400  
74500  
74600  
74700  
74800  
74900  
75000  
75100  
75200  
75300  
75400  
75500  
75600  
75700  
75800  
75900  
76000  
76100  
76200  
76300  
76400  
76500  
76600  
76700  
76800  
76900  
77000  
77100  
77200  
77300  
77400  
77500  
77600  
77700  
77800  
77900  
78000  
78100  
78200  
78300  
78400  
78500  
78600  
78700  
78800  
78900  
79000  
79100  
79200  
79300  
79400  
79500  
79600  
79700  
79800  
79900  
80000  
80100  
80200  
80300  
80400  
80500  
80600  
80700  
80800  
80900  
81000  
81100  
81200  
81300  
81400  
81500  
81600  
81700  
81800  
81900  
82000  
82100  
82200  
82300  
82400  
82500  
82600  
82700  
82800  
82900  
83000  
83100  
83200  
83300  
83400  
83500  
83600  
83700  
83800  
83900  
84000  
84100  
84200  
84300  
84400  
84500  
84600  
84700  
84800  
84900  
85000  
85100  
85200  
85300  
85400  
85500  
85600  
85700  
85800  
85900  
86000  
86100  
86200  
86300  
86400  
86500  
86600  
86700  
86800  
86900  
87000  
87100  
87200  
87300  
87400  
87500  
87600  
87700  
87800  
87900  
88000  
88100  
88200  
88300  
88400  
88500  
88600  
88700  
88800  
88900  
88900  
89000  
89100  
89200  
89300  
89400  
89500  
89600  
89700  
89800  
89900  
90000  
90100  
90200  
90300  
90400  
90500  
90600  
90700  
90800  
90900  
91000  
91100  
91200  
91300  
91400  
91500  
91600  
91700  
91800  
91900  
92000  
92100  
92200  
92300  
92400  
92500  
92600  
92700  
92800  
92900  
93000  
93100  
93200  
93300  
93400  
93500  
93600  
93700  
93800  
93900  
94000  
94100  
94200  
94300  
94400  
94500  
94600  
94700  
94800  
94900  
95000  
95100  
95200  
95300  
95400  
95500  
95600  
95700  
95800  
95900  
96000  
96100  
96200  
96300  
96400  
96500  
96600  
96700  
96800  
96900  
97000  
97100  
97200  
97300  
97400  
97500  
97600  
97700  
97800  
97900  
98000  
98100  
98200  
98300  
98400  
98500  
98600  
98700  
98800  
98900  
98900  
99000  
99100  
99200  
99300  
99400  
99500  
99600  
99700  
99800  
99900  
100000

FIG. 22.

## EFFECT OF PRESSURE ON DIELECTRIC RECOVERY

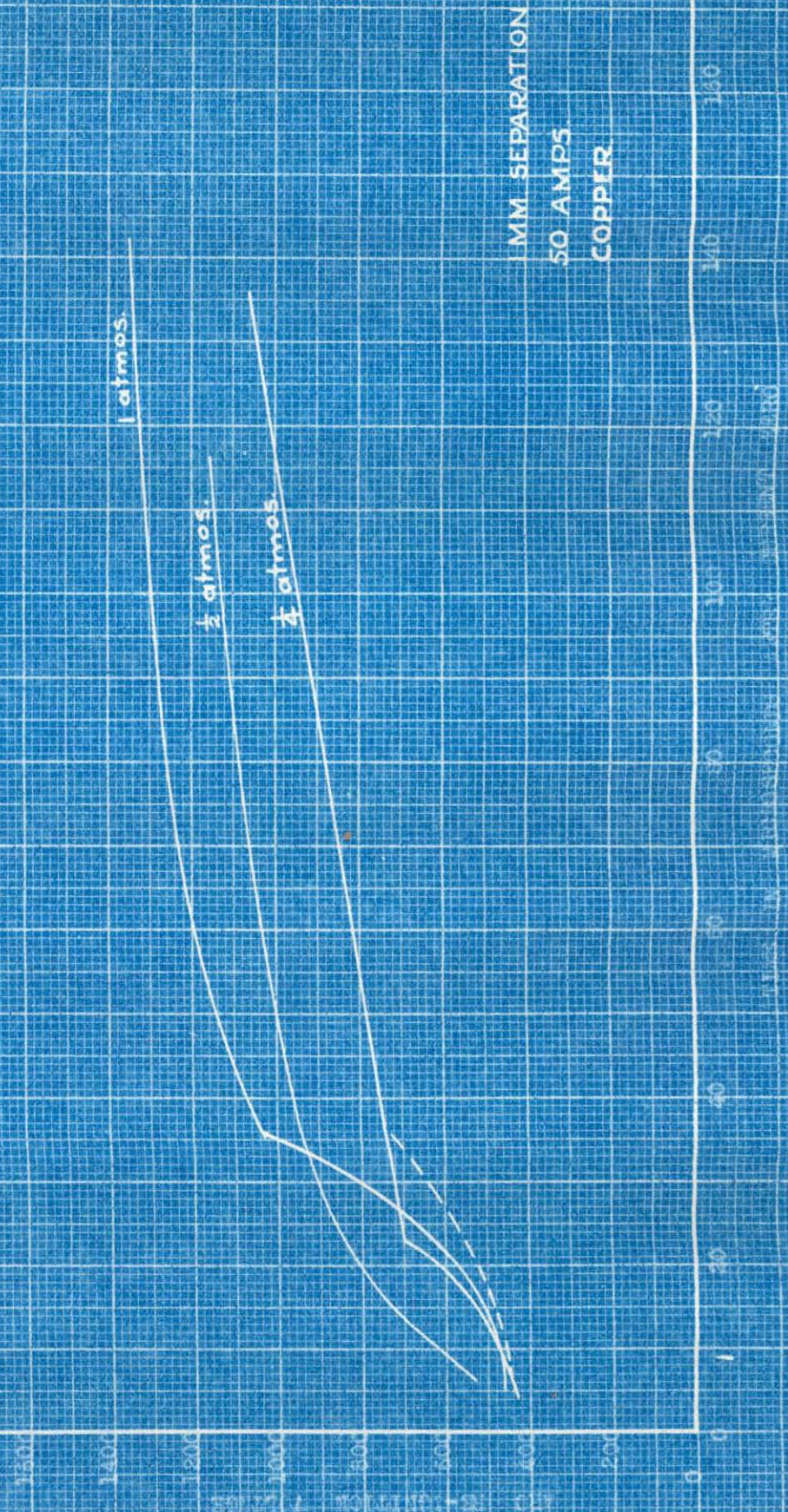


FIG. 23.

## EFFECT OF PRESSURE ON DIELECTRIC RECOVERY

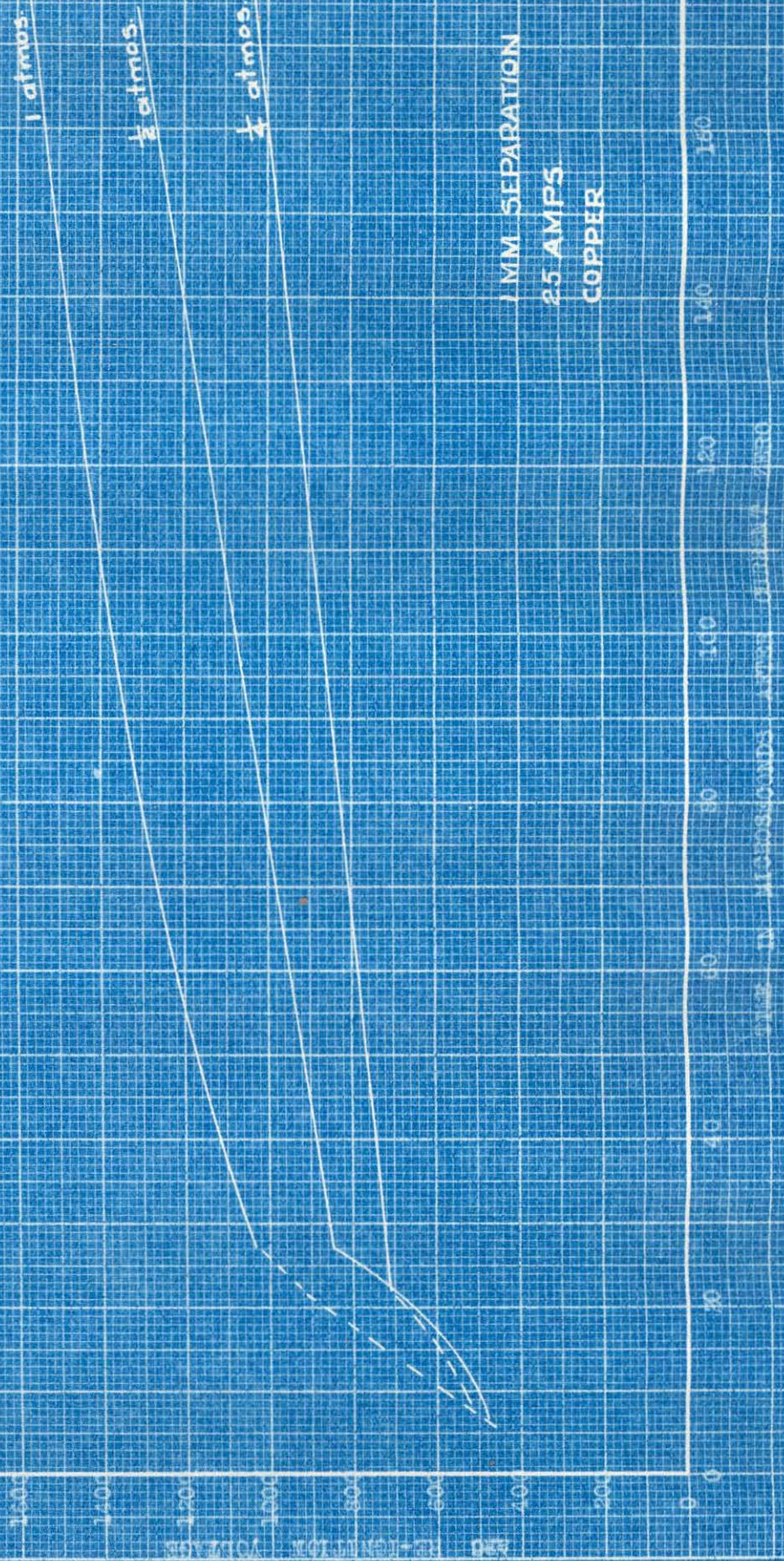
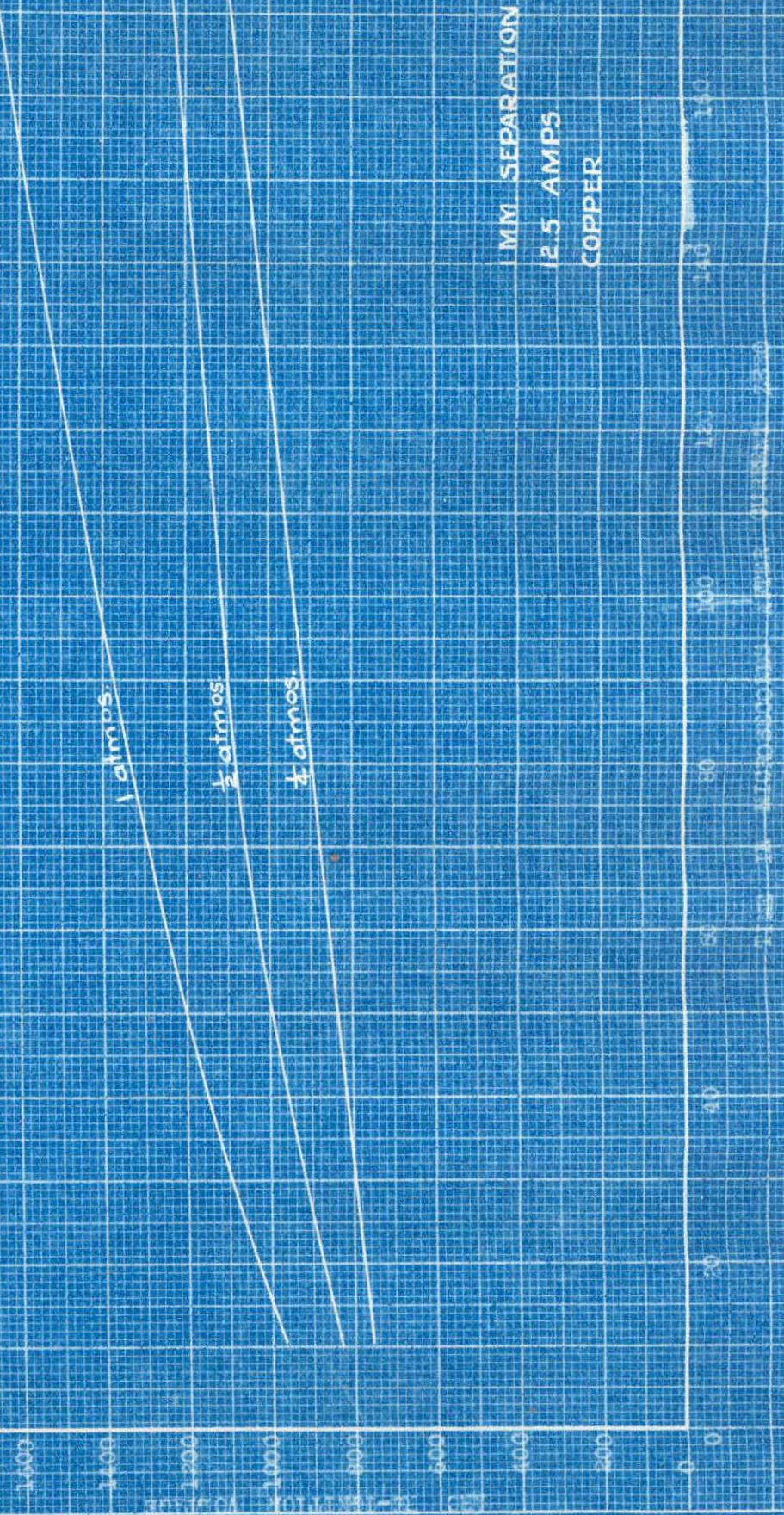


FIG. 24.

## EFFECT OF PRESSURE ON DIELECTRIC RECOVERY



## EFFECT OF PRESSURE ON DIELECTRIC RECOVERY

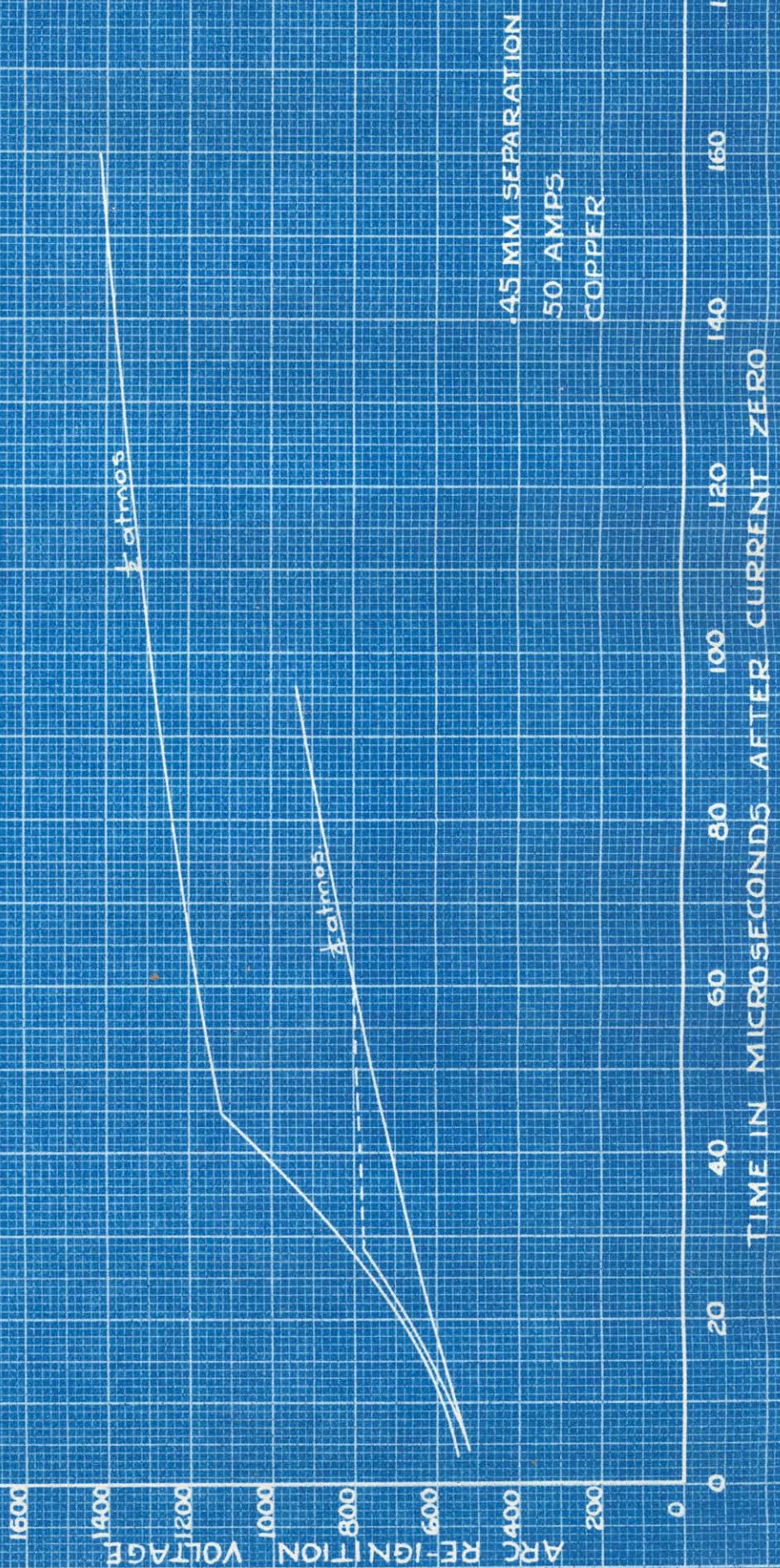


FIG. 26.

## EFFECT OF PRESSURE ON DIELECTRIC RECOVERY

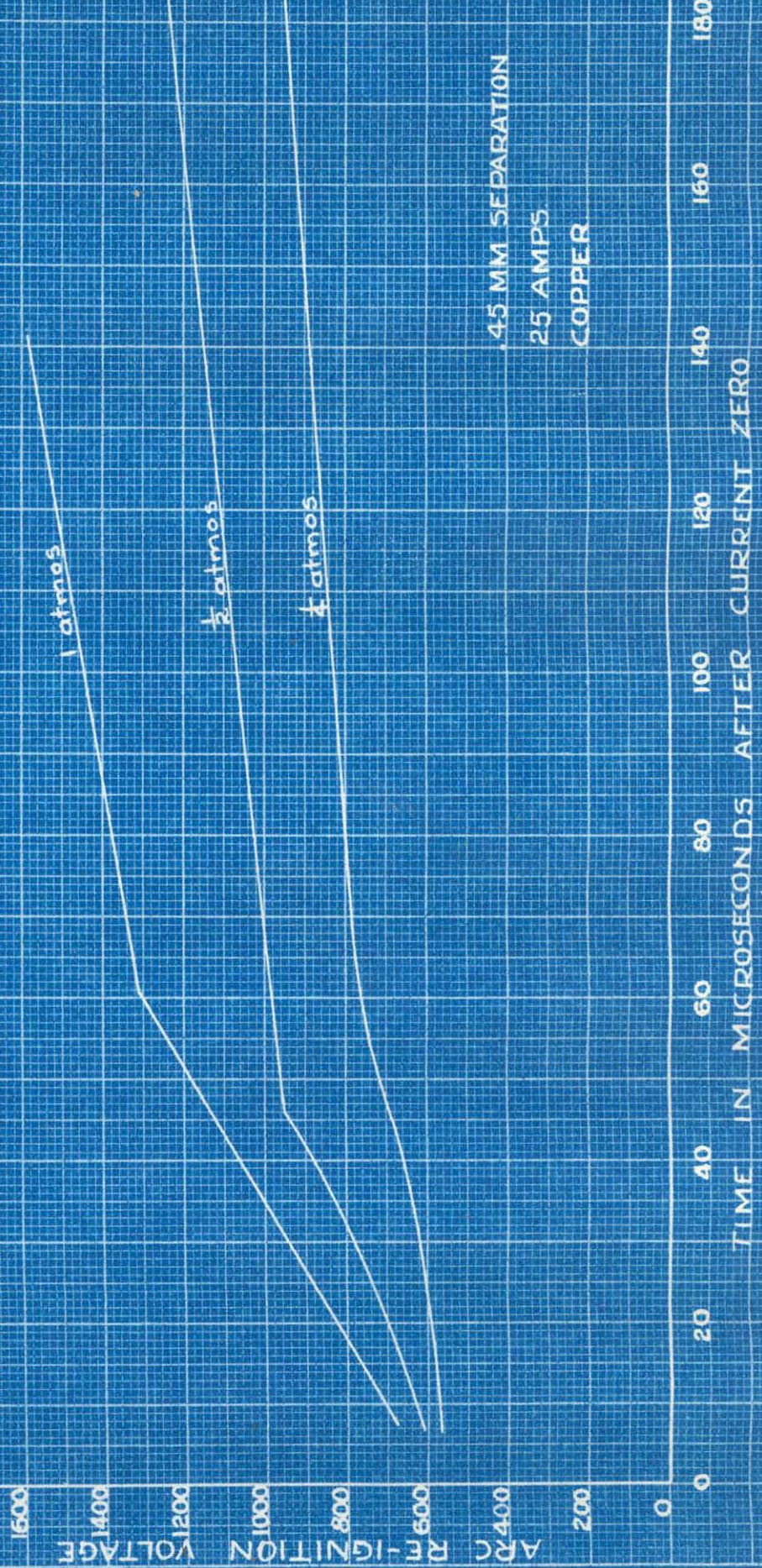


FIG. 27.

## EFFECT OF PRESSURE ON DIELECTRIC RECOVERY

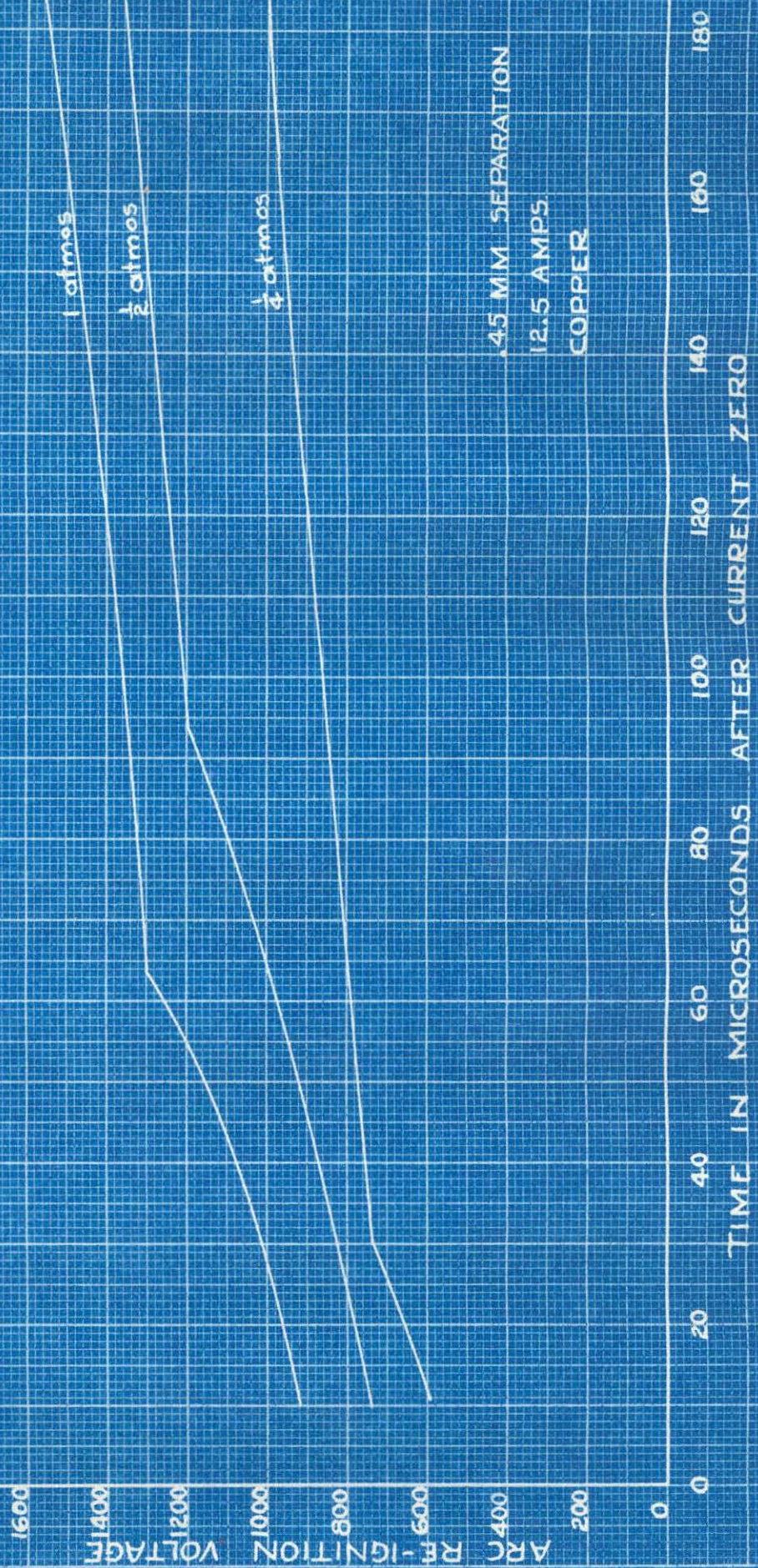


FIG. 26.

EFFECT OF ARC LENGTH ON DIELECTRIC RECOVERY

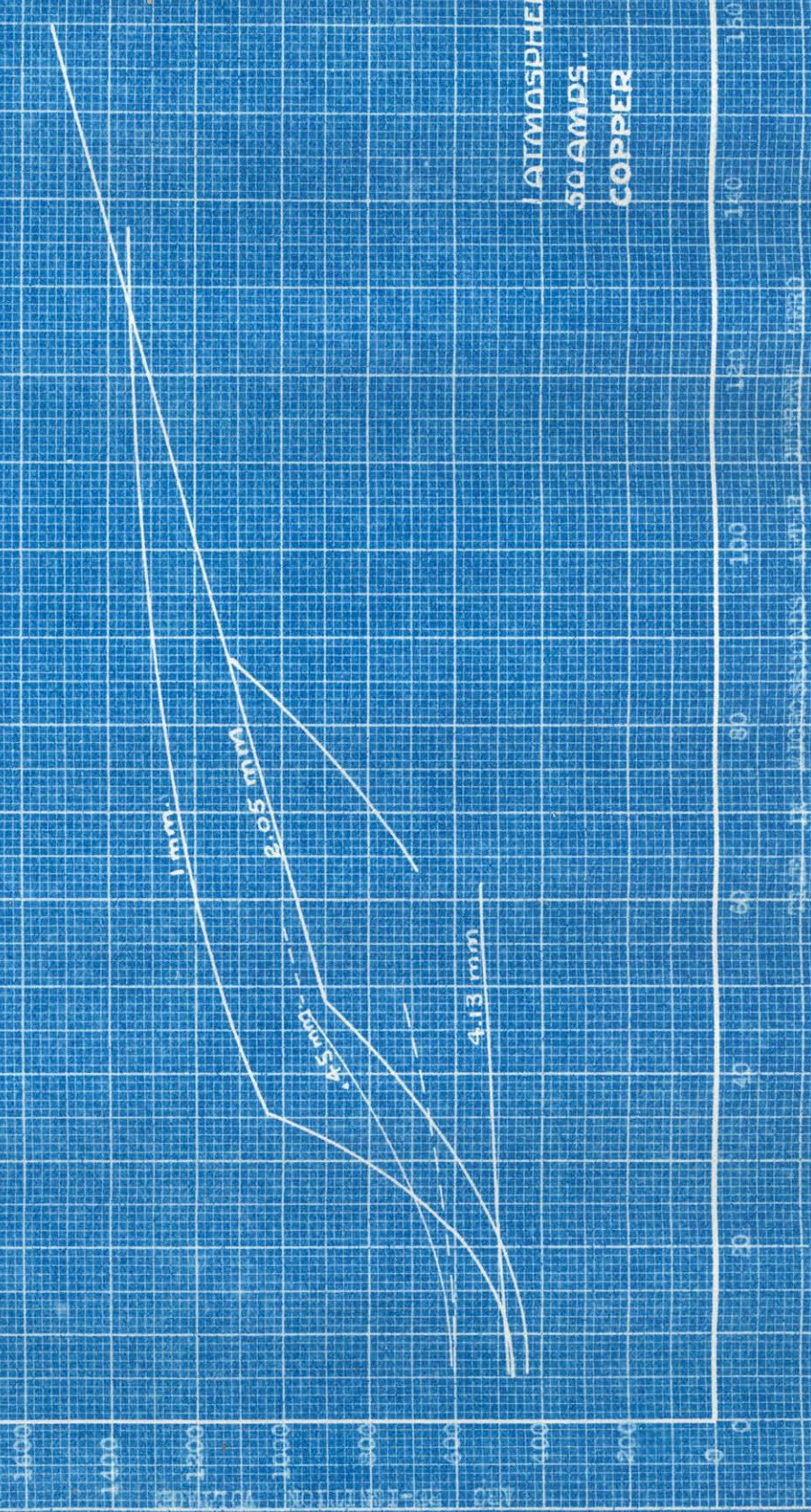


FIG. 29.

## EFFECT OF ARC LENGTH ON DIELECTRIC RECOVERY

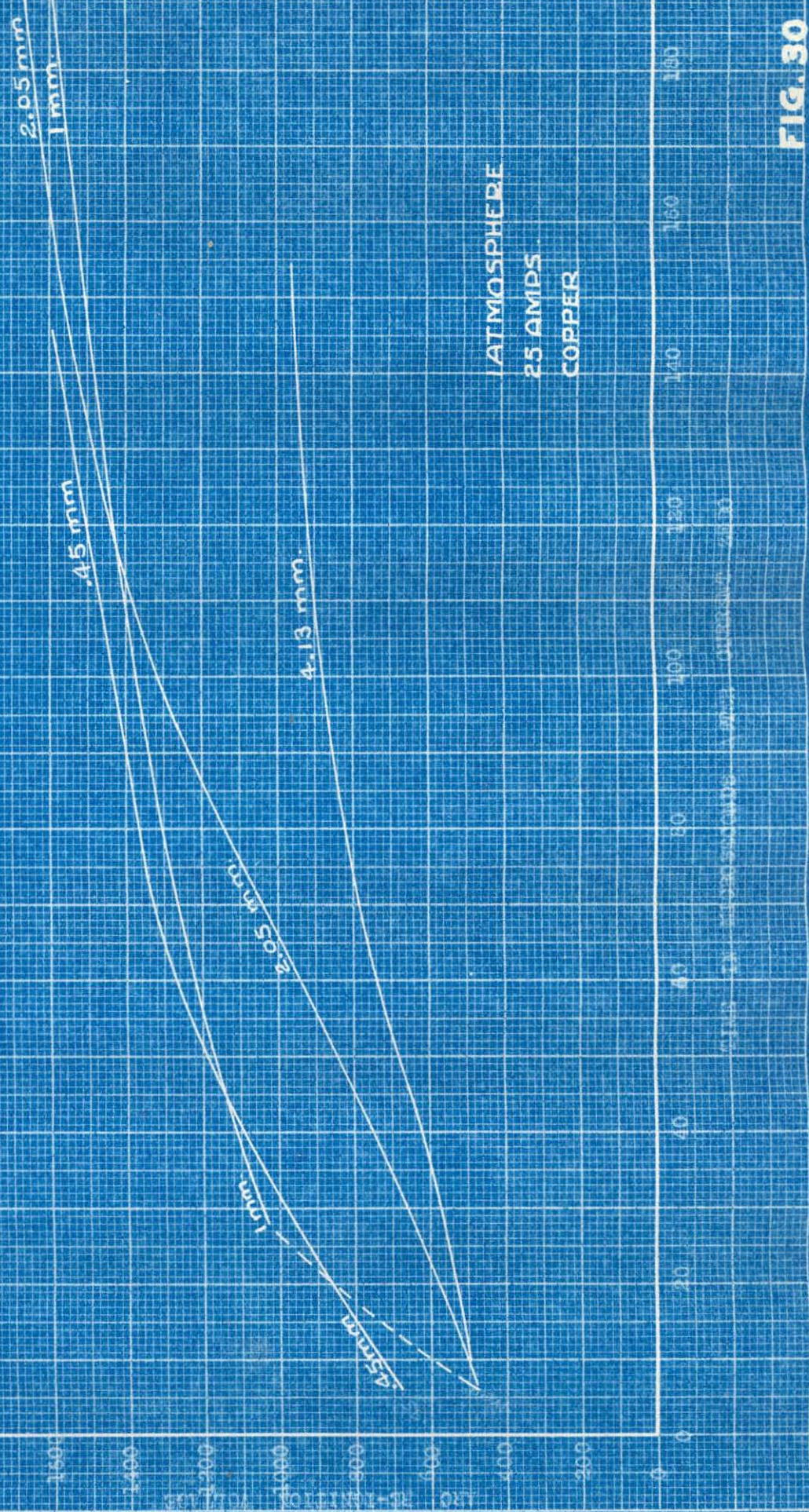
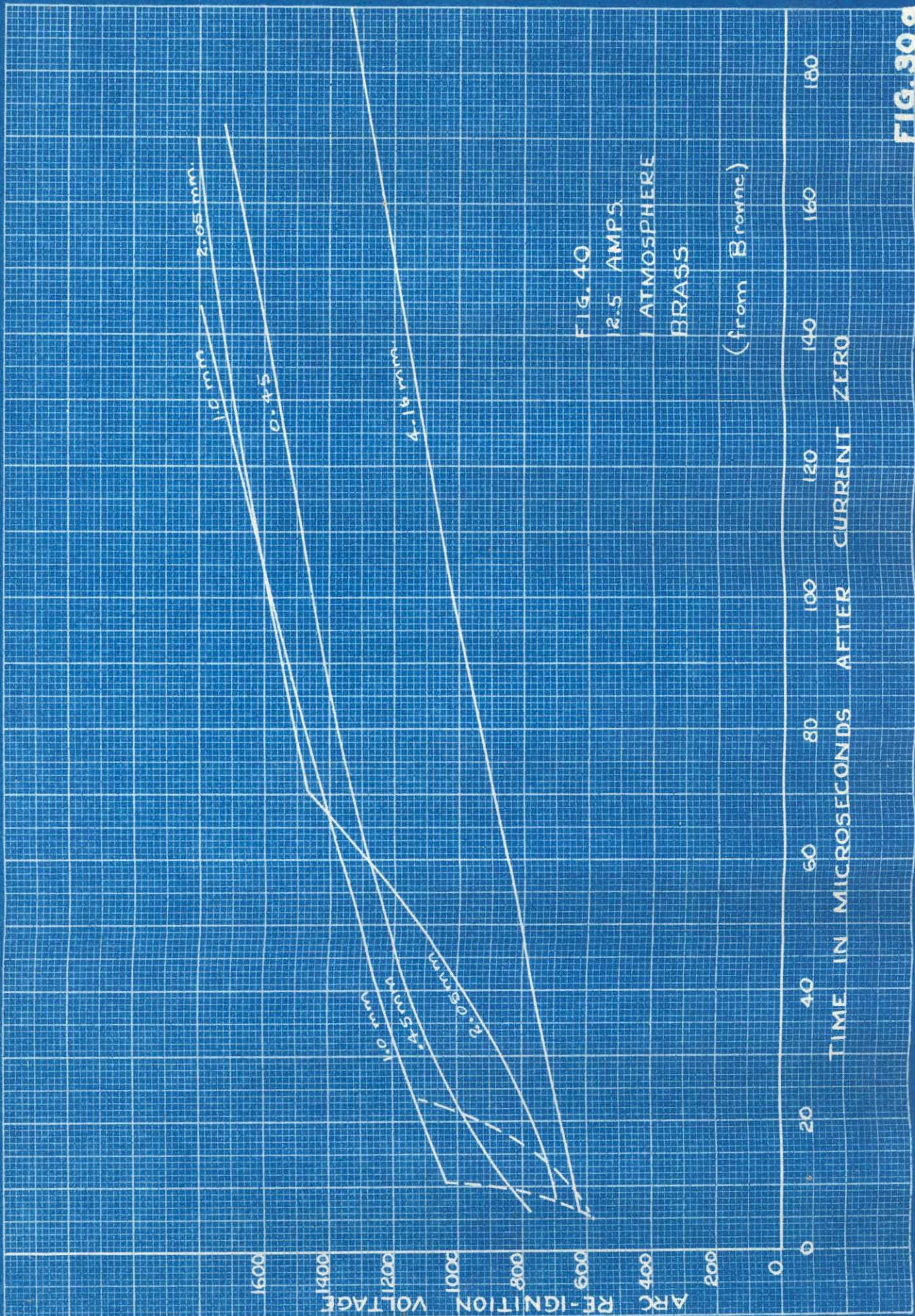


FIG. 30



## EFFECT OF ARC LENGTH ON DIELECTRIC RECOVERY

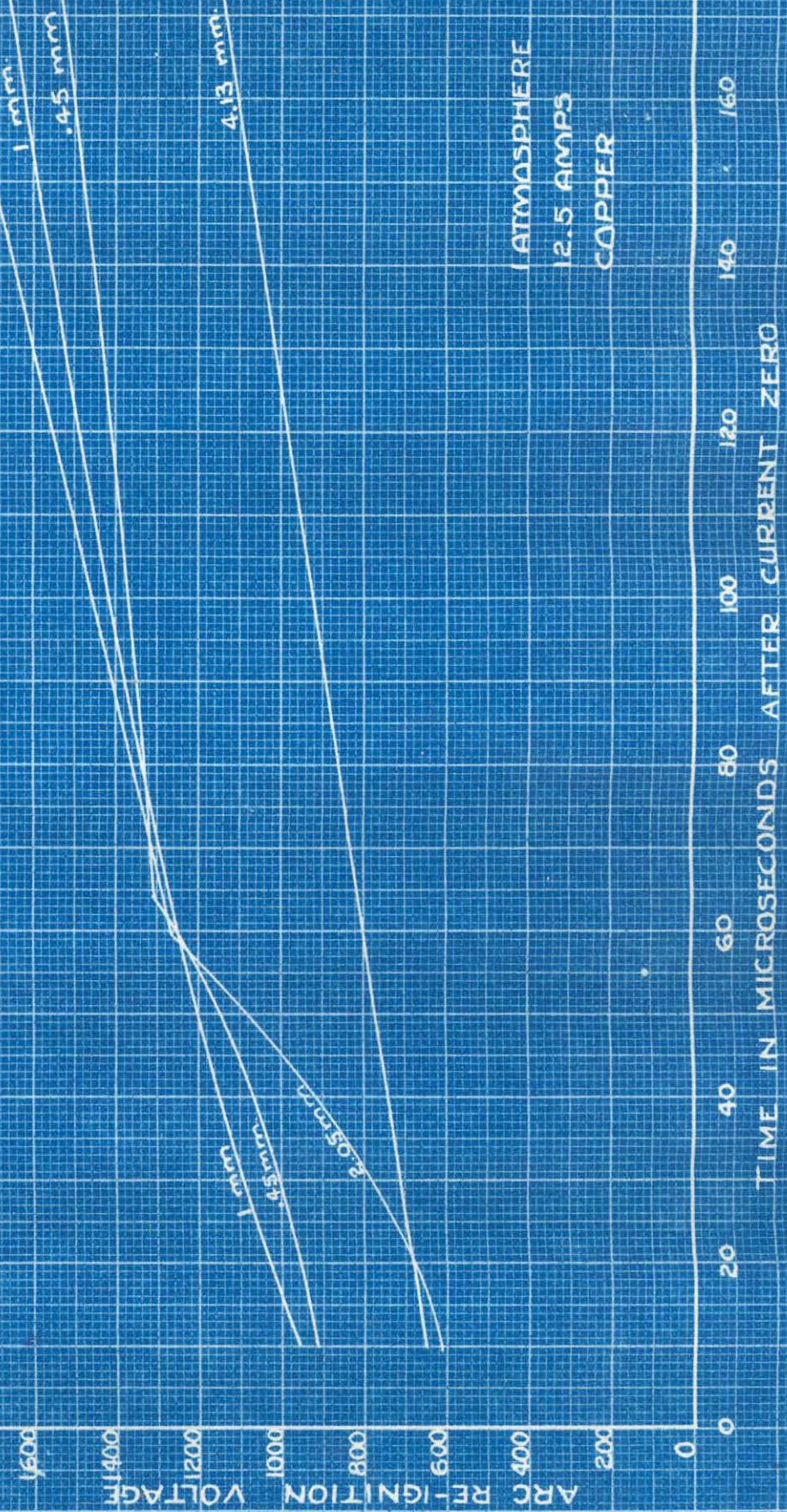


FIG. 31

## EFFECT OF ARC LENGTH ON DIELECTRIC RECOVERY



FIG. 312.

EFFECT OF ARC LENGTH ON DIELECTRIC RECOVERY

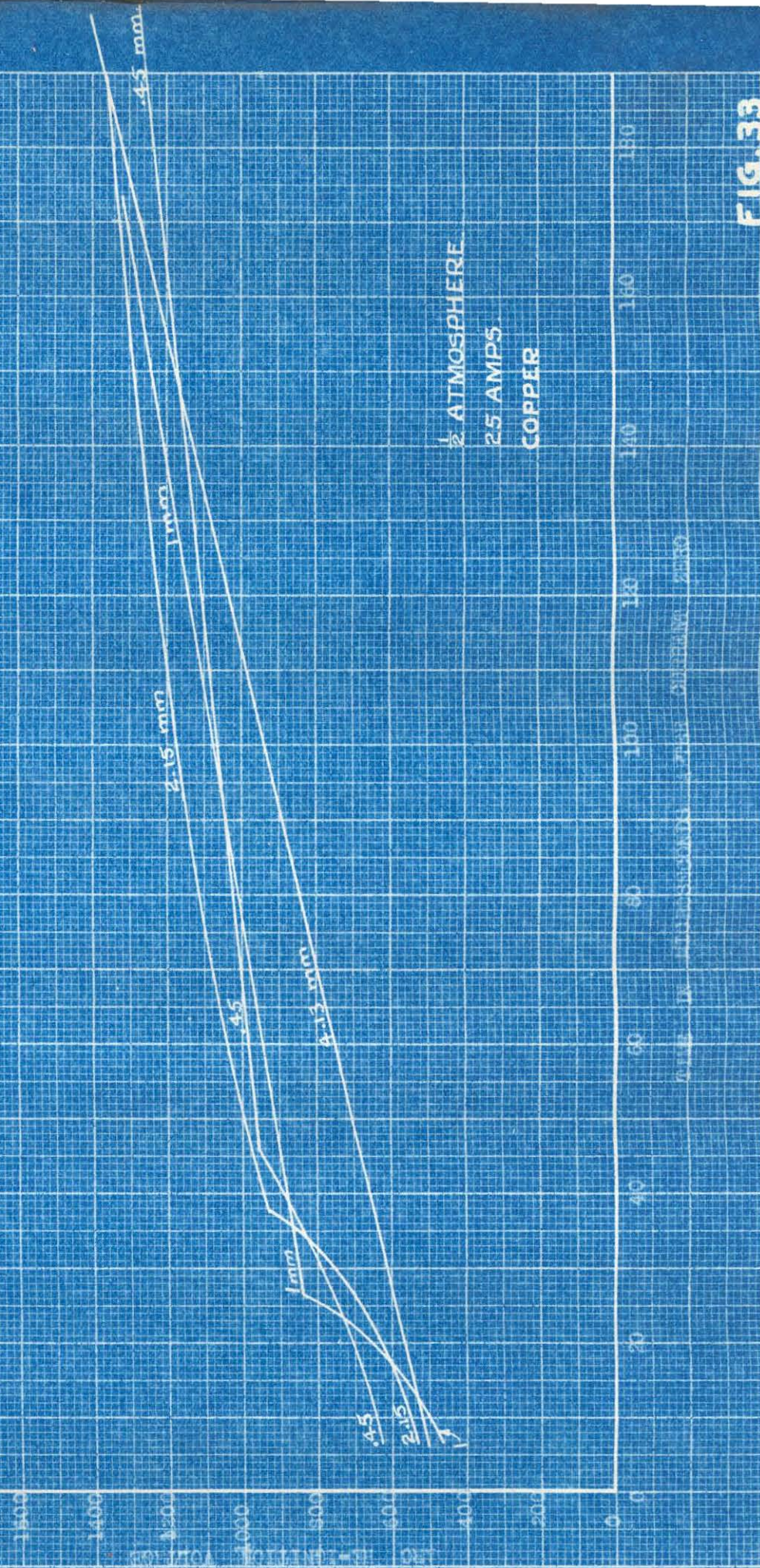


FIG. 33

EFFECT OF ARC LENGTH ON DIELECTRIC RECOVERY

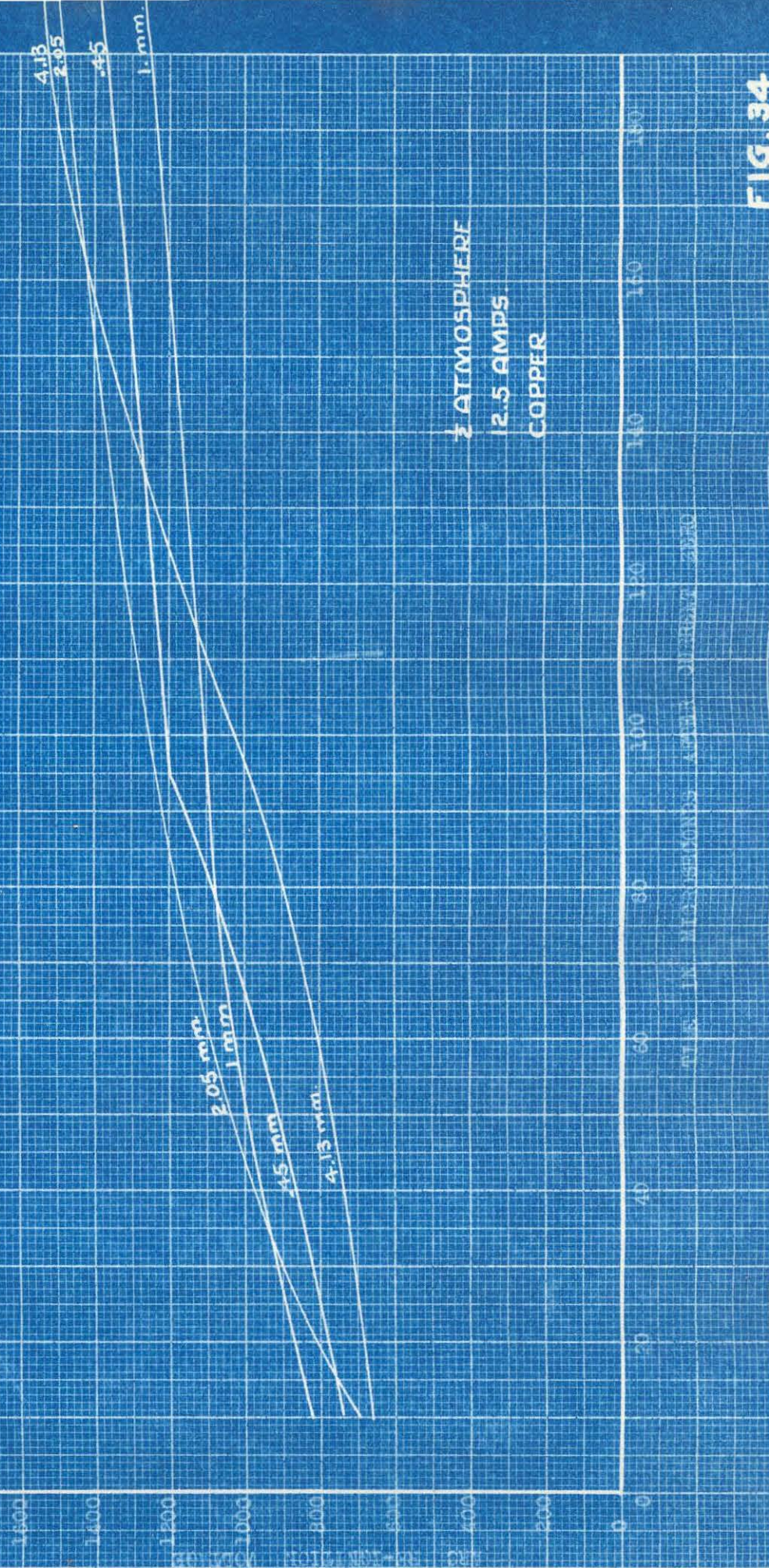


FIG. 34

EFFECT OF ARC LENGTH ON DIELECTRIC RECOVERY

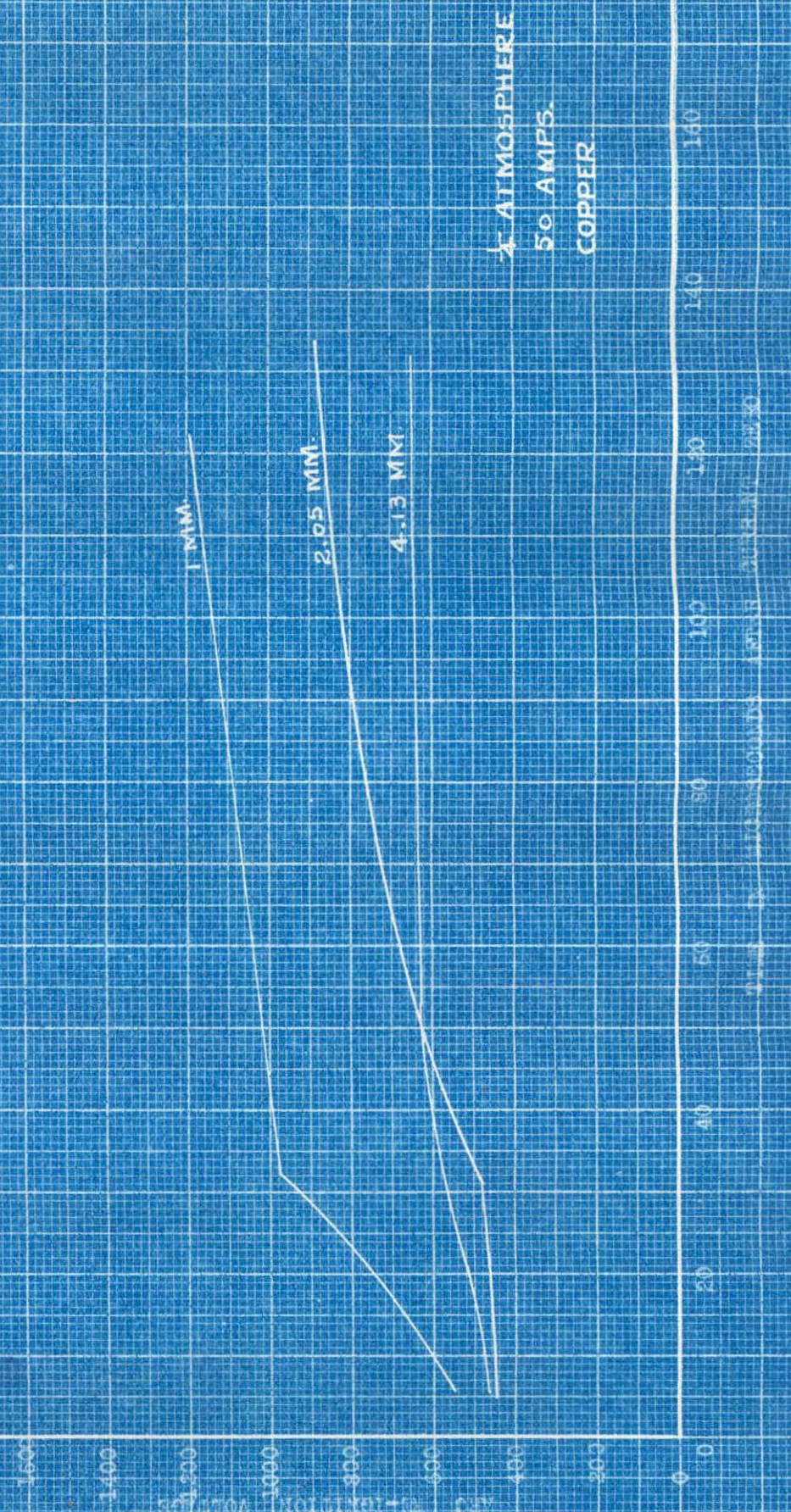


FIG. 35

## EFFECT OF ARC LENGTH ON ELECTRIC RECOVERY

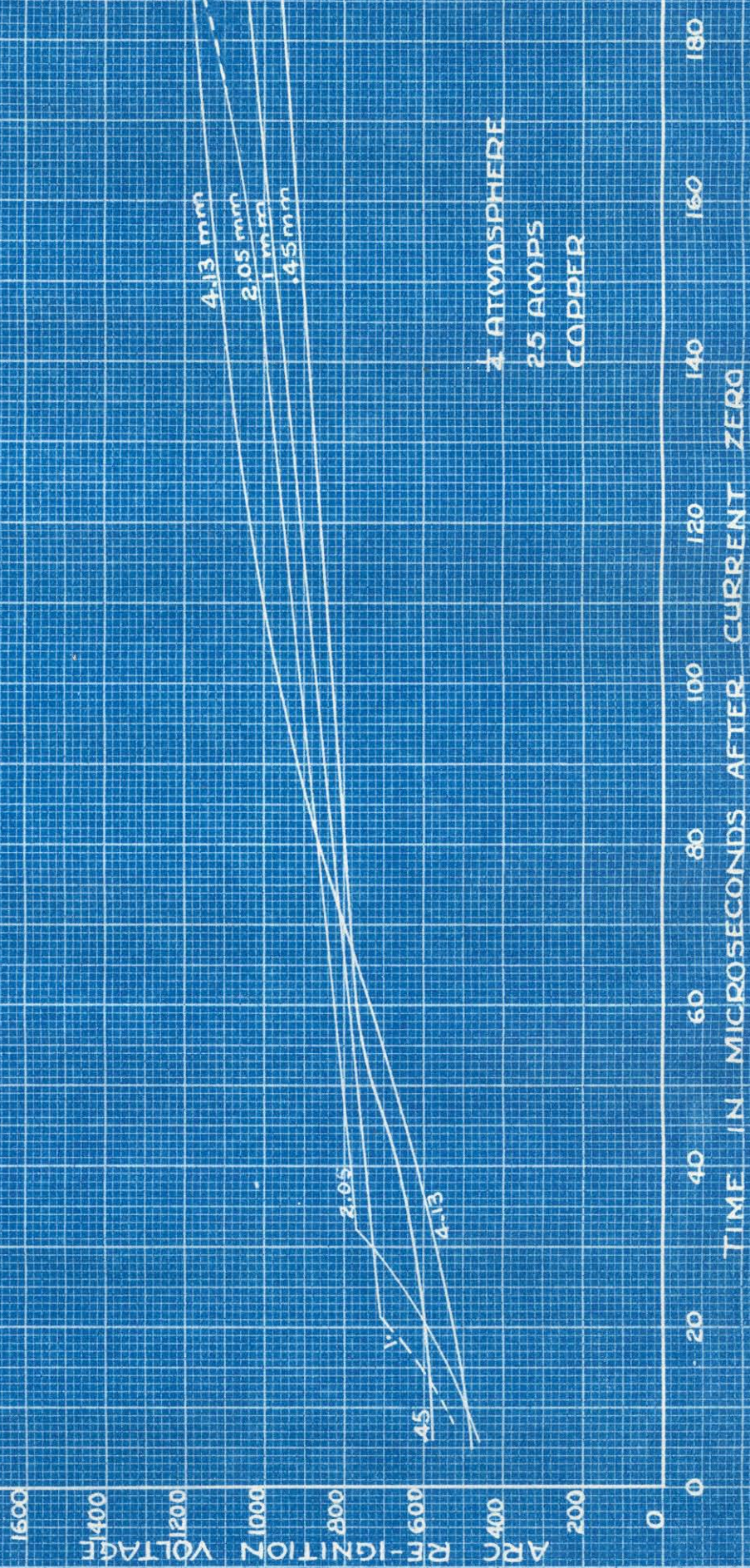


FIG. 36.

## EFFECT OF ARC LENGTH ON DIELECTRIC RECOVERY

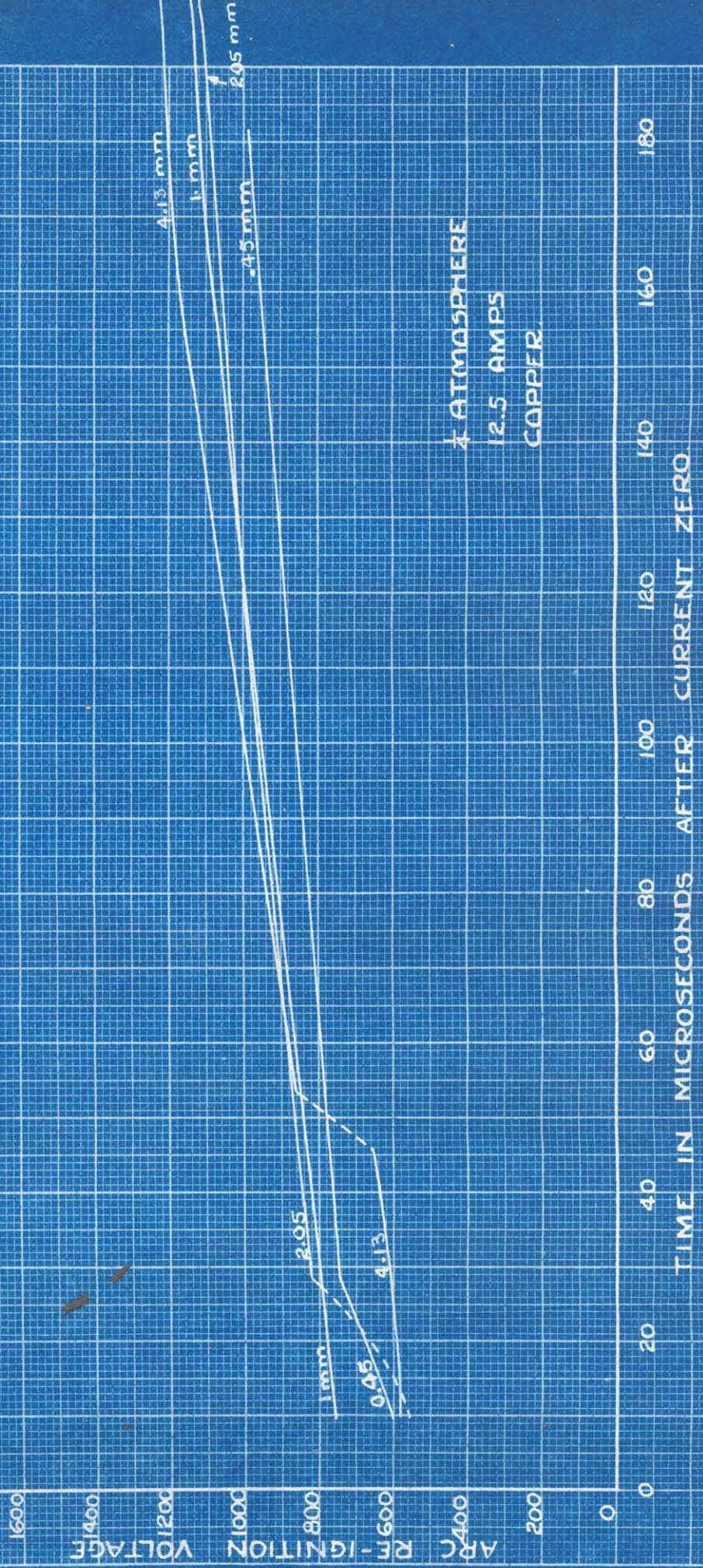
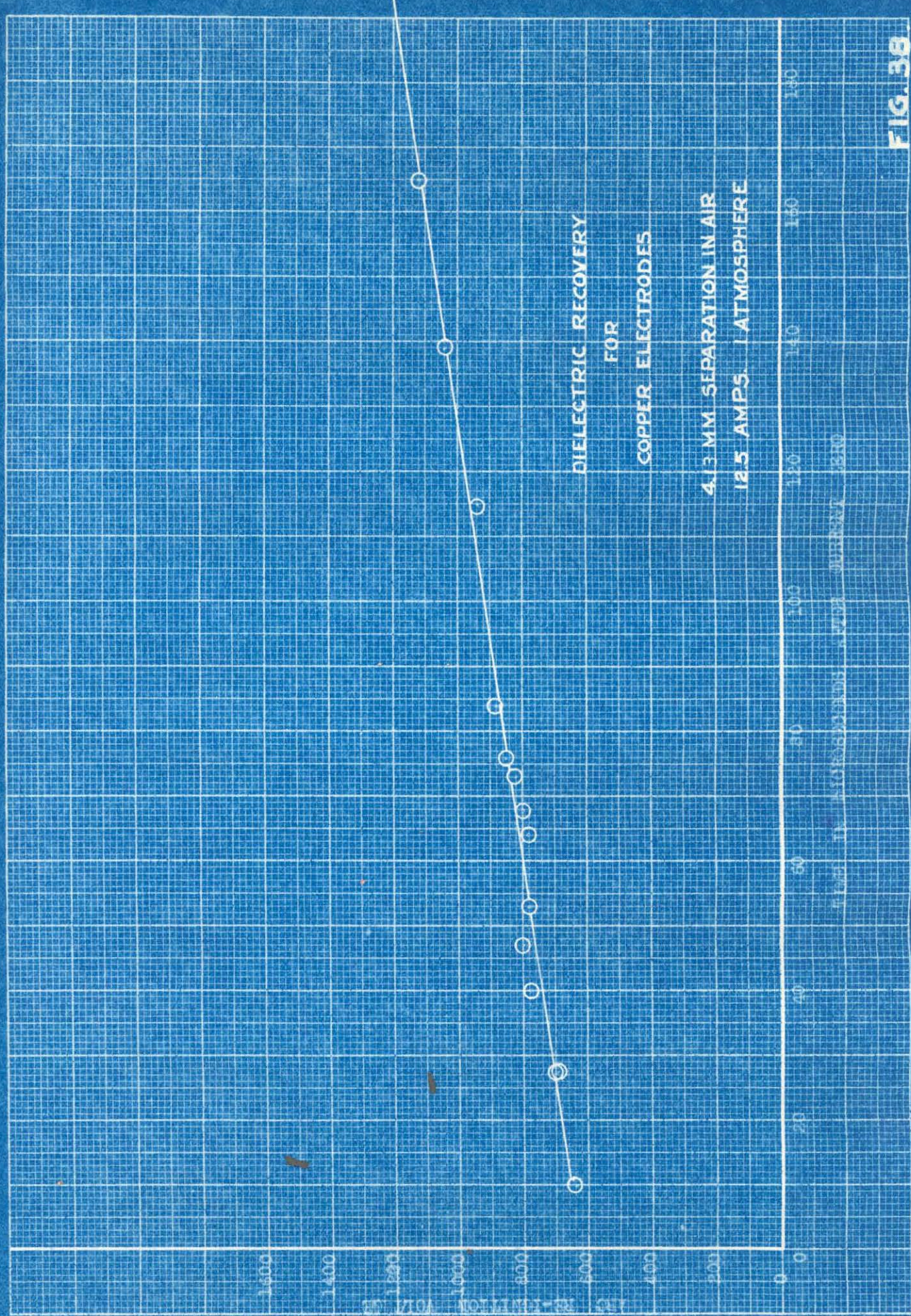


FIG. 37.

FIG. 38



2. Effect of Current - (Copper)

Figures 5 through 11, show the definite effect that increasing the current lowers the initial recovery voltage and also the subsequent sparking voltage. However, at 1/2 atmos. and 1 mm. (Fig. 12), the dielectric recovery curve for 50 amps. is higher than that for 12.5. Figure 13 (1/4 atmos. and 1 mm.) and Figure 14 (1 atmos. and 0.45 mm.) show this same effect.

The curves shown on Figures 15 and 16 show the anomalous relation that the dielectric recovery curve for 12.5 amps is higher than that for 25 amps. but less than that for 50 amps. The initial recovery rate, however, is still smaller for the higher currents. It should be noted that with the exception of Figure 12, these latter results all occur at 0.45 mm. separation.

Assuming that current density is invariant in the arc, neglecting lateral diffusion from the ionized core, and treating diffusion and cooling as one-dimensional processes, then the reignition curves for various currents should all coincide. The results obtained show then the variations in these assumptions. Lateral diffusion must be appreciable for the longer arcs - 4.13, 2.05, and 1.0 mm. For, still assuming uniform current density, the ratio of core perimeter to core area is greater for 12.5 amps. than for a greater current, so that diffusion is relatively more important for the smaller currents.

The effect occurring in Figures 13 to 16, that of a higher recovery curve for 50 amps. than for 12.5 amps., can be explained by the fact that it was very difficult to maintain an arc at 0.45 mm. and 1/2 or 1/4 atmos. with 12.5 or 25 amps. Almost immediately after initiation the arc appeared as a diffuse discharge and quickly (in less than a second) changed to a glow discharge. For these cases then, the relations existing were obviously very different from those holding at the other spacings and there could be no assumption of uniform current density.

### 3. Effect of Pressure - (Copper)

Figures 17 through 28 show the effect of gas pressure on dielectric recovery, all other quantities being kept constant for any set of curves. The Figures show that in general the curves cross at some point, showing that the effect of pressure is different for the first and the latter part of the curves. Equation (5), Appendix (E), shows that the dielectric strength of the space charge sheath should vary directly with the pressure (since pressure varies inversely as temperature) and inversely as the ion density. Because of the relation existing between the ion density and coefficient of diffusion, Equation (5) shows that for deionization by diffusion the early recovery rate should be almost independent of pressure. After deionization of the space, the only effect of pressure is upon the density of the gas between the electrodes.

For the same temperature the dielectric strength should be higher for the higher pressure and directly proportional to it. The fact that this condition does not hold for later recovery times, shows that the temperatures are different, which is easily appreciated since the cooling rate is higher for a lower pressure. These relations of low dielectric strength for short reignition times and of high dielectric strength for later times with increasing pressure are well shown in the curves of this set.

Figures 18, 21, 24, and 27 agree identically in form with Browne's Figures 45, 44, 43, and 42, respectively, for brass, differing only somewhat in magnitude.

#### 4. Effect of Arc Length - (Copper)

Figures 29 through 37 show the effect of arc length on dielectric recovery. With only the exceptions noted below, the shorter arcs are seen to have a higher short-time voltage strength than the longer ones. Inasmuch as this property has hitherto been held to hold only for the low-boiling-point electrodes, this is a very significant fact.

Considering first the 50 amp. curves at 1, 1/2, and 1/4 atmosphere (Figures 29, 32, and 35) as being of most practical interest, it is seen that the 4.13 mm. arc has the lowest restriking voltage. In Figure 35 (50 amps. 1/4 atmos.) deionization takes place for all spacings at 30 microseconds. Both in these curves (Figure 35)

and in those of Figure 32, the 4.13 mm. arc has a slightly higher recovery voltage than the 2.05 mm. arc but the difference is within the range of possible experimental error. In Figures 29 and 32, complete deionization does not take place for the 4.13 mm. spacing within the time range shown. It was impossible to continue this curve further, because of the explosive violence with which the arc behaved. For as the arc shunting capacity was increased to obtain longer reignition times, the arc movement became very rapid often reaching the electrode edges and bowing out into an arc length of a foot or more. It is unfortunate that readings were not taken on spacings between 2.05 mm. and 4.13 mm., for there appears to be a rather significant large variation in dielectric recovery between these curves (Figures 29 and 32). Figures 29, 30, and 32 show that as the time gets longer the dielectric strength of the 2.05 mm. space becomes greater than that of the 1 mm. or 0.45 mm. arcs. At still later times it is to be expected, as shown in subsequent curves, that the 4.13 mm. arc strength will rise to a value greater than any of the others shown.

The 25 amp. curves at 1, 1/2, and 1/4 atmosphere (Figures 30, 33, and 36) are also very interesting. They show again that for short times the breakdown voltage varies inversely as the arc length, and then as diffusion becomes more important the long arc spaces reassert their higher voltage strength. Figure 36 is indeed an excellent presentation of these phenomena.

Figures 31, 34, and 37 for the 12.5 amp. arcs show another effect which is also evident on Figure 35. It is that even for short recovery times the 1 mm. arc has a higher dielectric strength than the 0.45 mm. This shows very definitely that for 12.5 amps. at least, there is a separation between 1.0 mm. and 2.05 mm. at which the dielectric strength of a copper arc is a maximum.

Figures 30, 31, and 33 of this thesis agree very closely with data taken under the same conditions for brass<sup>5</sup>-(Figures 39, 40, and 41, respectively). These Figures 40 and 41 also show that an optimum spacing exists between 1 mm. and 2.05 mm. These results show that short time dielectric recovery is not dependent on boiling points, as far as copper and brass are concerned, unless indeed their boiling points are not sufficiently different, - which is a rather untenable hypothesis since the boiling point of zinc is only 930°C. and that of copper is 2310°C.

The extremely close relation between Figure 31 for copper and Figure 40 for brass is a good check on the consistency of the experimental apparatus, for data, for these curves were taken exactly eighteen months apart.

Results are given for steel electrodes under the following  
Figure numbers:-

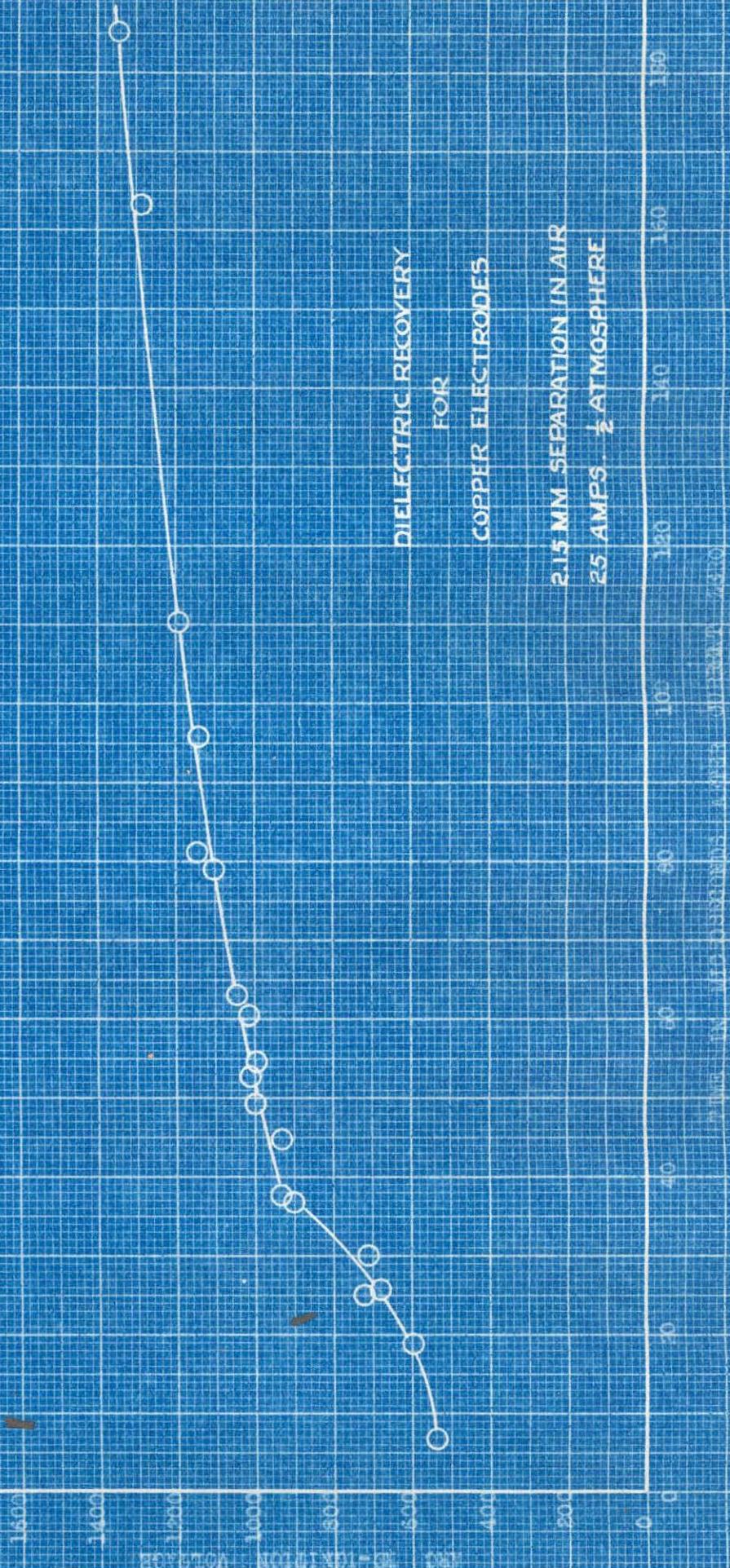
STEEL ELECTRODES

	Separation	Pressure Atmos.		Fig. Nos.
Effect of Current	4.13 mm.	1	1/2	1/4
	2.05 mm.	1	1/2	1/4
	1.0 mm.	1	1/2	1/4
	Separation	Current		Fig. Nos.
Effect of Pressure	4.13 mm.	50,	25,	12.5
	2.05 mm.	50,	25,	12.5
	1.0 mm.	50,	25,	12.5
	Pressure	Current		Fig. Nos.
Effect of Arc Length	1 atmosphere	50,	25,	12.5
	1/2 "	50,	25,	12.5
	1/4 "	50,	25,	12.5

FIG. 35.

DIELECTRIC RECOVERY  
FOR  
COPPER ELECTRODES

2.15 MM SEPARATION IN AIR  
25 AMPS  $\frac{1}{2}$  ATMOSPHERE



## EFFECT OF CURRENT ON DIELECTRIC RECOVERY

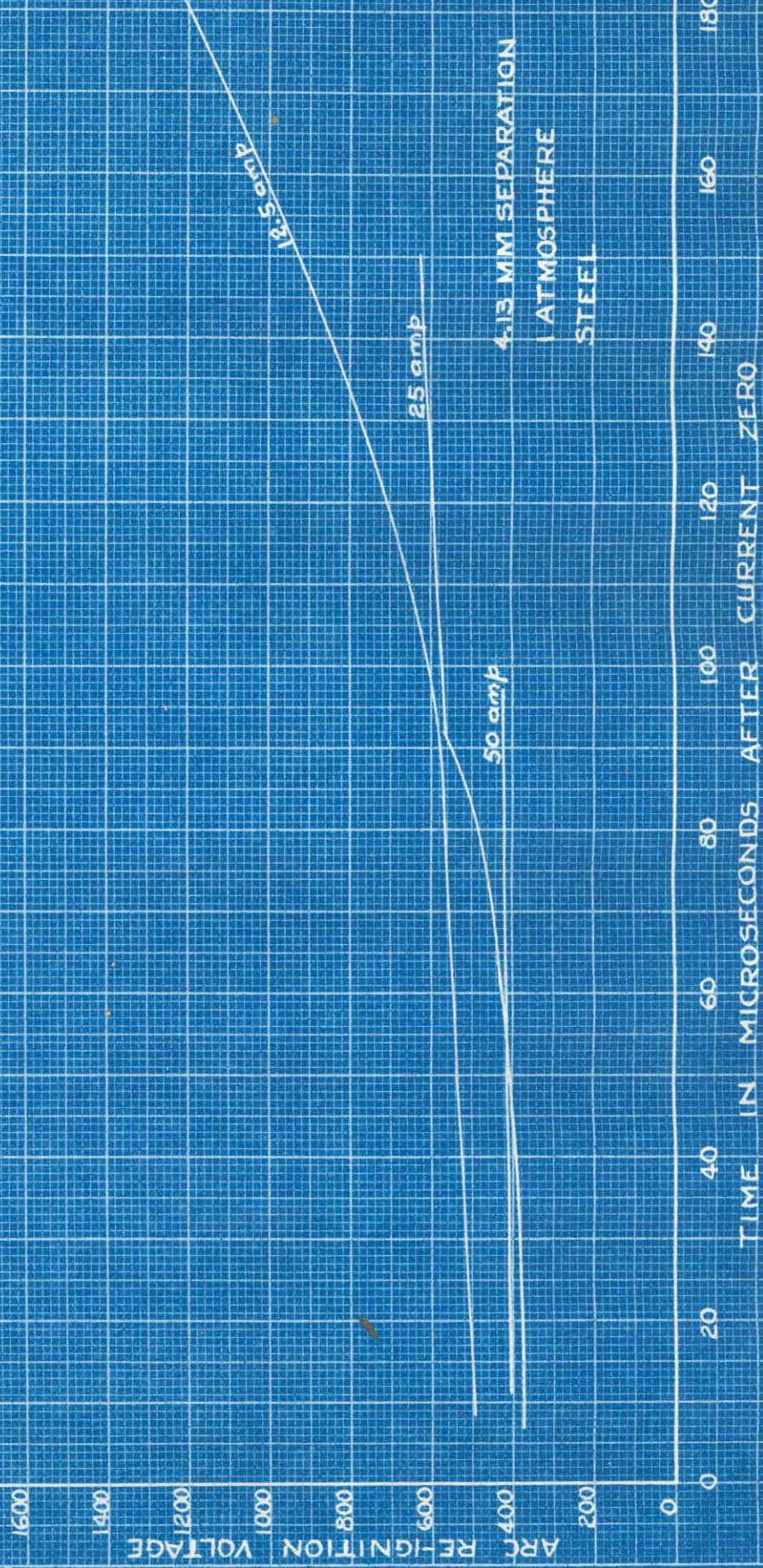


FIG. 40

## EFFECT OF CURRENT ON DIELECTRIC RECOVERY

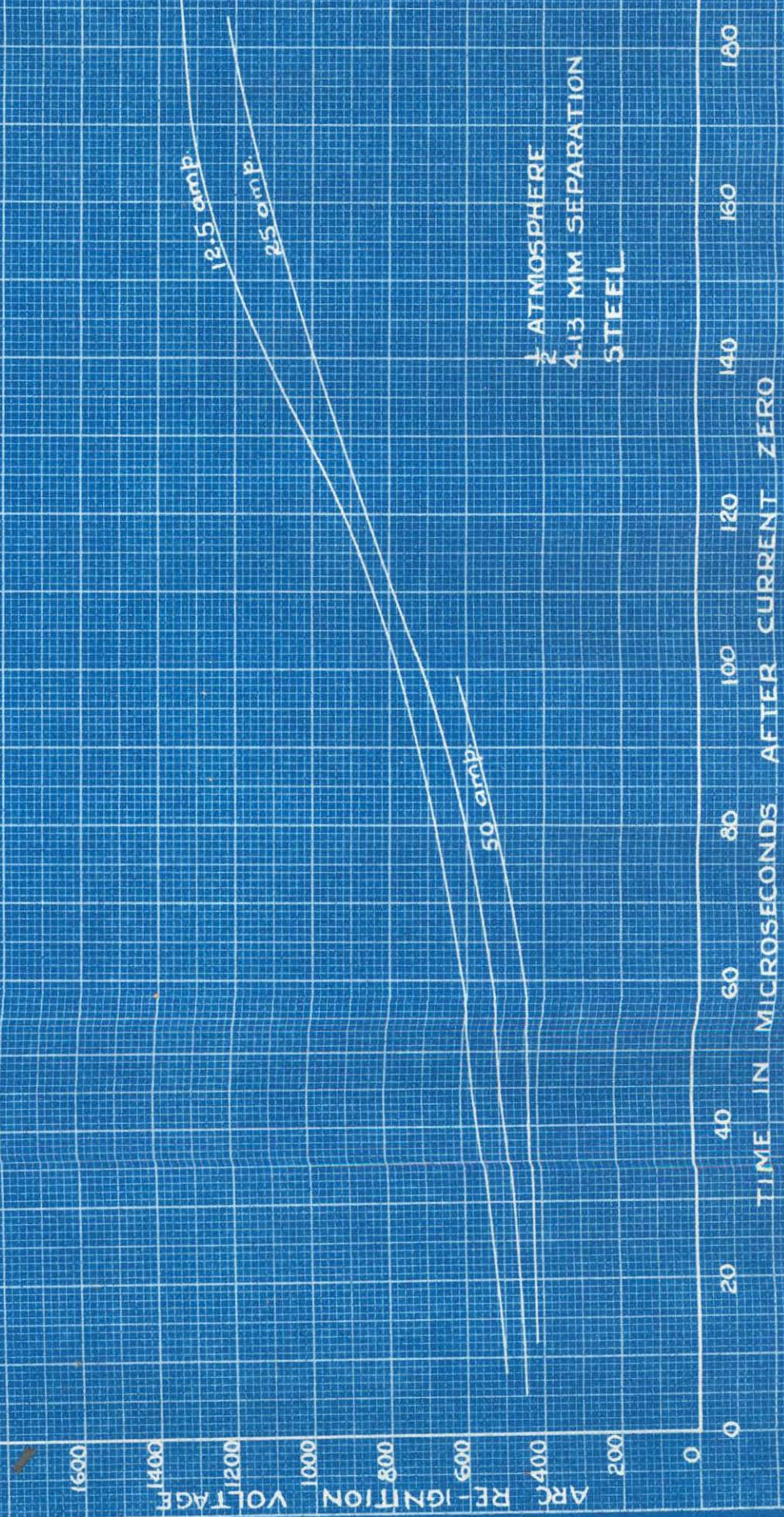


FIG. 41.

## EFFECT OF CURRENT ON DIELECTRIC RECOVERY

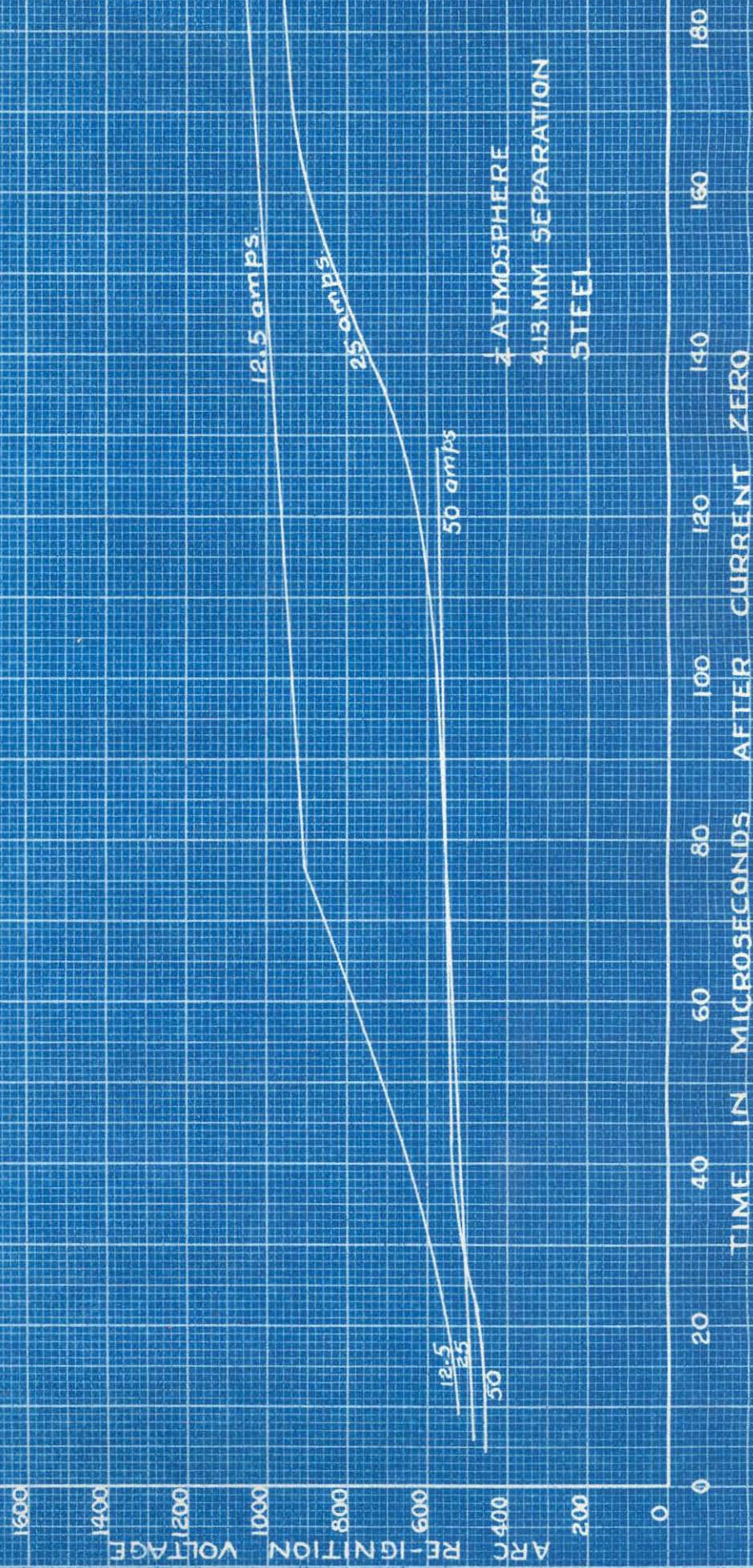


FIG. 42.

## EFFECT OF CURRENT ON ELECTRIC RECOVERY

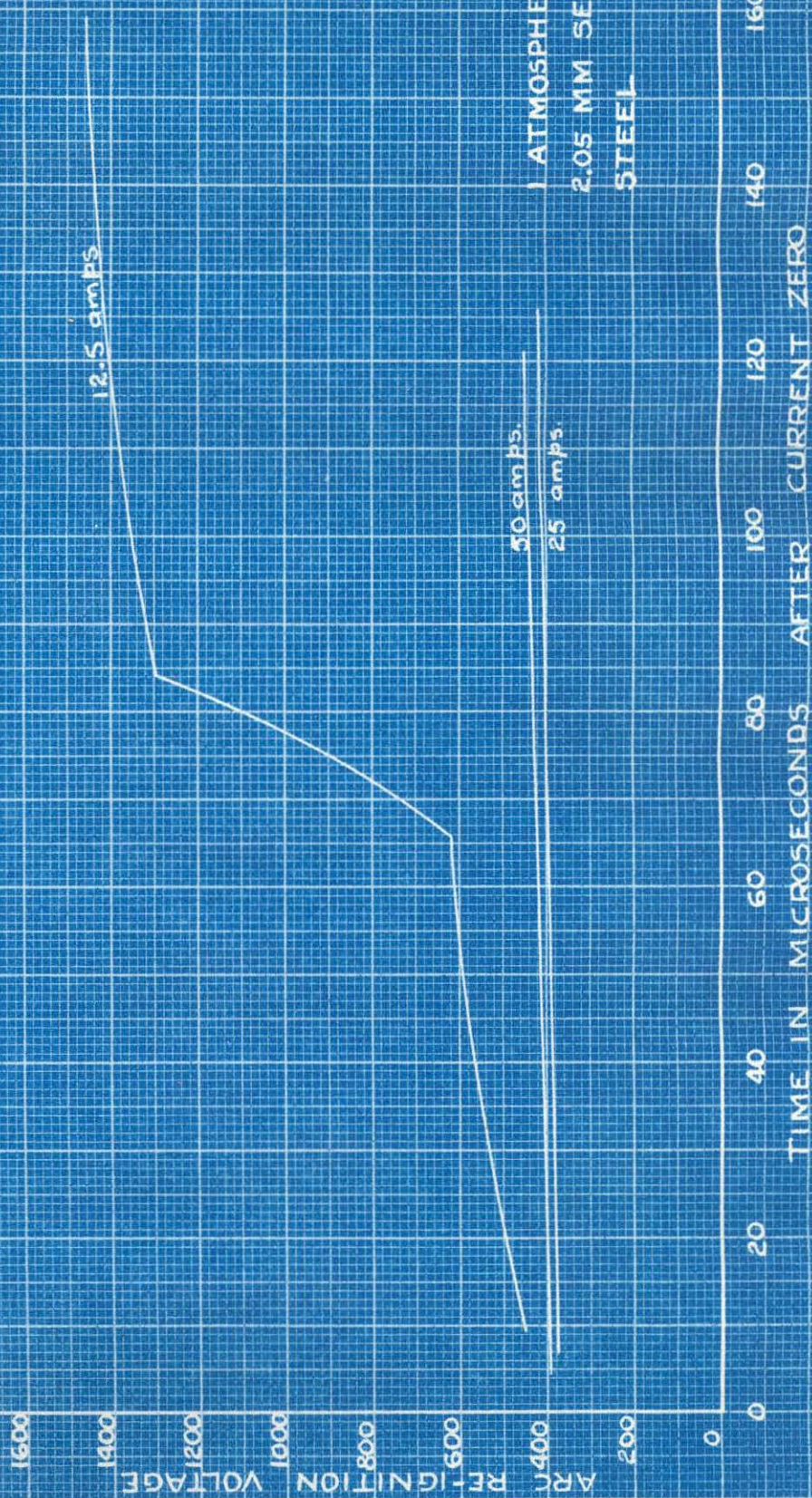


FIG. 43

## B. Steel Electrodes

### 1. Data

Figures 40 through 46 show 27 sets of curves. These curves were made up from 472 readings. As for copper, all combinations of 50, 25, and 12.5 amps; 4.13, 2.05, and 1 mm.; and pressures of 1, 1/2, and 1/4 atmosphere were used. These Figures are divided into three main groups:-

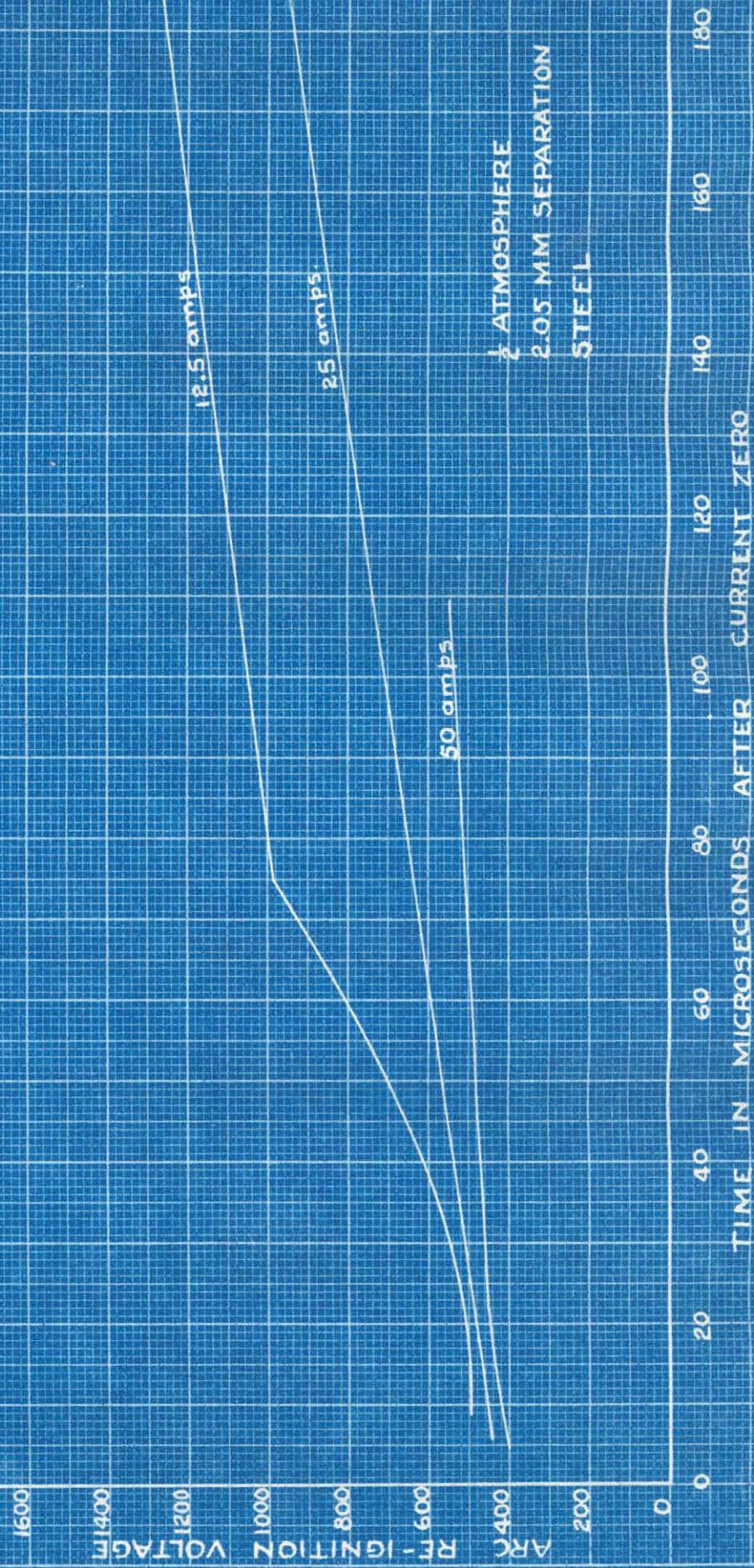
- (1) Figures 40 to 48 show the effect of current on dielectric recovery;
- (2) Figures 49 to 57 show the effect of pressure on dielectric recovery;
- (3) Figures 58 to 66 show the effect of arc length on dielectric recovery.

### 2. Effect of Current - (Steel)

The nine sheets, Figures 40 to 48, show definitely that increasing the current does not have much effect on the initial voltage-time recovery rate but that after a short time, of the order of 30 microseconds, the recovery voltage rises very much more rapidly for the 12.5 amp. arc.

In none of the curves, except perhaps in Figure 41 (1/2 atmos. 4.13 mm.), did complete deionization take place for the 50 amp. arc up to 130 microseconds. All 26 curves, if projected back to cut the zero time axis, show an initial arc reignition voltage

## EFFECT OF CURRENT ON DIELECTRIC RECOVERY



## EFFECT OF CURRENT ON DIELECTRIC RECOVERY

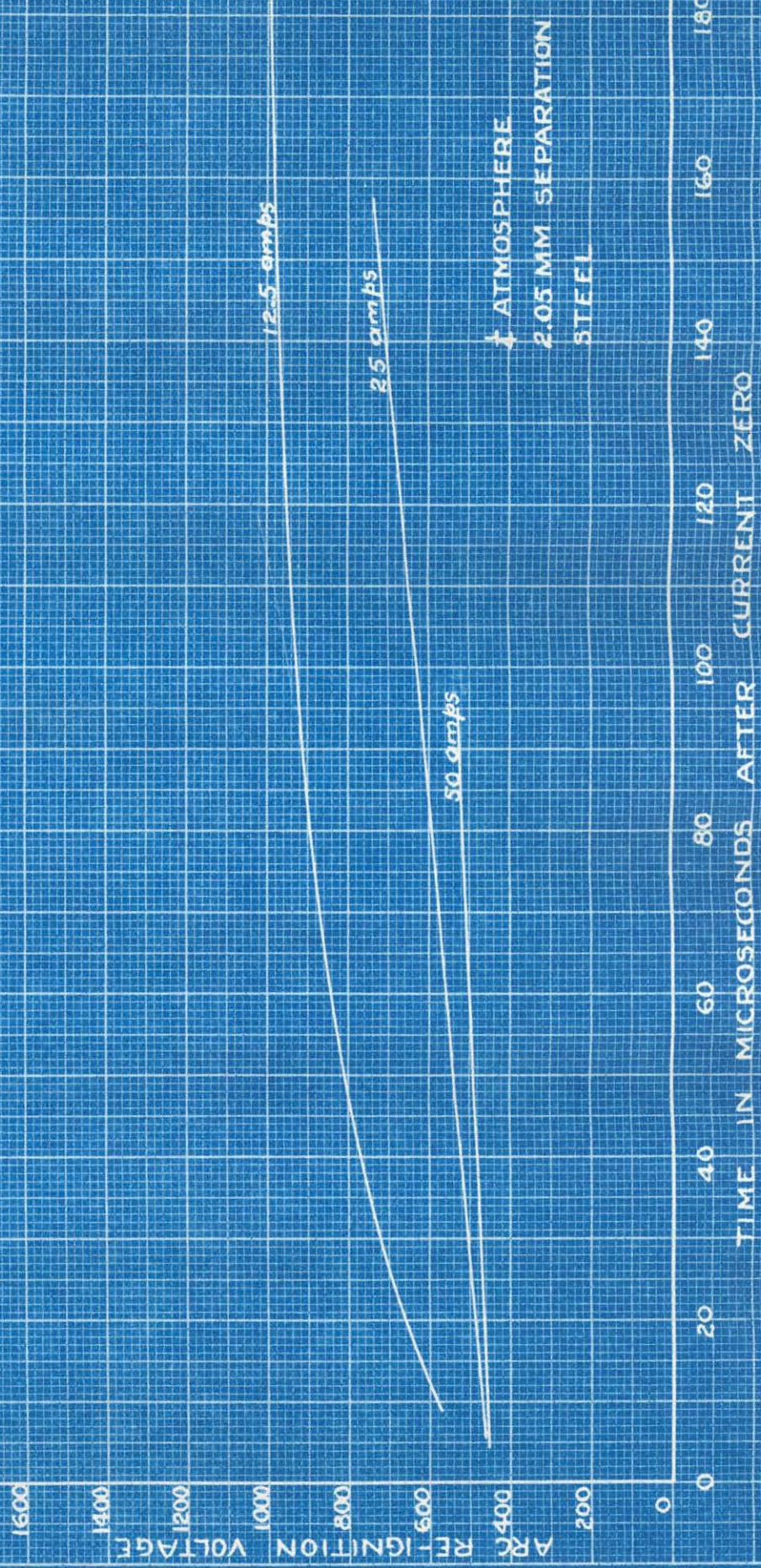
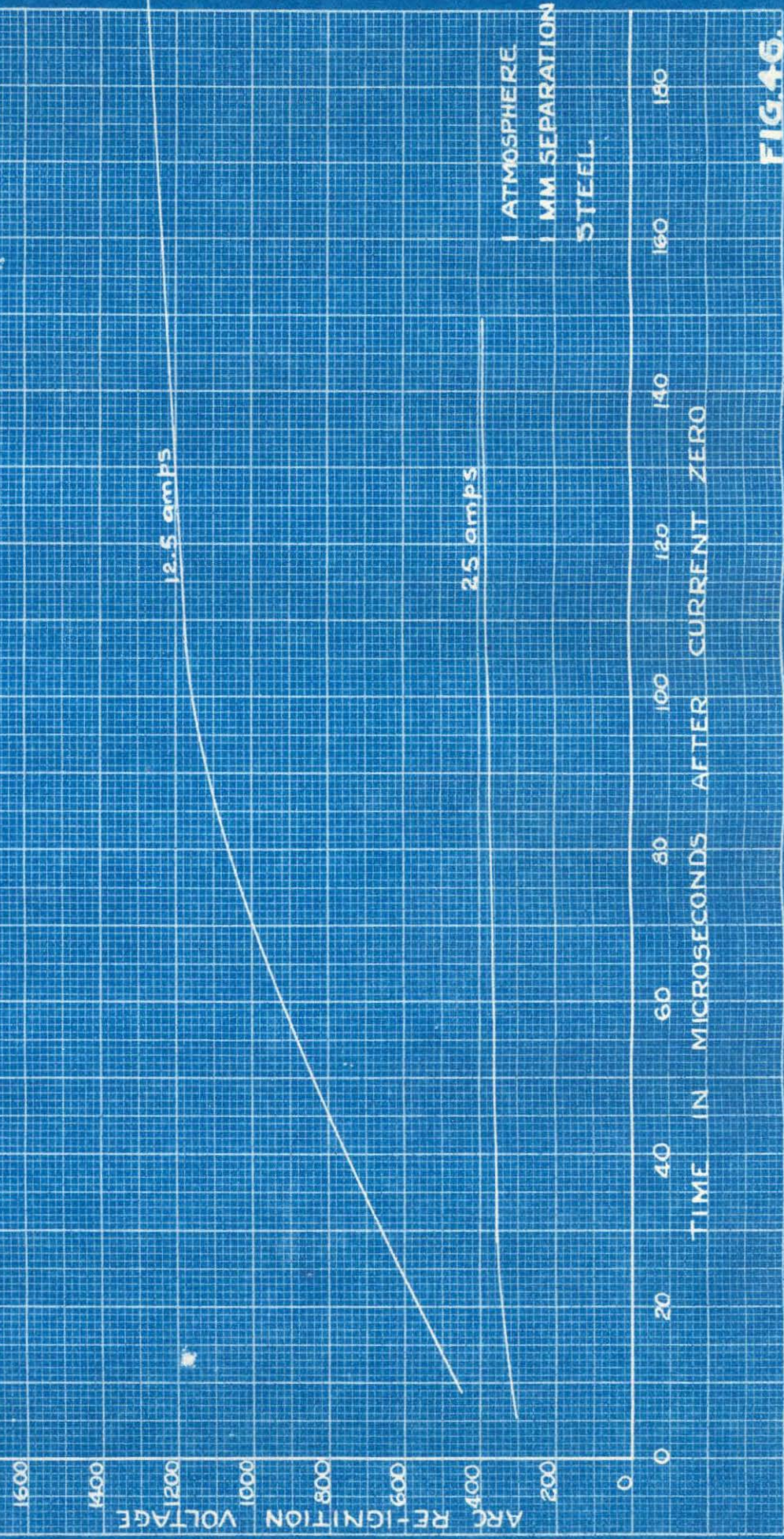


FIG. 45.

## EFFECT OF CURRENT ON DIELECTRIC RECOVERY



between 400 and 500 volts. This value is of the order of the minimum sparking potential for air and undoubtedly represents that value for iron electrodes in air. These variations of voltage with current show definitely that no simple one-dimensional process of cooling or diffusion is adequate to explain recovery rates. However, the observations made for the case of the copper electrodes apply with equal force to this case.

### 3. Effect of Pressure (Steel)

Figures 49 through 57 show the effect of pressure on dielectric recovery for the 50, 25, and 12.5 amp. arc at 4.13, 2.05, and 1.0 mm. separations.

Looking first at Figures 49, 52, and 55 (50 amps.; 4.13, 2.05 and 1.0 mm.), it is seen that the dielectric recovery curves are practically horizontal. The dielectric strength is greater for 1/4 atmos. than for 1/2 or 1 atmos., but the difference is indeed small, being principally the difference existing at earliest restriking. For this case it is true that the initial striking voltage should be slightly higher for the lower pressure, since cooling takes place in the arc space immediately after current zero at a rate depending on the mean free path which is inversely proportional to the pressure. Complete deionization does not occur for any of the 50 amp. curves up to 130 microseconds. It was impossible to obtain points beyond this time, because of the very unstable arc which then existed.

## EFFECT OF CURRENT ON DIELECTRIC RECOVERY

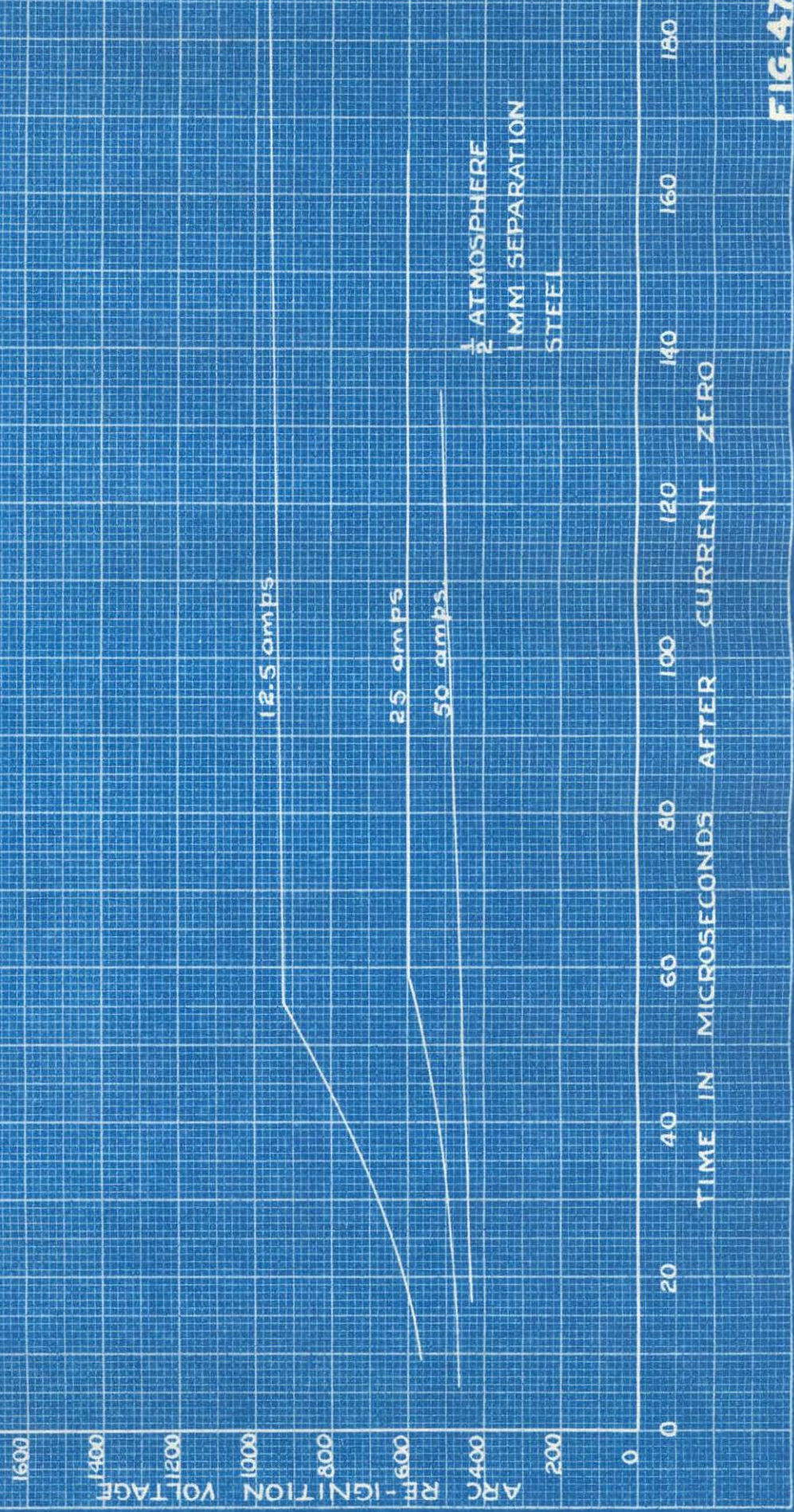


FIG. 47

## EFFECT OF CURRENT ON DIELECTRIC RECOVERY

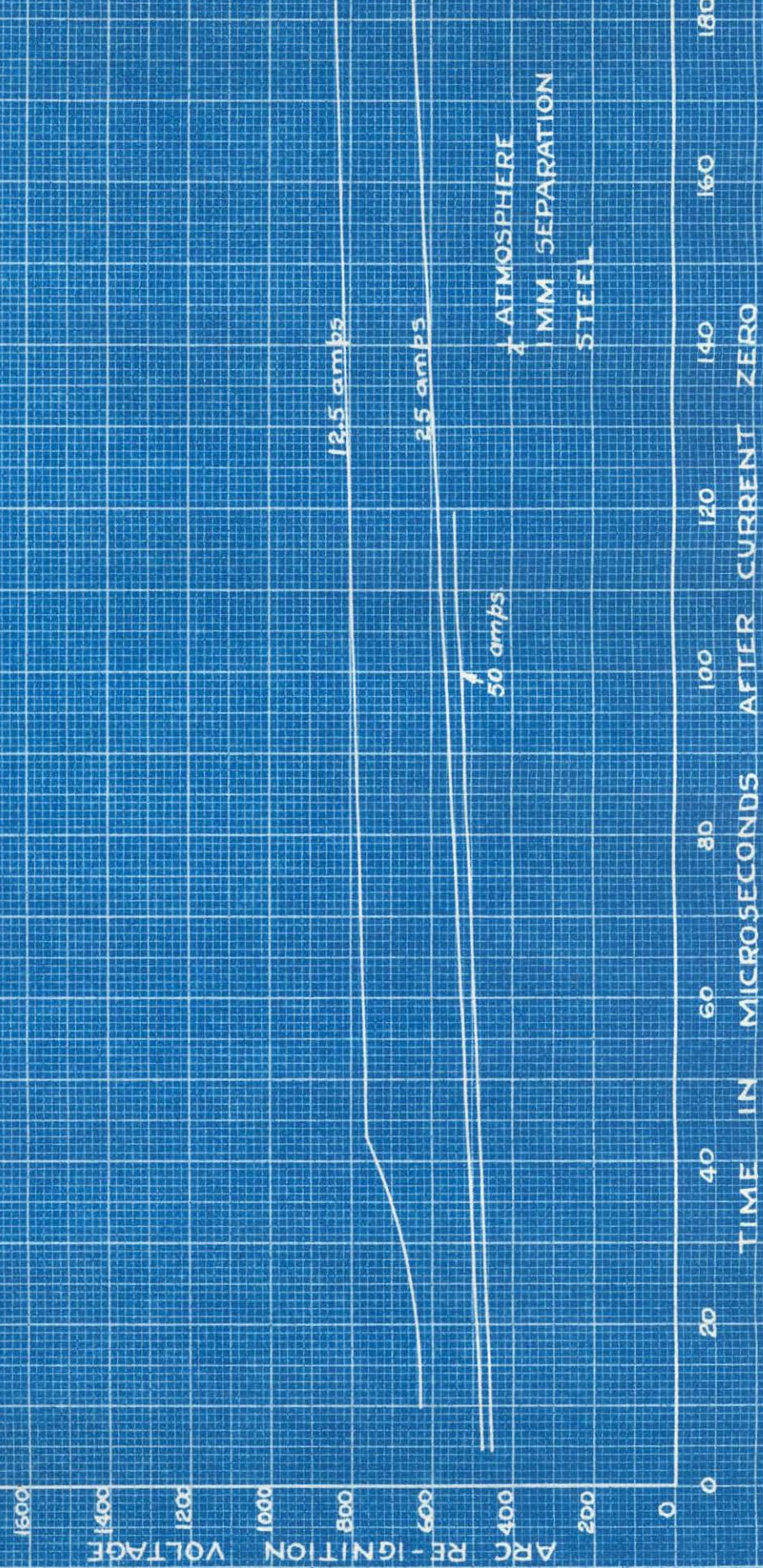


FIG. 48

## EFFECT OF PRESSURE ON ELECTRIC RECOVERY

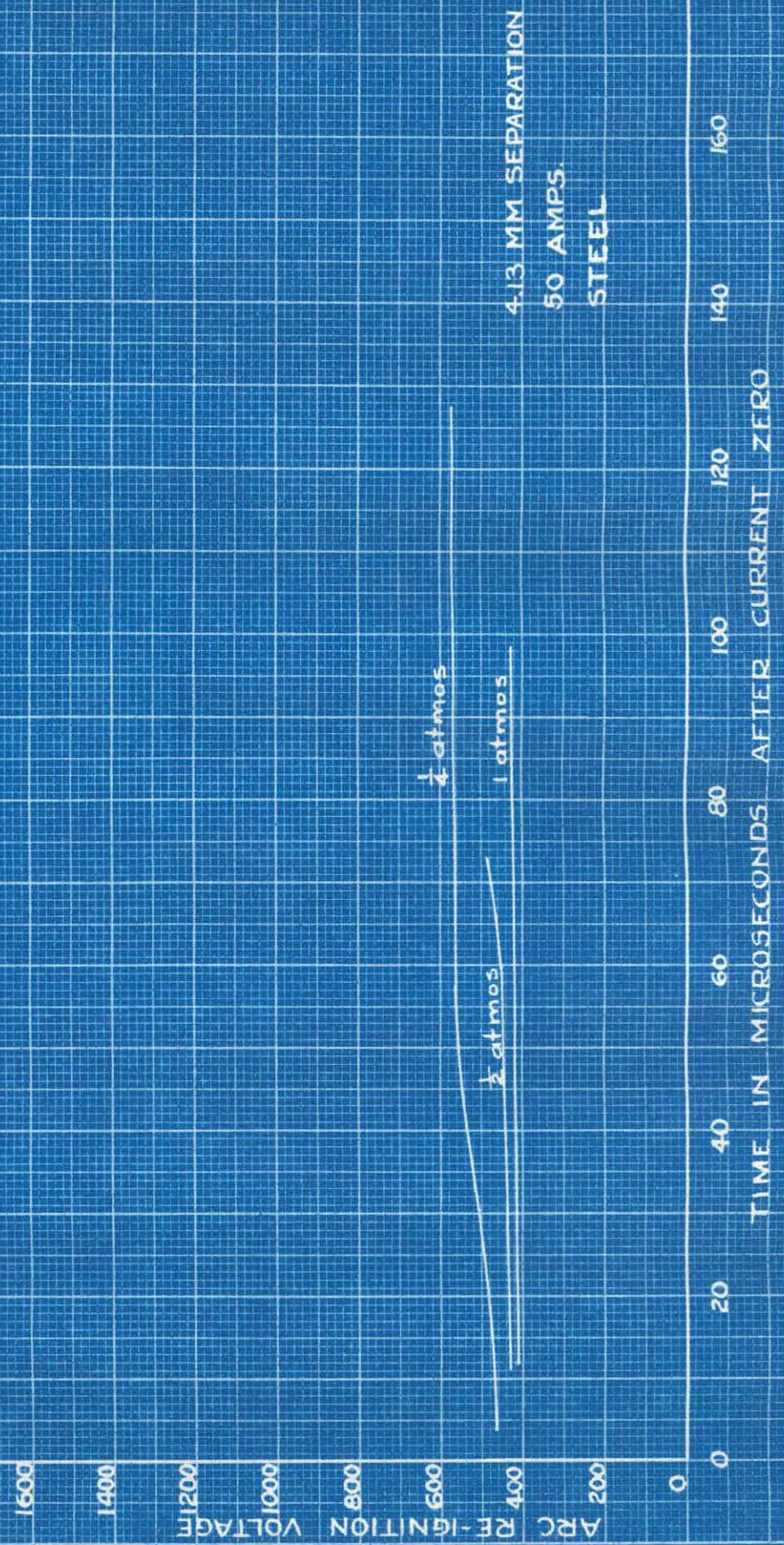


FIG. 4.9.

## EFFECT OF PRESSURE ON DIELECTRIC RECOVERY

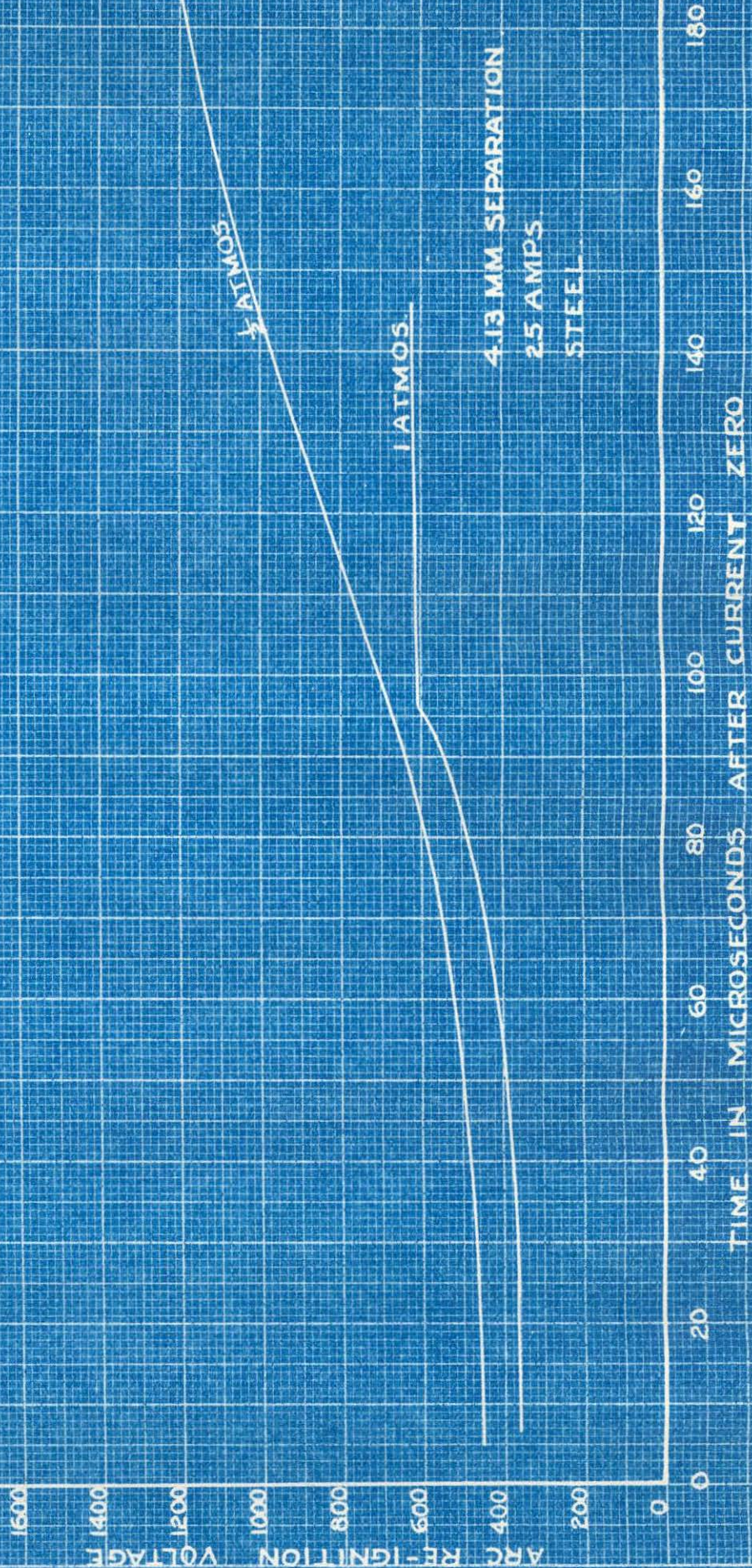
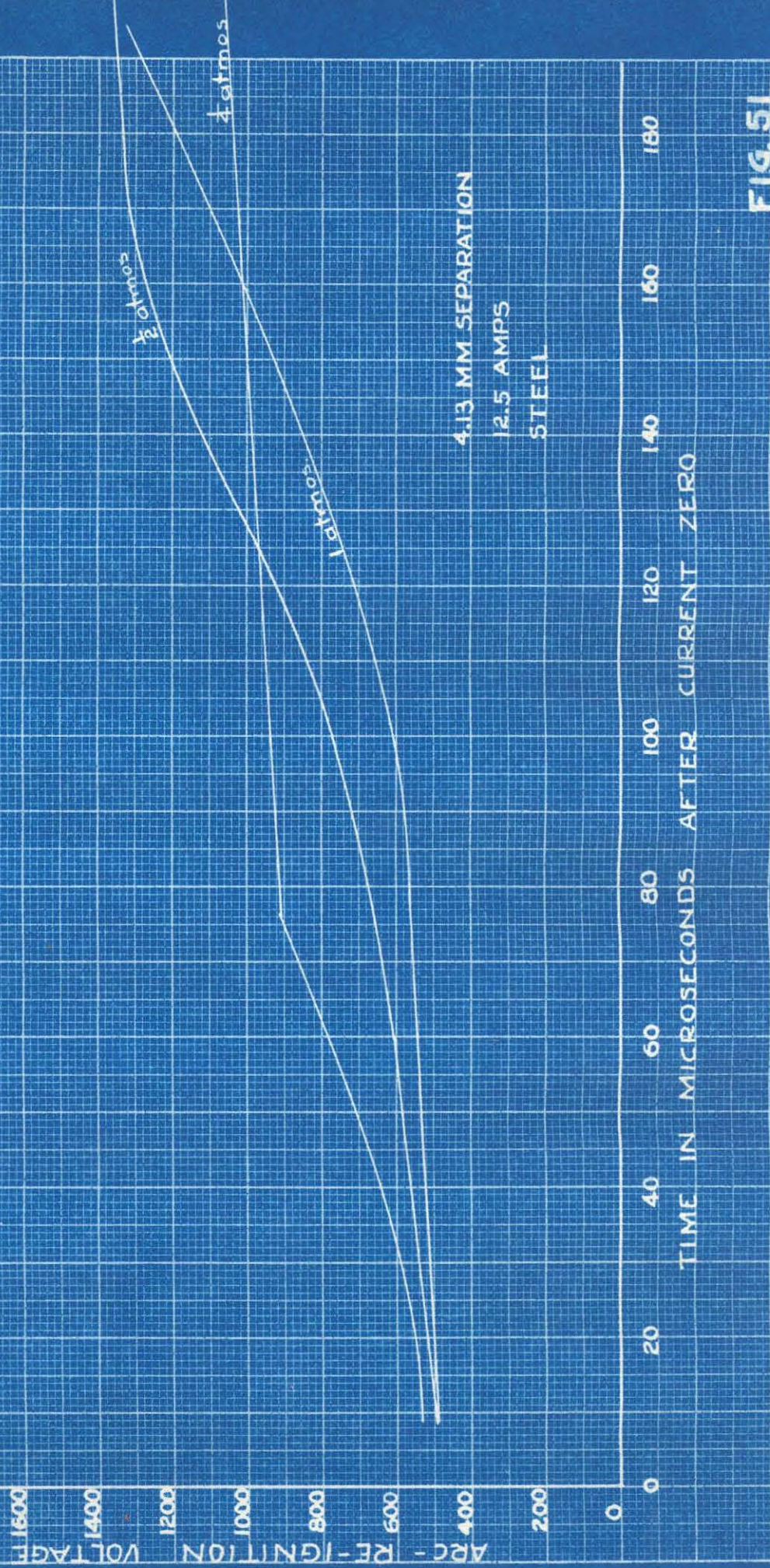


FIG. 50.

### EFFECT OF PRESSURE ON ELECTRIC RECOVERY



EFFECT OF PRESSURE ON DIELECTRIC RECOVERY

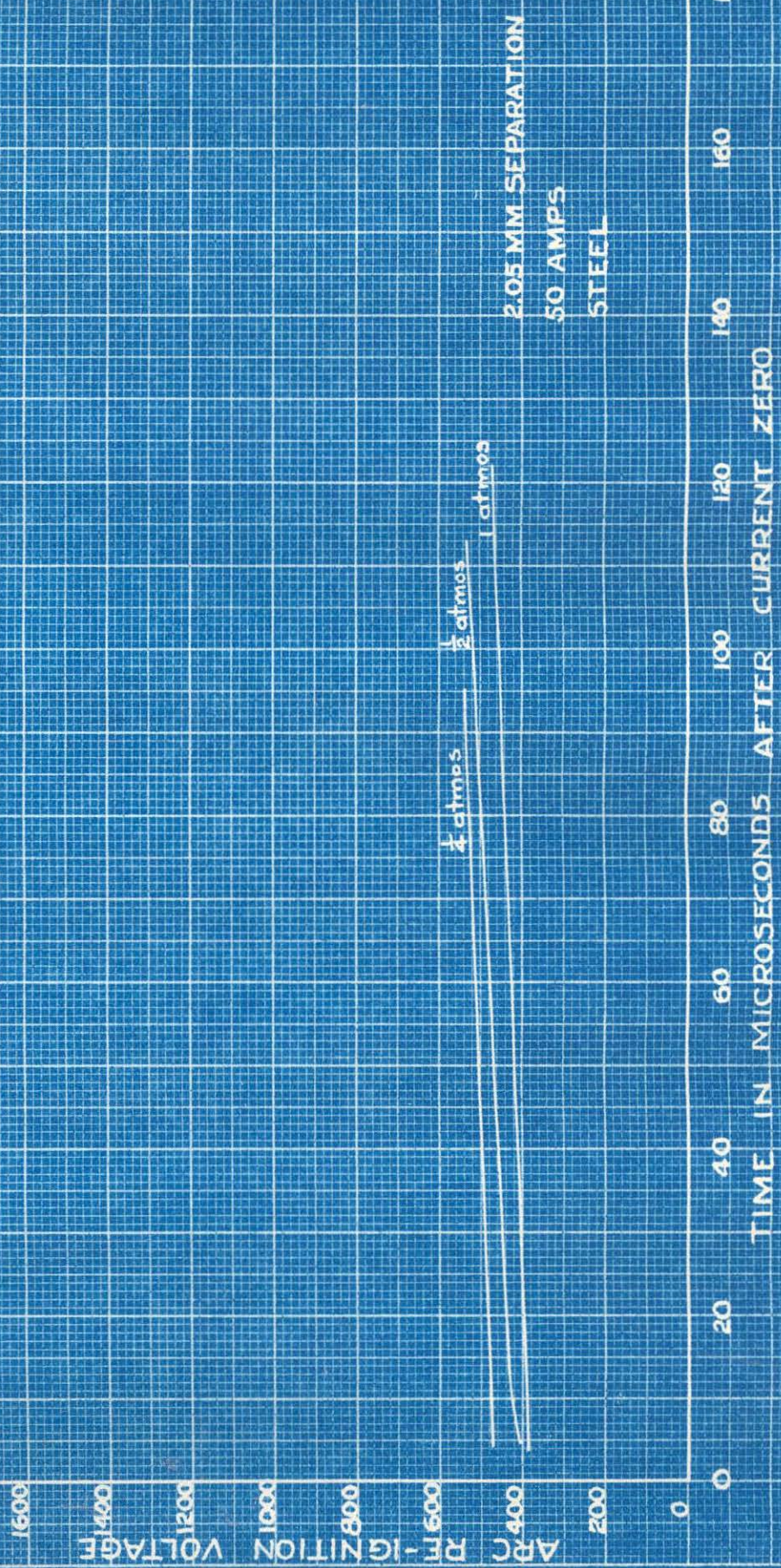


FIG. 52.

# EFFECT OF PRESSURE ON DIELECTRIC RECOVERY

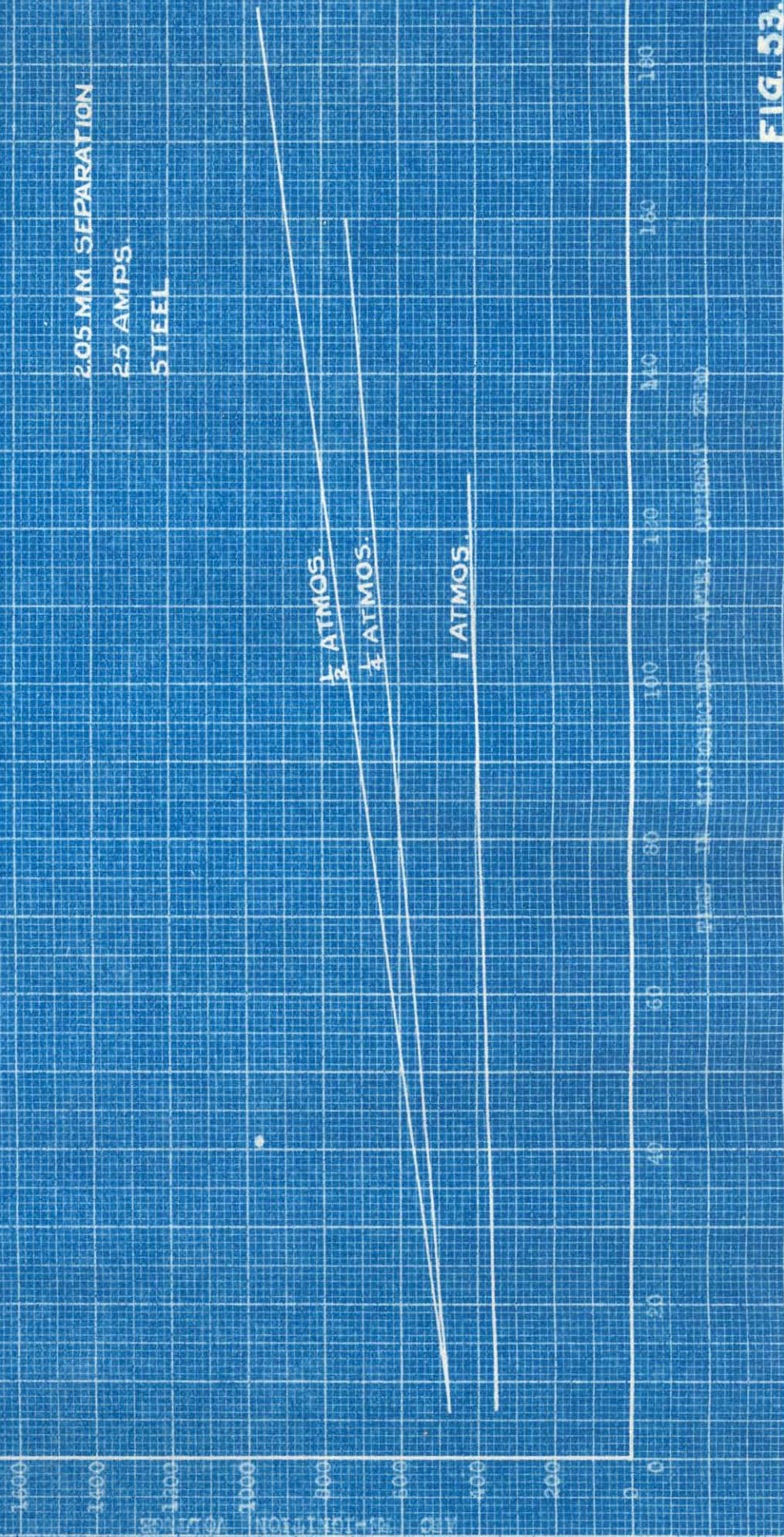


FIG. 53.

EFFECT OF PRESSURE ON DIELECTRIC RECOVERY

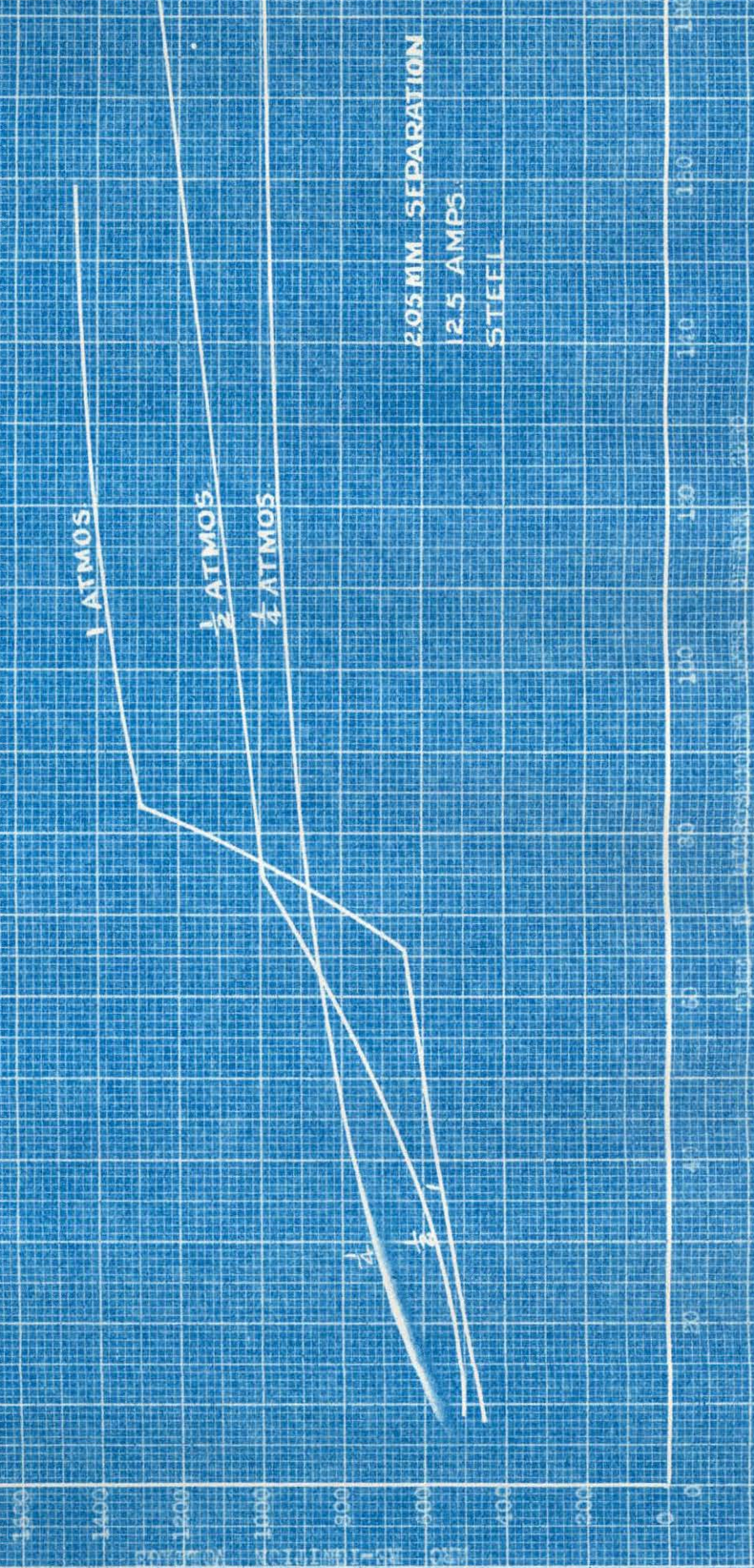


FIG. 54.

## EFFECT OF PRESSURE ON DIELECTRIC RECOVERY

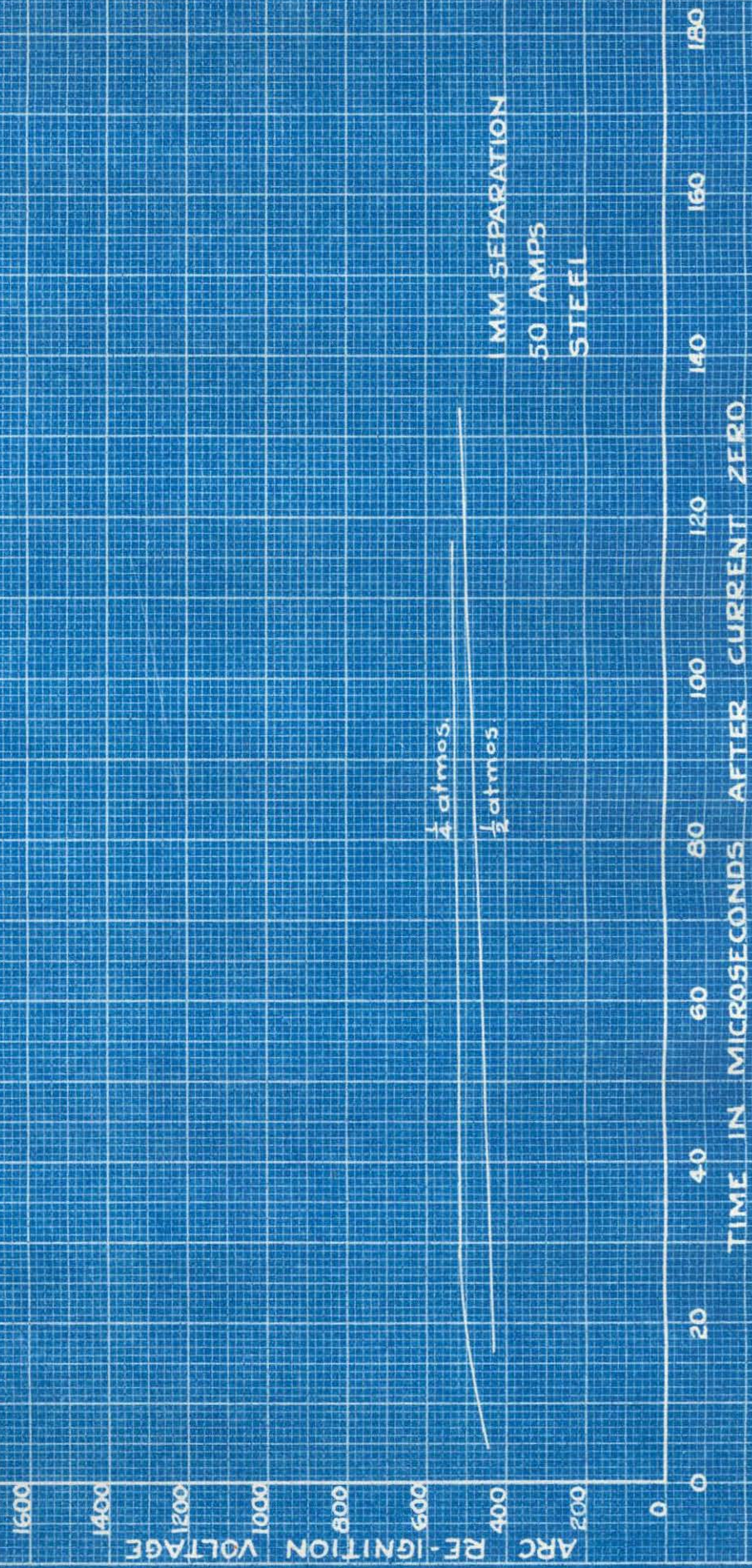


FIG. 55.

## EFFECT OF PRESSURE ON DIELECTRIC RECOVERY

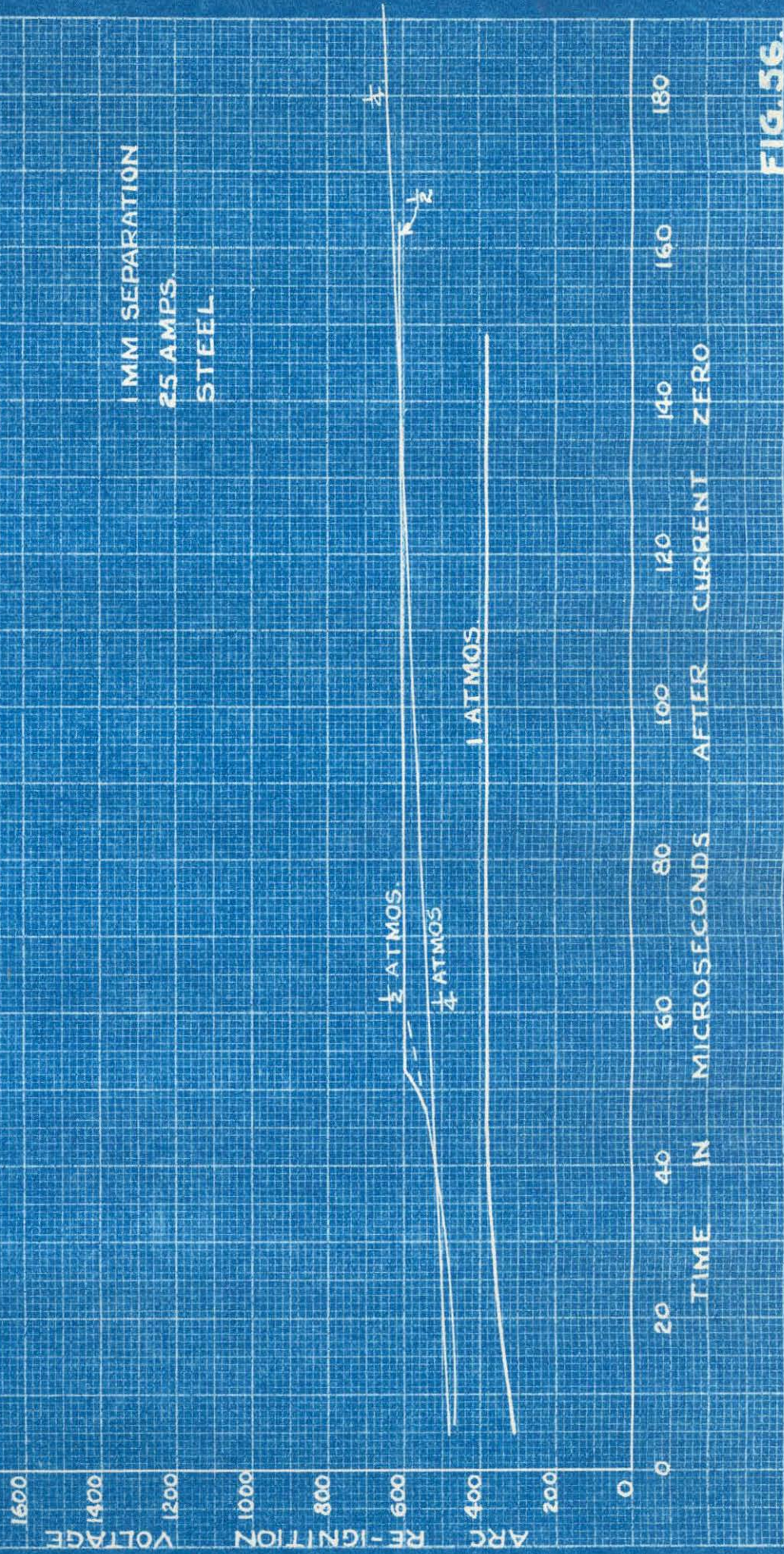


FIG. 56

## EFFECT OF PRESSURE ON DIELECTRIC RECOVERY

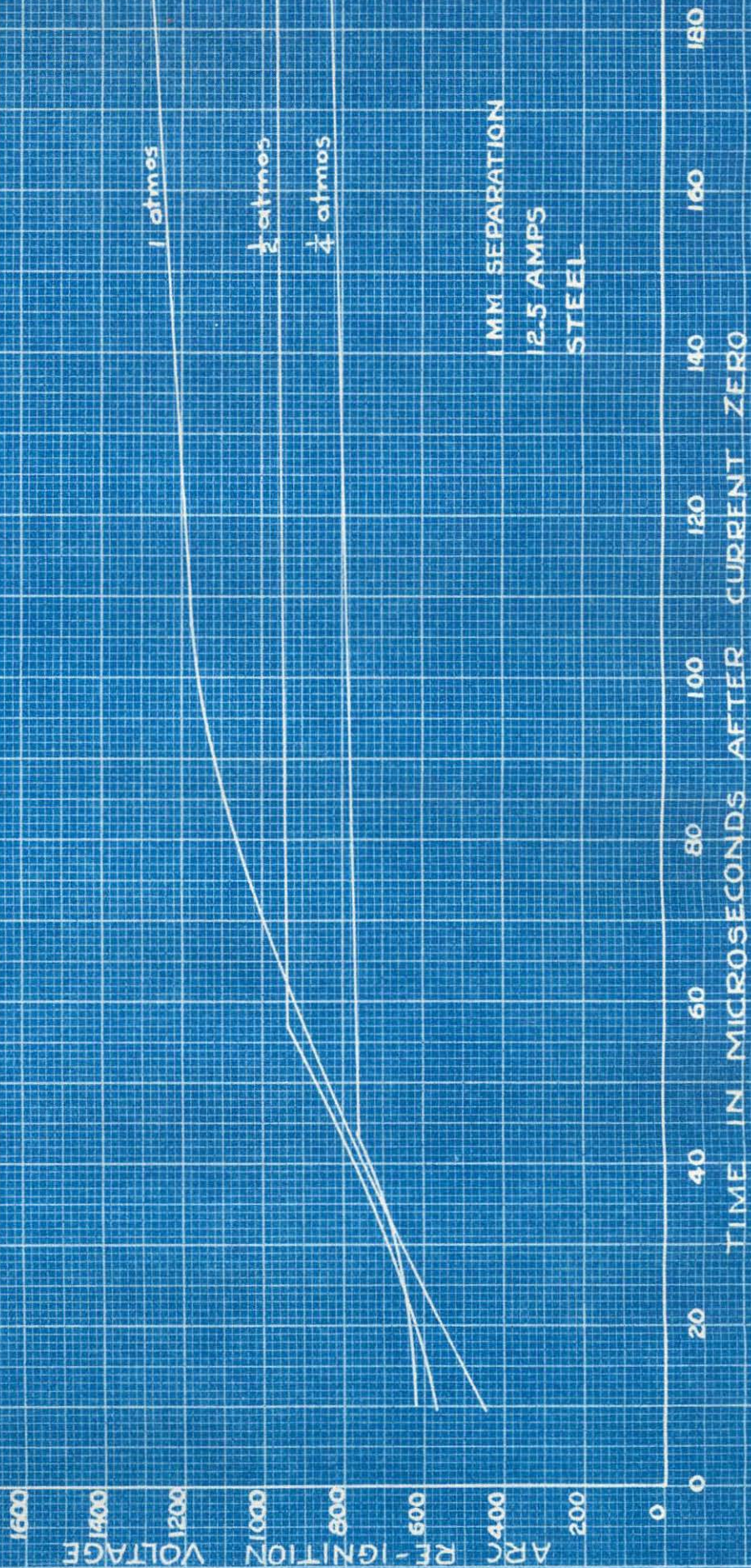


FIG. 57

Proceeding now to a consideration of Figures 50, 53, and 56 (25 amps.; 4.13, 2.05 and 1 mm.), we find that the 4.13 mm. arc shows complete deionization at about 80 microseconds. The 2.05 mm. gap shows a somewhat greater gain in dielectric strength for the 1/2 atmos. case, deionization appearing to take place very quickly. For 1 atmos. pressure, however, as for 50 amps., deionization is not completed in 130 microseconds. The minimum breakdown voltage, which we should expect to be independent of current, is very nearly the same for 50 as for 25 amps..

Figures 51, 54, and 57, showing the effect of 12.5 amps. at the various spacings, give results which are very similar in form to those obtained for copper. After deionization takes place, the dielectric strength of the air space should be directly proportional to the density; i.e., to the pressure; the temperature being assumed constant for all pressures. A significant fact to note is that for the 12.5 amp. arcs the initial breakdown voltage is about 100 volts higher on the average for similar spacings than that existing for the 50 or 25 amp. case. This lends weight to the theory that the air is partially replaced by vapor from the electrode material, which has a much lower recombination rate, thus lowering the initial breakdown voltage. The 50 amperage arc would, of course, produce a much greater evolution of vapor than an arc one-quarter its magnitude.

#### 4. Effect of Arc Length - (Steel)

Figures 58 to 66 show the effect of arc length on reignition voltage versus time. Figures 58, 61, and 64, (at 50 amps., and 1, 1/2 and 1/4 atmos.), show that arc length has very little effect for this value of current either on initial restriking voltage or subsequent rate of rise which is very slow. As is expected, for later times the longer arcs show slightly higher breakdown strengths.

Examining the curves for 25 and 12.5 amps., the same type of voltage recovery takes place as was discussed for the copper electrodes. Here again we find that the short arc lengths have a higher dielectric strength for short times after current zero than do the longer arcs. This is clearly shown in Figures 60, 61, 62, 63, 64, and 66. Again a preferred arc length exists somewhere between 1 mm. and 2.05 mm. for the 12.5 amp. case at which short-time reignition voltage is a maximum. Again there is a remarkable similarity between Browne's Figure 40 for brass, Figure 60 for steel, and Figure 31 for copper. These curves show conclusively that the dielectric strength of short arcs is independent of boiling point.

#### C. Results - General

Although it is not the purpose of this thesis to correlate data obtained with that found for brass, still results are so analogous, especially for the case of copper electrodes, that

## EFFECT OF ARC LENGTH ON DIELECTRIC RECOVERY

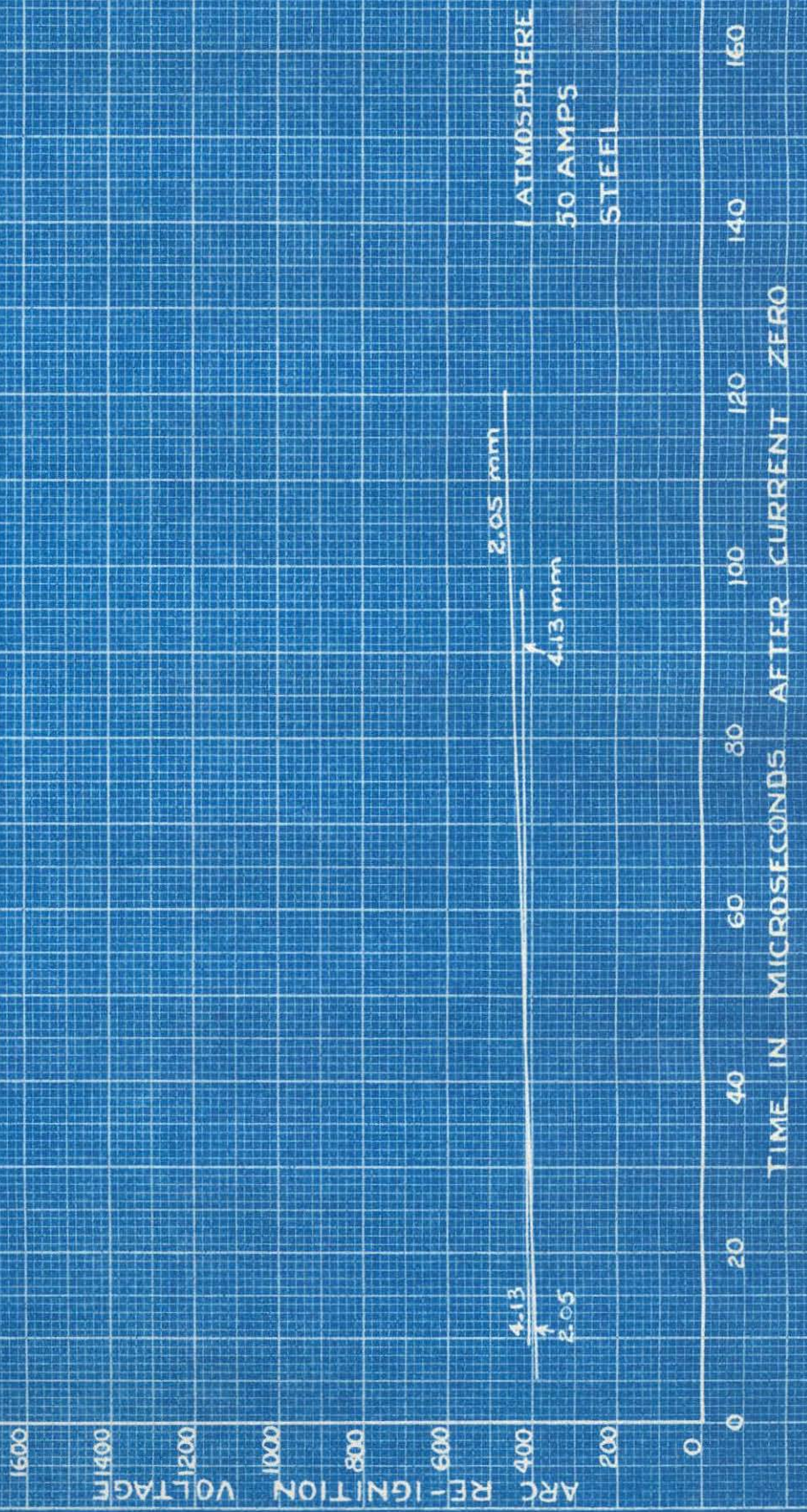


FIG. 58

EFFECT OF ARC LENGTH ON DIELECTRIC RECOVERY

ATMOSPHERE

25 AMPS

STEEL

4.13 mm.

2.05 mm.

1 mm.

TIME IN MILLIONTHS OF A SECOND

100 120 140 160 180

0

20

40

60

80

100

120

FIG. 59.

## EFFECT OF ARC LENGTH ON ELECTRIC RECOVERY

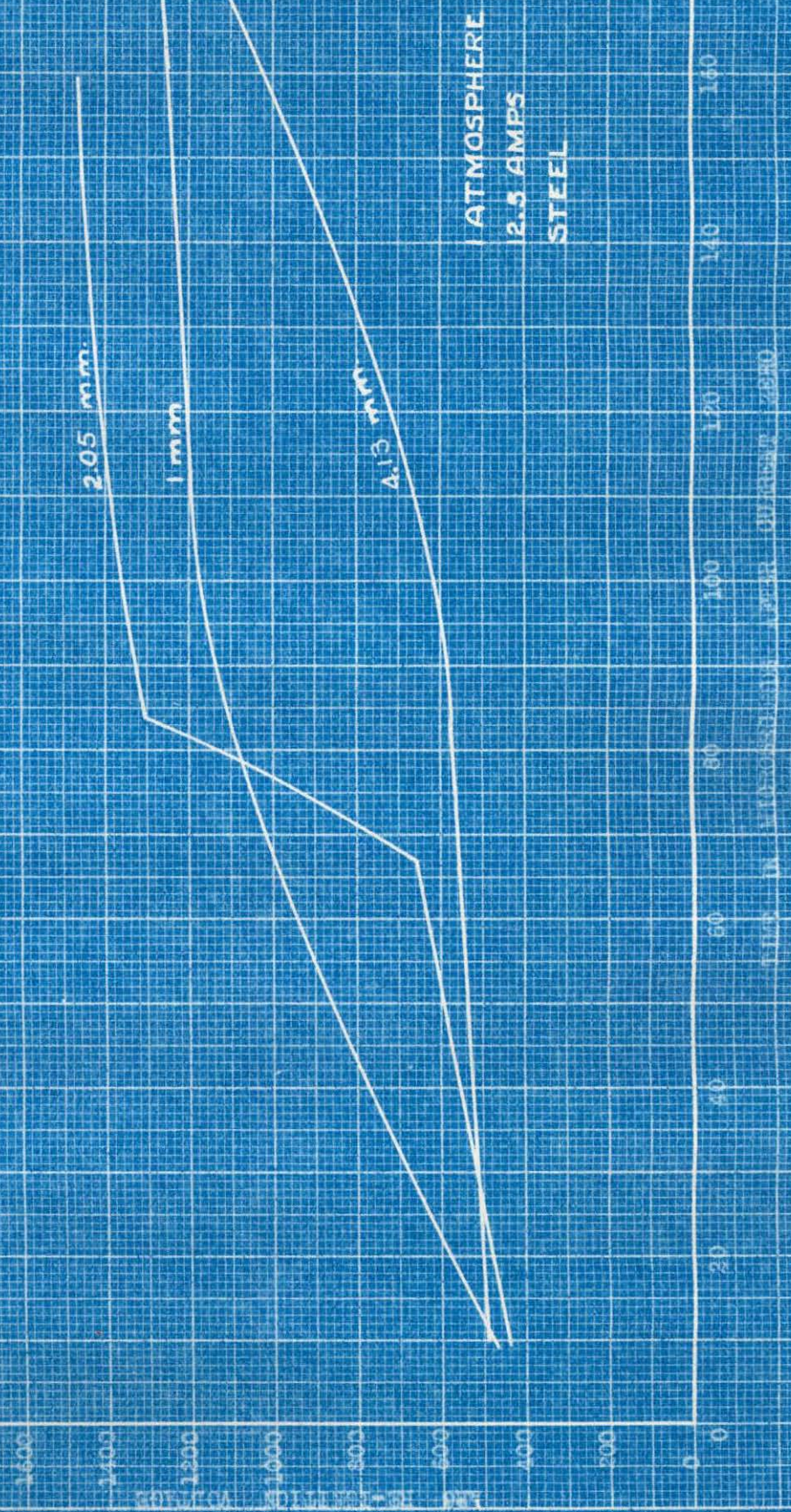


FIG. 60

EFFECT OF ARC LENGTH ON DIELECTRIC RECOVERY

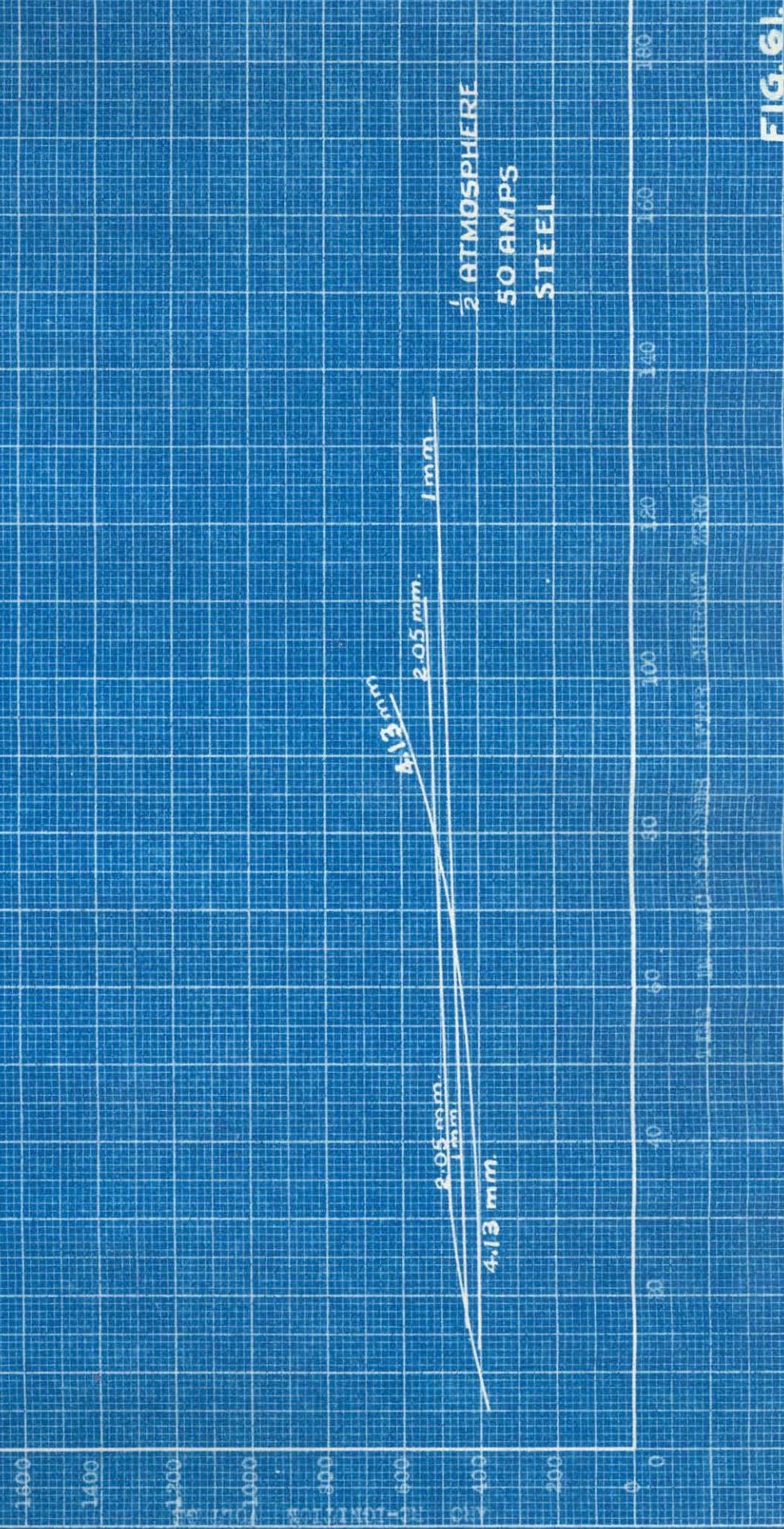


FIG. 6.

## EFFECT OF ARC LENGTH ON DIELECTRIC RECOVERY

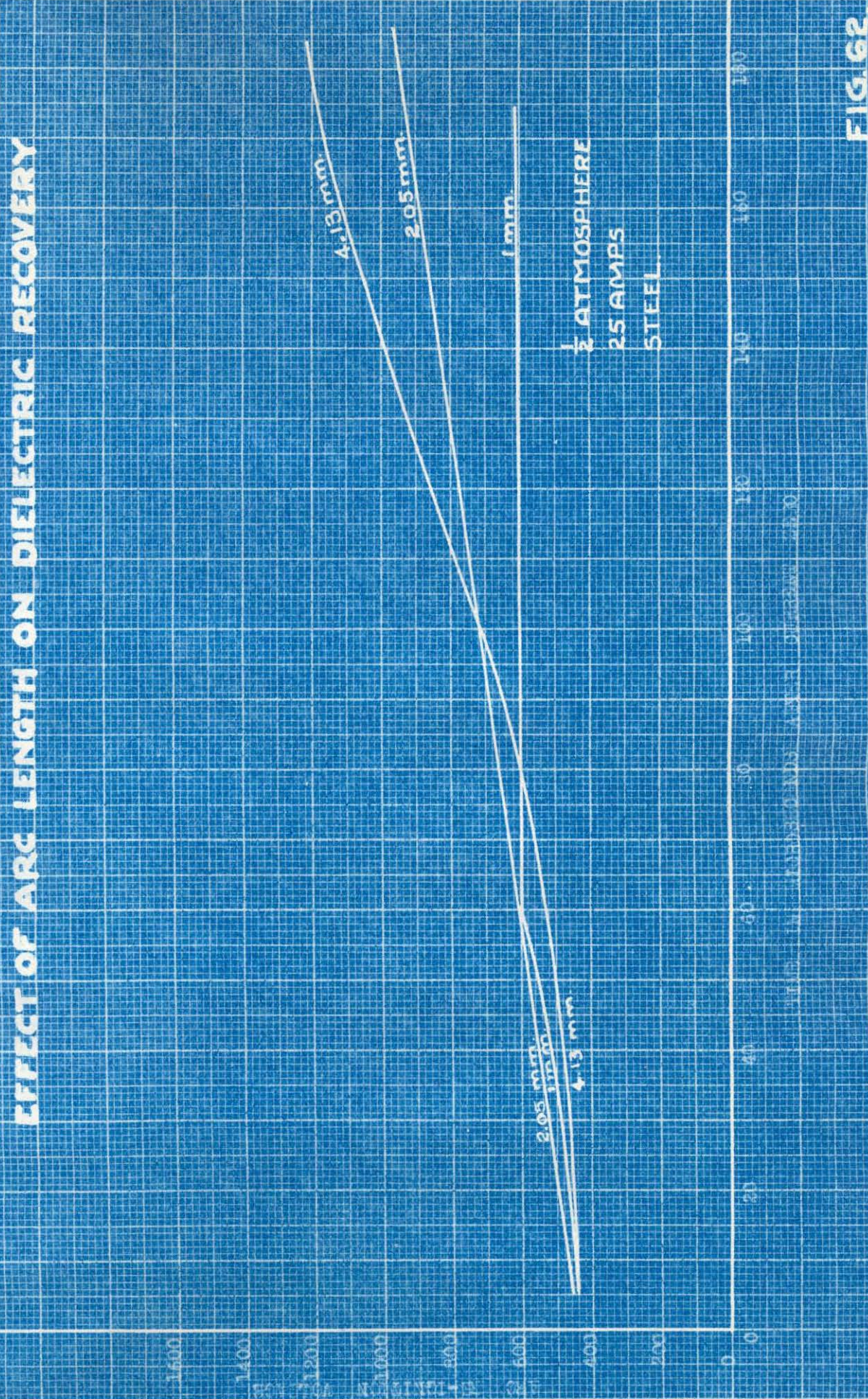


FIG. 62

# EFFECT OF ARC LENGTH ON DIELECTRIC RECOVERY

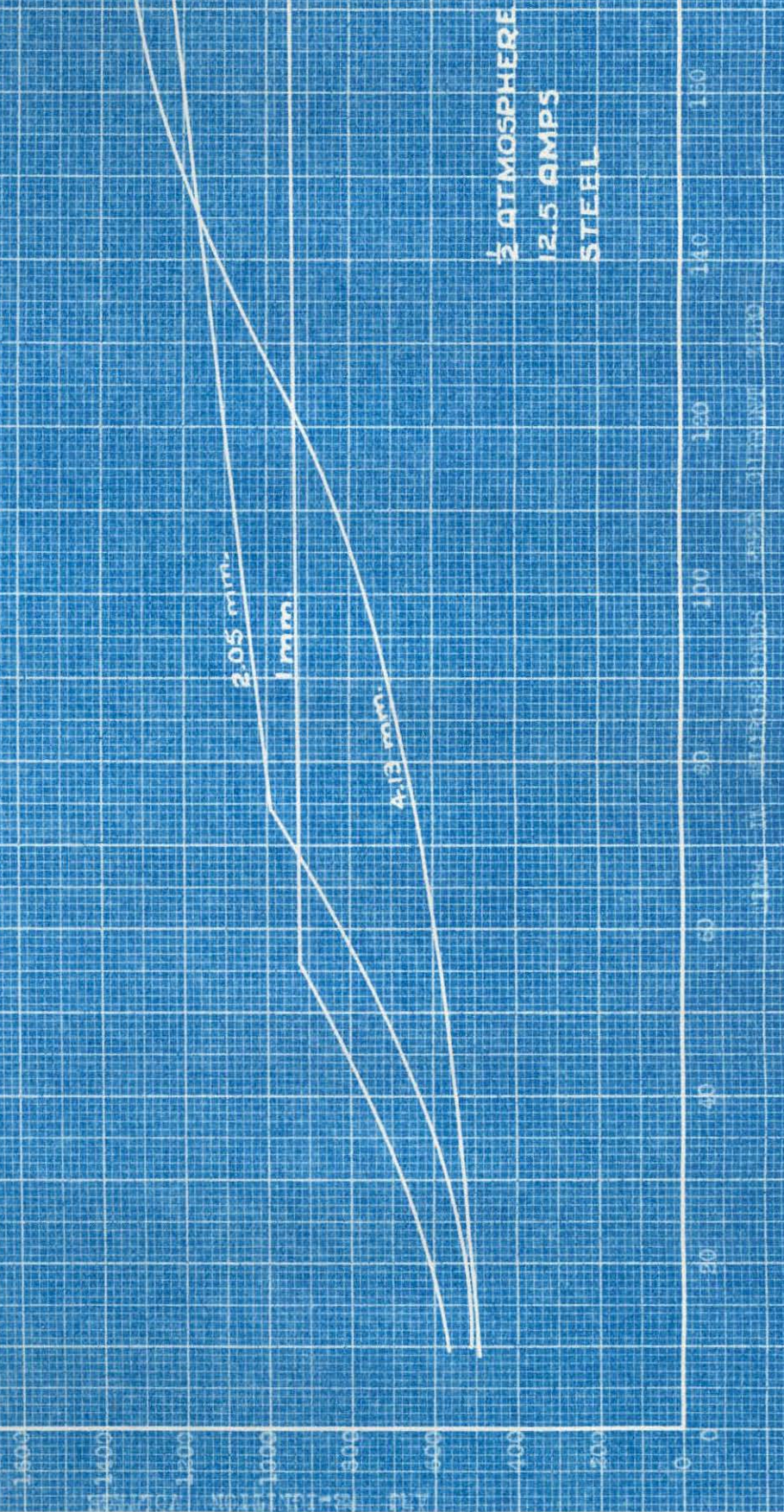


FIG. 63.

## EFFECT OF ARC LENGTH ON DIELECTRIC RECOVERY

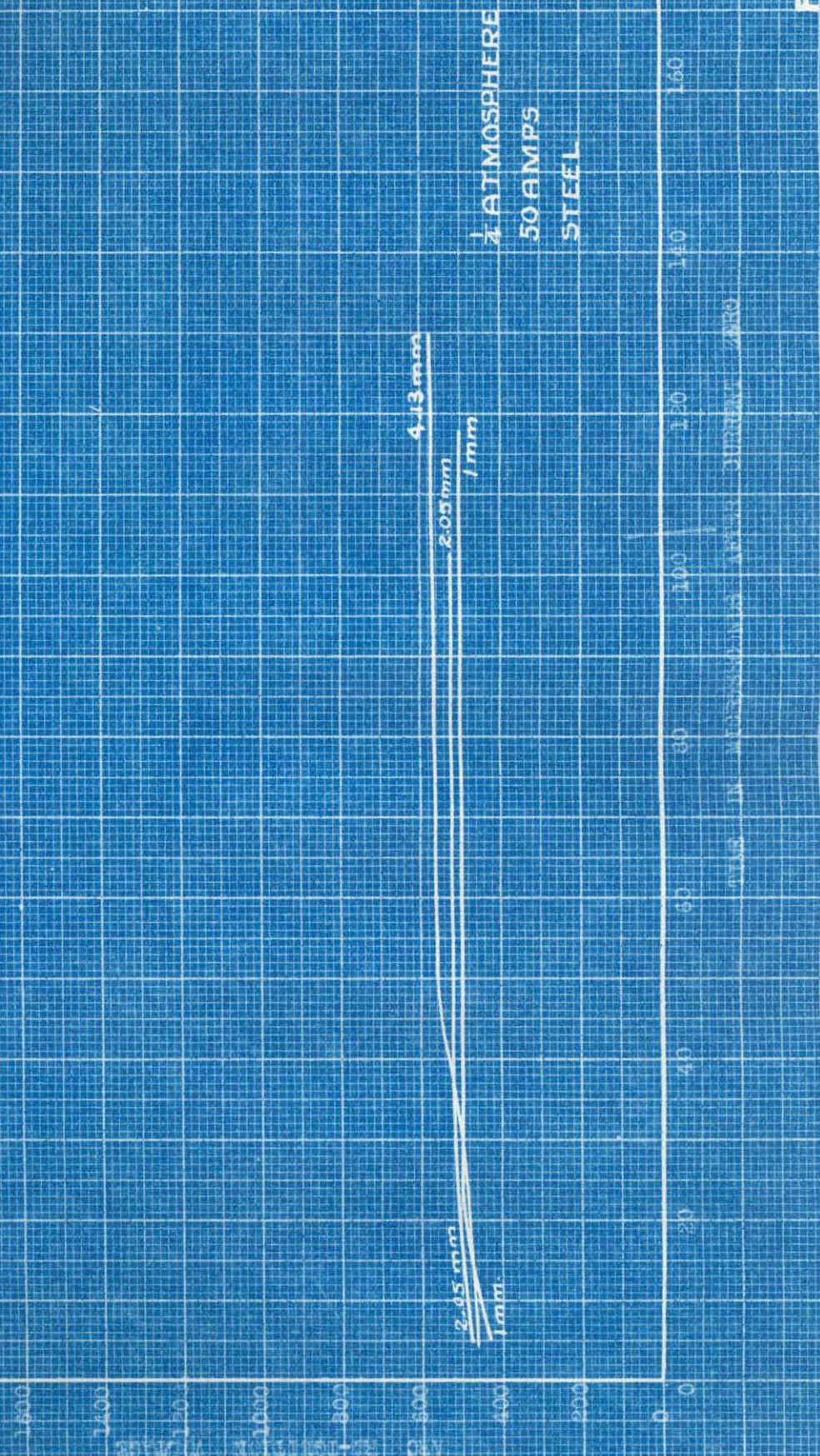


FIG. 64.

# EFFECT OF ARC LENGTH ON DIELECTRIC RECOVERY

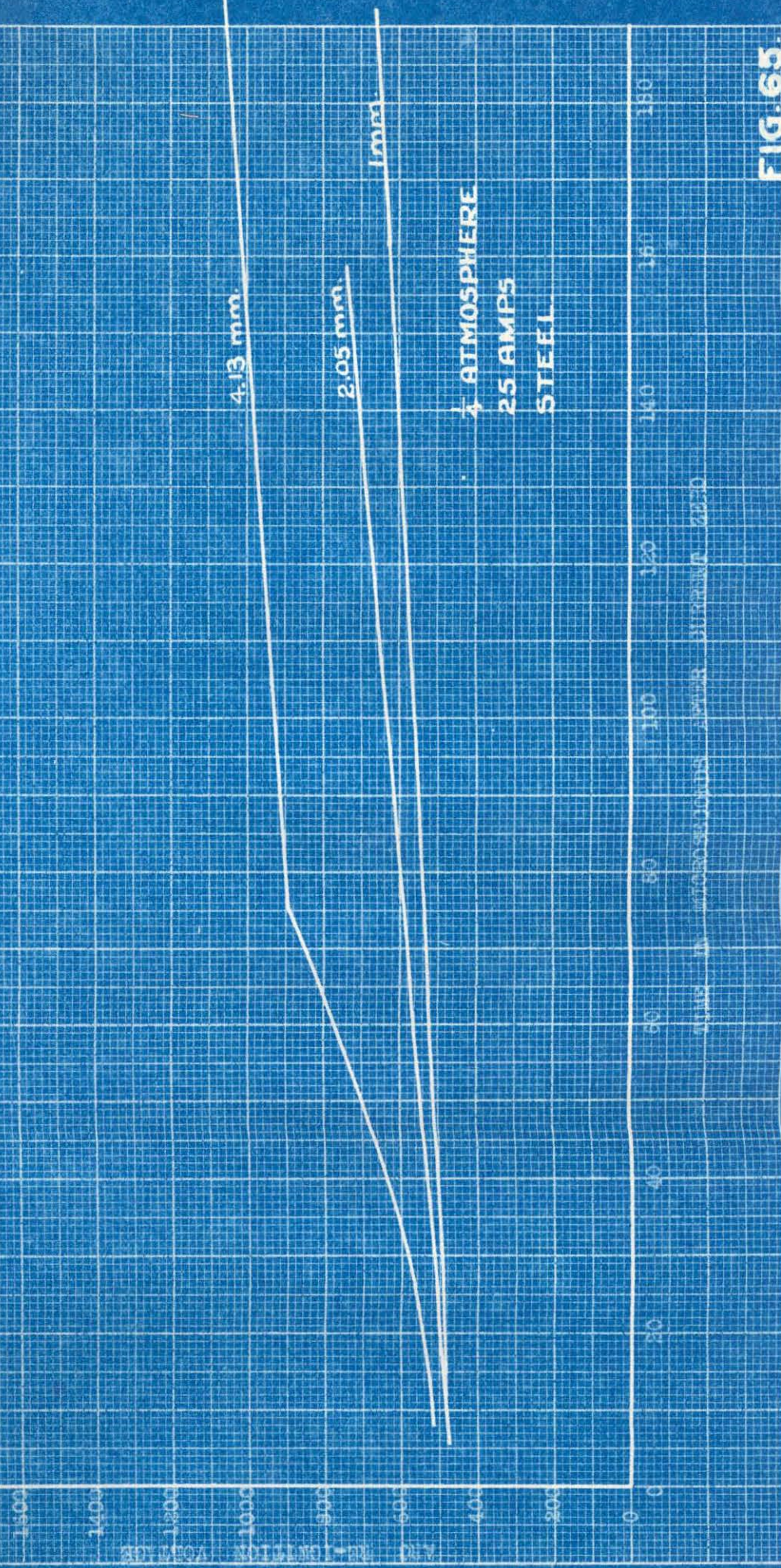


FIG. 65.

EFFECT OF ARC LENGTH ON DIELECTRIC RECOVERY

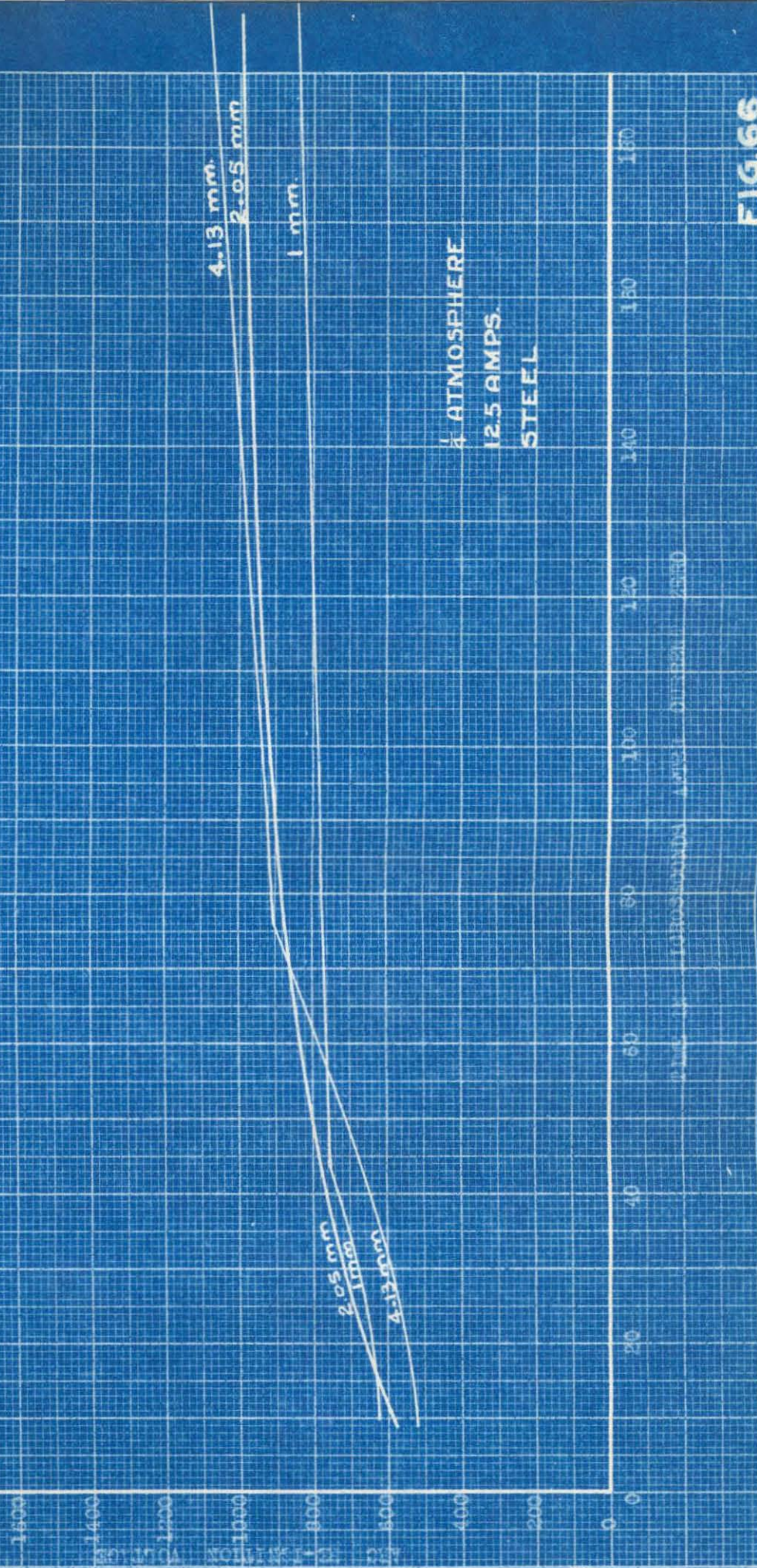


FIG. 66.

results obtained there can be applied directly to this case.

It will be noticed that the curves almost without exception show a definite transition point between two distinct regions: the first, a concave upward curve; and, the second, a nearly straight line. The first concave-upward portion represents dielectric recovery due to space charge growth associated with deionization, as given by Equation 5, Appendix E, and as discussed earlier under "Results". The second, usually a straight-line recovery, represents increase in dielectric strength due to the effect of cooling on the gas density. Assuming the latter to be true, the temperatures indicated by the striking voltage in air in this second region were calculated for three cases, (Appendix D). For steel at 1 atmosphere and 1 mm., the extrapolated temperature curve gives for the arc temperature a value of 2750° K.; for 2.05 mm., a value of 4500° K. is obtained. Both these values are for 12.5 amps.. A calculated point for copper at 1 mm., 1 atmos. and 50 amps. shows an arc temperature of 3500° K. Brass electrodes under the same conditions yielded 3800° K., - close enough agreement. For a D-C arc between copper electrodes, Suits obtained a value of temperature of 4050° K.

V. CONCLUSIONS

The following conclusions may be drawn:-

- (1) Dielectric recovery by the arc space after current zero is due to the formation of a space charge sheath, as predicted by Slepian.
- (2) The chief deionizing process for short arcs is not recombination, but is diffusion.
- (3) The initial recovery voltage is lowered by increasing current.
- (4) An optimum spacing exists between 1.0 and 2.05 mm. for copper electrodes at which the reignition voltage is highest for short times after current zero.
- (5) Short arcs in copper have a higher dielectric strength than long arcs over the range shown by the curves; i.e., over the same range at which brass exhibits this property. This definitely disproves the theory that this property holds only for low boiling point electrodes.
- (6) For steel electrodes the very short time breakdown voltage is about 100 volts higher for 12.5 amps. than for either 25 or 50 amps., supporting the theory that the air is partially replaced by electrode vapor.

(7) Short arcs in steel have a higher breakdown strength than the longer ones. This is very definitely shown for all currents and pressures used, except at 1 atmosphere and 25 and 50 amps., where the curves are too closely grouped for any analysis.

(8) A preferred arc length between 1.0 and 2.05 mm. exists for steel electrodes also, for which the breakdown voltage is a maximum.

(9) Temperatures are calculated which agree in order of magnitude (4000° - 6000° K.) with recent determinations.

There still remains considerable work to more thoroughly analyse the curves contained herein. It is hoped that further correlation can be made in the near future and the results published.

VI. ACKNOWLEDGMENT

The writer wishes to express his gratitude to the Electrical Engineering Faculty of the California Institute of Technology for their cooperation, to Dr. T. E. Browne for his excellent instruction and inspiration in this work; to Mr. T. Fahrner for aid in obtaining data; and to Miss Esther Gilbert for her invaluable help in preparing this thesis.

To the National Youth Administration a special acknowledgment is due, - for without the aid of the two assistants whom it supplied for six months, the very laborious and long machine work and calculations would have very much curtailed the scope of this investigation.

APPENDIX A.APPARATUS

Figure 4 shows in more detail the actual circuit used. Three, single-phase, 1 K.V.A., transformers in parallel, together with a 7.5 K.V.A. transformer in series, provided the power supply at 690 volts. The reactors, air-core, three in number, were designed for minimum distributed capacitance and consisted of 19 layers, each of 19 turns of No. 7 wire. Each coil had a resistance of 0.63 ohms, an inductance of 0.0334 henry, and capacity of 18 micro-microfarads. The inductance of the circuit was varied by taps on the reactors and also by varying the coupling between the coils.

The electrodes were square blocks, 5 cm. per side initially 1.27 cm. thick. The lower electrode was drilled with a No. 59 hole (0.9 mm. diameter) through which a tungsten wire was projected by means of an extensible bellows (Silfon) seal to make contact with the upper electrode and then, falling back, to start the arc. The steel electrodes were shaped after each reading, polished smooth and plane with carborundum paste on a flat disc and then cleaned. With the copper electrodes it was possible to obtain clean surfaces by sandpapering; when they became at all pitted, they were reshaped also. The electrode supporting structure was mounted on a drilled glass base, ground to make good contact with

a 12" belljar and the whole connected to a vacuum pump and a closed tube mercury manometer.

The voltage divider was composed of six identical resistor-capacitance sections in series. Each section consisted of a 600,000 ohm carbon resistor in parallel with a small, 50 to 100 micro-microfarad "trimming" condenser. The resistors were adjusted by filing to give equal D-C resistances, and the condensers by insertion into a tuned circuit to give equal voltage ratios at 50,000 cycles. For small displacements on the oscilloscope a voltage-divider ratio of one was used by connecting the leads directly across the arc, and for larger deflections a ratio of 2 or 3 was used. The divider was symmetrically arranged above ground to eliminate errors due to ground currents flowing through non-symmetrical capacitances to ground of other parts of the circuit. The rest of the circuit, as much as possible, was also balanced with respect to ground to eliminate distortion in the electro-static deflecting field caused by high frequencies if one plate is closer to ground potential than the other.

The oscilloscope had only one pair of electro-static plates which was connected across the arc through the voltage divider. Deflection for the sweep was obtained by magnetic field coils connected through a phase-shifting transformer to the same supply as the arc. The coils were so designed that deflection of the spot across the tube screen took place only when the field current

was near zero, and so a linear sweep was obtained. Condensers in series with the coils made the circuit a pure resistance. The reignition phenomena to be observed were centered on the screen by means of the phase shifting transformer. By applying a voltage of the same frequency as the arc supply, but displaced from it by  $90^\circ$ , the spot was cut off on its return path so that the reignition phenomena recurred for one polarity only.

The condensers used for shunting the arc were of two types: the smaller, mica insulated in molded composition; and the larger, ordinary "telephone" condensers of rolled paper. All were accurately measured at frequencies from 10 to 50 kilocycles, the smaller in a tuned circuit, and the larger with a condenser bridge.

The arc and all measuring equipment were about 15' from, and on a line perpendicular to the axis of the reactors, to avoid the latters' magnetic field.

The transformer voltage was read by means of a standard 20-1 potential transformer. A 200 volt D-C supply with voltmeter was also available for calibrating small deflections on the oscilloscope.

APPENDIX B.EXPERIMENTAL TECHNIQUE

Data were taken in such a manner as to obtain curves of reignition volts versus time after current zero. The current pressure, and electrode separation were kept fixed for each set of readings and the arc shunt capacitance was varied to act as a parameter for the required curve.

The arc current was taken to be the short circuit current flowing when the system was shorted on itself. This current was checked regularly and its value altered by changing the taps or the coupling of the reactors. The pressure was adjusted and controlled by the vacuum pump and manometer. The separation was obtained by the use of gauges of the correct thickness. The lower electrode was first clamped into its supporting structure with the initiating tungsten wire near the bottom of the centrally drilled hole. The top electrode was then laid on the lower and its movable holder brought down to it and clamped. The top holder and electrode were then backed off and clamped firmly, using the gauges as separators. By this means it was unnecessary to do any complicated levelling to make sure the faces were parallel. The tungsten was then pushed through the lower electrode to make contact with the upper one, a quick return being obtained by a fairly strong spring.

Since the oscillograph sensitivity varied somewhat, depending on the width and intensity of line used, settings on the focusing

or acceleration anodes, and line voltage, it was calibrated for every reading. All deflections were read by means of two glass slides which moved vertically across the whole face of the tube. A millimeter scale capable of small lateral adjustment was fastened horizontally below and above the screen so that positive and negative distances from the zero mark could be read. Before every reading the zero on the scale was adjusted to correspond to the position of the electron beam.

The line voltage was applied to the plates and the deflections measured in both positive and negative directions. The applied voltage was read through a standard 20-1 potential transformer and a voltmeter. This deflection was usually 33 mm. in the positive direction, and 35 mm. in the opposite direction, using a voltage divider ratio of 2 and peak applied voltage of 1000. A 200 volt D-C supply was used for reading directly the voltage corresponding to any deflection up to 15 mm. (V.D.R. = 1). Between these two points a constant mm. per volt sensitivity existed.

As soon as the arc was started, one slider was moved to read  $E_s$ , the average reignition voltage and the other to read average  $E_m$ . The arc circuit was broken and restarted several times to check these values and also to obtain a reading of  $E_l$ . Wherever possible, a voltage divider ratio of one was used. With steel electrodes at other than 1/4 atmosphere, the initiating hole was usually blocked with molten metal just after the arc was struck so that all three

readings  $e_s$ ,  $e_m$ , and  $E_1$ , had to be obtained while the arc was burning the first time. When it was felt that these readings were not sufficiently definite or reliable, a new set of electrode surfaces was used and the reading repeated under the same conditions.

Several precautions were observed. In some cases, particularly at the lower values of shunt capacitance, the arc did not move. In these cases, it was necessary to obtain the reading of  $e_s$  very quickly, before it fell as it invariably did when the arc stayed on burned metal. Often by extinguishing and restriking the arc several times, it was possible to make it move around on clean metal, in which case, the values on the screen were very uniform and well defined. For the higher values of capacity, the arc usually moved with great rapidity toward the edges where it bowed outwards. This condition of burning could be noticed on the oscilloscope screen and no readings were taken when this condition persisted.

The greatest variation in values appeared in  $-e_m$ , the negative maximum. Often two well-defined and consistently repeated values appeared simultaneously, either when two no glow traces appeared, or when the no glow and glow case appeared, which occurred near the point where the transition took place from no glow to glow. Readings were taken and recorded of all such consistently appearing values.

For each reading the following data were recorded:-

Open circuit volts.

Short circuit volts.

Deflection in mm. corresponding to open circuit  
volts in both directions.

S.C. amps.

Shunt capacity.

Separation in mm.

Pressure.

Reignition volts,  $e_s$ .

Negative maximum,  $e_m$ .

Initial voltage,  $E_1$ .

Glow frequency.

Behavior of arc, - kind of movement, etc.

APPENDIX C.PROBABLE ACCURACY OF THE METHOD

A very complete and searching analysis of the accuracy of the experimental method followed, is given by Browne<sup>5</sup> and will only be summarized here.

Readings of deflections were probably accurate to within five percent on the large deflections and ten percent on the small deflections.

Errors due to non-linearity in oscilloscope deflection were eliminated by calibrating as much of the scale as possible for each set of readings, and then plotting a curve of voltage versus deflection for the screen. The maximum probable error was perhaps ten percent.

Voltmeters and ammeters were checked against standards and were accurate to within one percent. Inductance calculated from these readings  $L = \frac{E}{2\pi f I}$  is thus accurate to at least two percent. The actual current in the arc was less than the measured short circuit current by about 5 percent, due to the neglect of the arc voltage.

The capacitance of the condensers used was measured to within two to five percent. The distributed capacitance of the circuit, found from the inductance and observed resonant frequencies of the circuit, was taken as the mean of several readings to be 150 micro-microfarads.

Measurement of electrode separation was easily accurate to five percent, and pressure to one percent.

Browne investigated fully the error occurring due to calculation of time by means of the simplified equations (X) and (Y), which neglect series resistance and conductance in parallel with the arc. Using the full equation, including series resistance:-

$$e = E - \mathcal{E}^{\frac{-R}{2C}t} \left\{ (E - E_1) \cos wt + \frac{1}{wC} \left[ -I_1 + \frac{R}{2L} (E - E_1) \right] \sin wt \right\}$$

where  $w = \sqrt{\frac{1}{LC} - \frac{R^2}{4L^2}}$

and calculating with typical constants and  $R = 5$  ohms, the effect of resistance of this magnitude was found to be quite negligible.

From an analysis of several oscillograms, Browne found that leakage conductance rose only when the arc voltage was above 600 or 800 volts. Since the greater portions of the normal voltage transients preceding reignition for the cases tested are below this figure, the evidence showed that leakage conductance could be entirely neglected without much error.

The total overall accuracy was estimated to be about five percent for voltage and ten percent in the calculated values of time.

APPENDIX D.TEMPERATURE CALCULATION

Slepian and Mason give a curve of sparking voltage versus  $p\ell$  for plane parallel electrodes in air, (Figure 70). Knowing a sparking voltage then, the corresponding value of  $p\ell$  can be found.

The apparent pressure is then:-

$$p = \frac{p\ell}{\ell}$$

Then since

$$\frac{p}{p_0} = \frac{d}{d_0}$$

where  $d_0$  is gas density at pressure  $p_0$  and temperature  $T_0$

Then since

$$T = T_0 \frac{d_0}{d} = 273 \frac{p_0}{p} \text{ in } {}^\circ \text{K.}$$

The assumptions included in this determination are:-

- (1) That Slepian's and Mason's curve can be extrapolated back as shown dotted.
- (2) That  $T_0$  can be taken as  $273^\circ$  K.
- (3) That the perfect gas law holds even though the arc space was not in thermal equilibrium.
- (4) That the gas temperature curves on Figures 67, 68, and 69 have been projected back with the correct slope.

APPENDIX E.SPARKING IN IONIZED GAS

A commonly used value for sparking voltage in air at ordinary pressure and temperature is:-

$$V = 30,000 d \text{ volts} \quad (1)$$

In more general form, applying Paschen's Law:-

$$V = 30,000 d \cdot \frac{T_0}{T} \quad (2)$$

where  $T_0 = 273^\circ \text{ K.}$

Now  $d = A \frac{V^{2/3}}{n^{1/3}} \quad (?)$  (3)

and  $A = (136) \left( \frac{k}{c} \right)^{1/3}$

Eliminating d,

$$V = \frac{(6.8)(10^{19}) k}{c} \cdot \frac{1}{n} \cdot \left( \frac{T_0}{T} \right)^3 \quad (4)$$

Taking into account changes in pressure by the use of (2) above, instead of (1), then:-

$$V = \frac{(6.8)(10^{19}) k_0}{c_0} \cdot \frac{1}{n} \cdot \left( \frac{T_0}{T} \right)^3 p^{5/2} \text{ volts} \quad (5)$$

where  $k_0$  = mobility at 1 atmos. and  $0^\circ \text{ C.}$

$\bar{c}_0$  = average thermal velocity at 1 atmos. and  $0^\circ \text{ C.}$

p = pressure in atmospheres.

k = ionic mobility.

T = absolute temperature of arc gas.

d = thickness of space charge sheath.

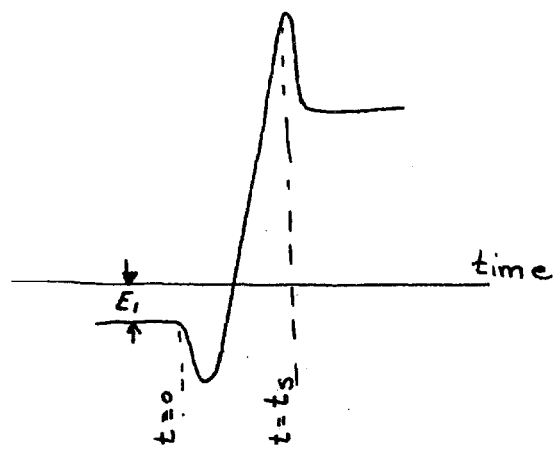
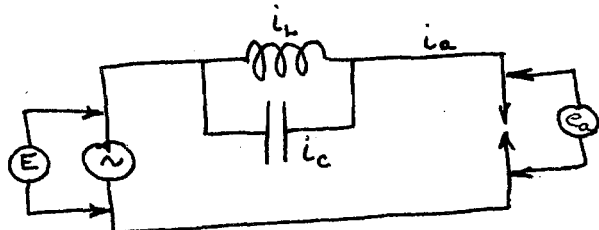
n = density of ionization.

7. Slepian, "Electrical Properties of Gases", (a book)  
Westinghouse Elec. & Mfg. Co. (1933).

# 36. Appendix "F"

## Reignition Voltage - Time Equations.

### Arc Voltage During Current Zero



$$E = E_a + L \frac{di_L}{dt} = E_a + \frac{q}{C} \quad (1)$$

$$\text{at } i_a = 0 \quad i_L + i_C = i_a = 0$$

$$\frac{di_L}{dt} = -\frac{di_C}{dt} = \frac{q}{LC} \quad (2)$$

$$\therefore L \frac{di_L}{dt} - \frac{q}{C} = 0 = L \frac{di_C}{dt} + \frac{q}{C}$$

$$L \frac{d^2q}{dt^2} + \frac{q}{C} = 0$$

$$q = A \cos \omega t + B \sin \omega t \quad \text{where } \omega = \frac{1}{\sqrt{LC}} \quad (3)$$

### Initial Conditions

At  $t=0$   $E_a = -E_1$  and  $i_L = I_1$ , for  $E$  is practically constant and

$$\therefore \frac{q}{C} = L \frac{di_L}{dt} = \text{const.}$$

$$\therefore i_C = \frac{dq}{dt} = 0 \quad \text{or} \quad i_L = I_1 = i_a$$

$$i_L = -\frac{dq}{dt} = -i_C = \omega A \sin \omega t - \omega B \cos \omega t$$

$$\text{From (1)} \quad E = -E_1 + \frac{1}{C_L} A \quad A = C_L (E - E_1)$$

$$\therefore (4) \quad I_1 = -\omega B \quad B = -\frac{I_1}{\omega}$$

$$\therefore E_a = E - \frac{q}{C} = E - (E - E_1) \cos \omega t + \frac{I_1}{\omega C} \sin \omega t$$

### Appendix "F" (Cont'd)

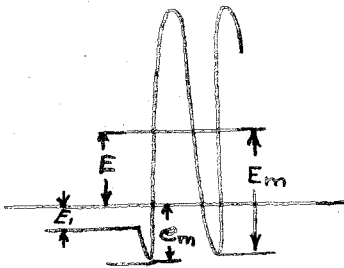
$$\begin{aligned}
 e_a &= E - L \left\{ \omega^2 C (E - E_1) \cos \omega t - \omega I_1 \sin \omega t \right\} \\
 &= E - \sqrt{(E - E_1)^2 + \left(\frac{I_1}{\omega C}\right)^2} \cos \left( \omega t + \tan^{-1} \frac{I_1}{\omega C (E - E_1)} \right) \\
 &= E - E_m \cos (\omega t + \theta)
 \end{aligned}$$

where

$$\theta = \tan^{-1} \frac{I_1}{\omega C (E - E_1)}$$

$$E_m = \sqrt{(E - E_1)^2 + \left(\frac{I_1}{\omega C}\right)^2}$$

$$I_1 = \omega C \sqrt{E_m^2 - (E - E_1)^2}$$



$$E_m = E - e_m$$

$$\therefore I_1 = \omega C \sqrt{(E - e_m)^2 - (E - E_1)^2}$$

$$e_a = E - (E - e_m) \cos (\omega t + \theta)$$

$$= E \left[ 1 - \left( 1 - \frac{e_m}{E} \right) \cos (\omega t + \theta) \right]$$

$$\cos (\omega t + \theta) = \frac{E - e_a}{E - e_m}$$

$$\omega t = \cos^{-1} \frac{E - e_a}{E - e_m} - \theta$$

$$t = \frac{1}{LC} \left[ \cos^{-1} \frac{E - e_a}{E - e_m} + \tan^{-1} \sqrt{\left( \frac{E - e_m}{E - E_1} \right)^2 - 1} \right]$$

$$f = \frac{1}{2\pi} \frac{1}{\sqrt{LC}} \quad T = \frac{1}{f} = 2\pi \sqrt{LC}$$

APPENDIX G.ARC BEHAVIOR

Due to the large variety of conditions under which the arc behavior was recorded, the data are given in note form below, with an explanatory summary following. In the notation used the first figure denotes current, the second separation, and the third the pressure.

COPPER

50 - 4.13 - 1      Rapid increase in gas pressure; violent flames when arc leaves the electrode edge.

50 - 1 - 1      For low shunting capacity, a soft sounding arc; as C increases, the arc becomes staccato, completely covering the electrode with a spotty trace; arc bowed out into length of 8 inches.

50 - .45 - 1      Arc self-starting.

50 - 2.05 - 1/2      Continuous spider-like trace to edge.

50 - 1 - 1/4      Large burnt spots, no depth of burning.

25 - 1 - 1/2      Arc goes out after 2-3 seconds.

25 - 4.13 - 1      Continuous trace up to 81 seconds, then goes into explosive movement.

25 - 2.05 - 1/2       $e_s$  drops by 50% when the arc reaches the edge.

25 - 1 - 1      Hard to keep arc going when C is increased.

25 - 4.13 - 1/2      Great increase in pressure.

25 - 4.13 - 1/4 Arc travels to the side very quickly but with no preferred direction;  $e_s$  drops by 30% and  $e_m$  increases; no violent flames as with 1 atmosphere; soft fuzzy electrode traces.

25 - .45 - 1/4 Self-starting; after surface is covered, arc turns to purple glow.

12.5 - 4.13 - 1 Start of staccato trace at 138 sec.

12.5 - 2.05 - 1 Start of staccato trace at 75 sec.

12.5 - 1 - 1/2 At high  $\Omega$  very diffuse arc; after electrode covered arc changes to diffuse purple glow; develops great heat.

12.5 - 1 - 1/2 Complete diffuse coverage of all electrode surface.

12.5 - 2.05 - 1/2 When oxidized around center hole, arc could not be restarted.

12.5 - .45 - 1/4 Arc changes to glow in 6-8 seconds.

12.5 - 1 - 1/4 Trace consisted of black spots mostly near edge.

#### STEEL

12.5 - .45 - 1 No readings could be taken at .45 mm. because arc was continuously shorted by thin spires of metal soon after arc started.

25 - 1 - 1 Two main craters; reading had to be taken quickly before characteristics changed.

25 - 4.13 - 1	Initiating hole welded over. Rapid movement only at high values of <u>C</u> .
12.5 - 1 - 1	Very rapid movement, maintained only for 2-3 cycles.
12.5 - 4.13 - 1	Difficult to maintain arc.
12.5 - 2.05 - 1	Difficult to maintain arc.
50 - 2.05 - 1/2	Dark, fine path; good movement. Arc sometimes shorted out by spire of metal.
50 - 1 - 1/4	Soft arc.
25 - 1 - 1/2	Good coverage - spotted trace.
25 - 1 - 1/4	Arc self-starting; electrode rough as though arc had passed but not stopped; some small molten spots also.
25 - 4.13 - 1/2	At low values of <u>C</u> total movement within 1/2" diameter circle. For higher values more movement.

#### SUMMARY

For low values of shunting capacity, the arc tended to burn near the center of the electrodes. As the capacity increased, the arc movement became more rapid. When it reached the edge for copper electrodes at 50 and 25 amps., the arc bowed out in violent flames. The manometer indicated a rapid increase in pressure, often great enough to send the mercury in the manometer tube surging from its

position recording a 1/2 or 1/4 atmospheric difference, to striking the top of the tube with considerable violence. This effect is well known and has been described in early literature<sup>8</sup>.

The different kinds of traces are shown in Figures 71 to 81. All the conditions holding at the time they were taken are noted under them.

Figure 81 shows an enlarged view of the center part of Figure 80. The hole shown is the initiating hole of diameter .9 mm. Measurements indicate a current density of approximately 10,000 amps. per square cm. for this case. Rougher calculations for Figure 79 show a current density of the same order of magnitude. This agrees with Langmuir's criteria for the high field theory of cathode spot.

In general  $e_s$  was much lower when the arc did not move, so that in such cases the circuit was broken and the arc restarted until it did move on new metal. It was also noticed (see 12.5 - 2.05 - 1/2) above, that it was harder to start the arc if the metal around the initiating hole had been previously burned, showing that the oxides and other products of burning when cold, support the arc with more difficulty than the parent metal.

Another point which is of interest is the fact that the arc ceased its continuous trace and broke into a fast spotty motion at roughly the same time when transition between the two kinds of dielectric recovery took place.

---

8. Thompson, J. J. and G. P., "Conduction of Electricity through Gases", (a book), Vol. II, page 566. Cambridge University Press, (1933).

The motion of the arc across the electrodes has been discussed in literature<sup>8</sup>, and its cause is fairly obvious. The addition of  $10^7$  ergs of energy to 1 c.c. of gas would increase the pressure by 6.6 atmospheres. Consider this same energy applied to  $\frac{1}{100}$  c.c., a very large over-estimate of the volume of a short arc, then the pressure rise of 660 atmospheres is experienced. This high pressure would spread as a wave giving the "bomb" effect described above, but would also cause the ionized gases in the core to move. The lowest dielectric path then usually occurs at a position slightly different from the previous arc position, and the arc then reignites at a new point.

FIG. 67

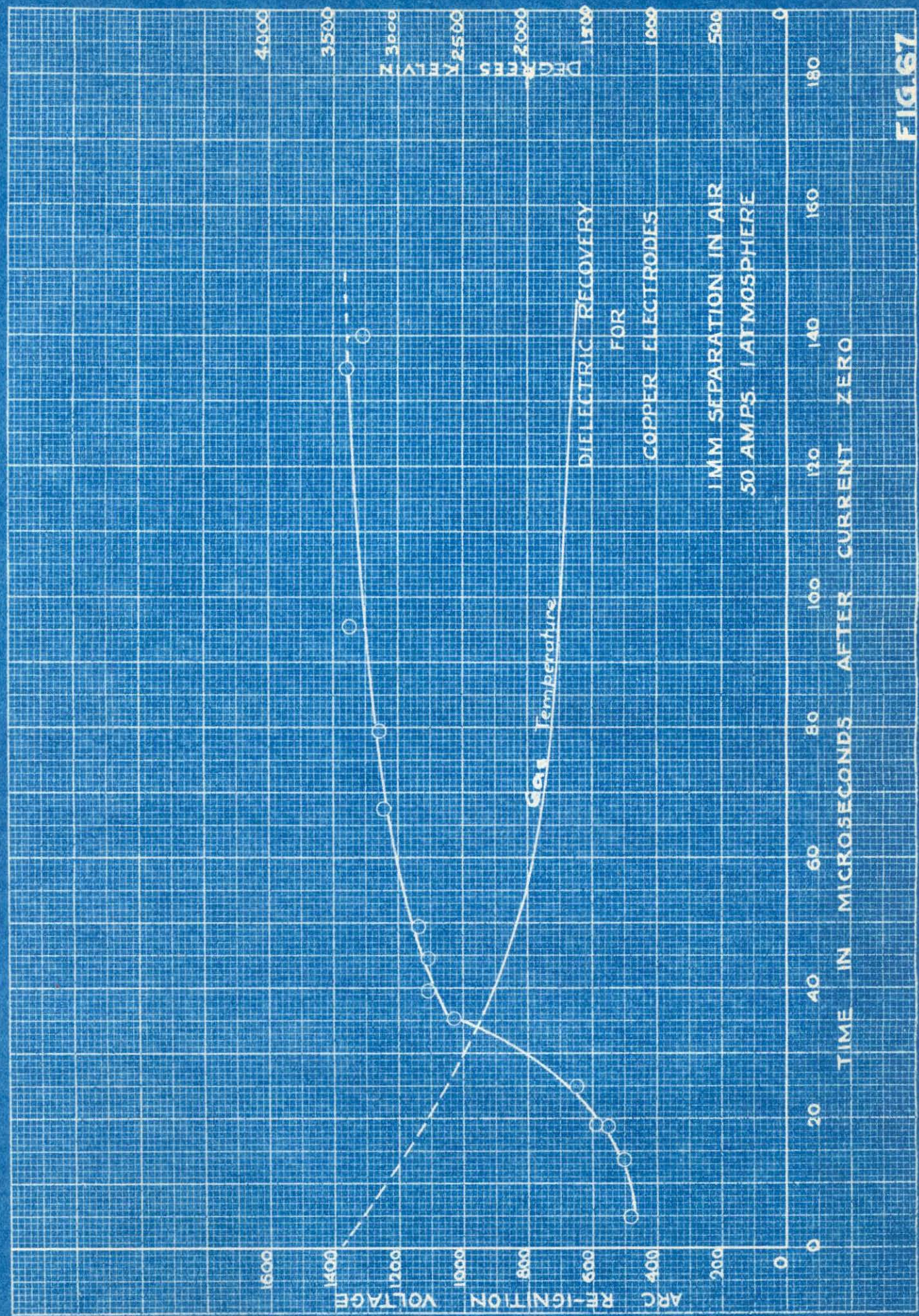


FIG. 68

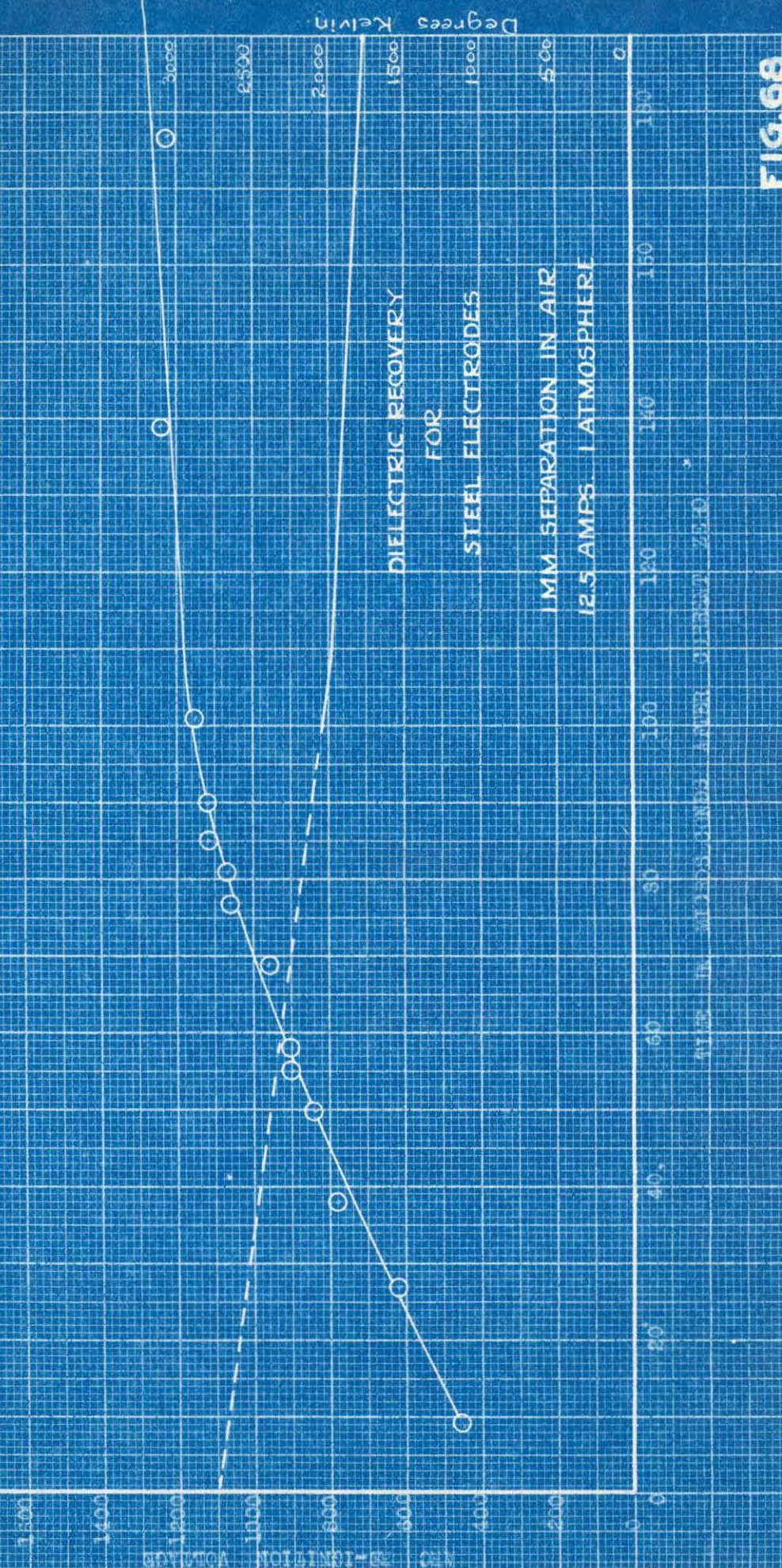
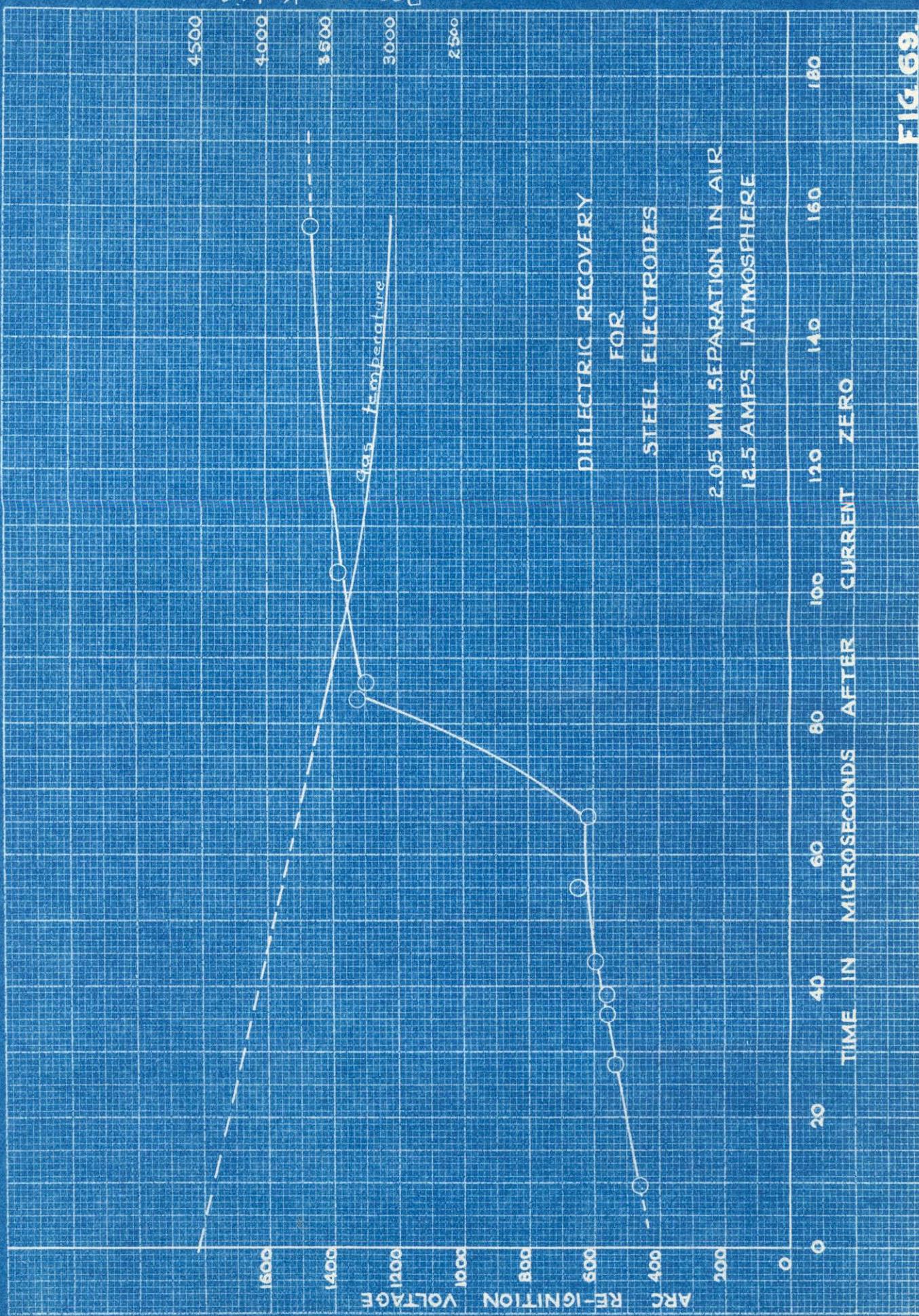
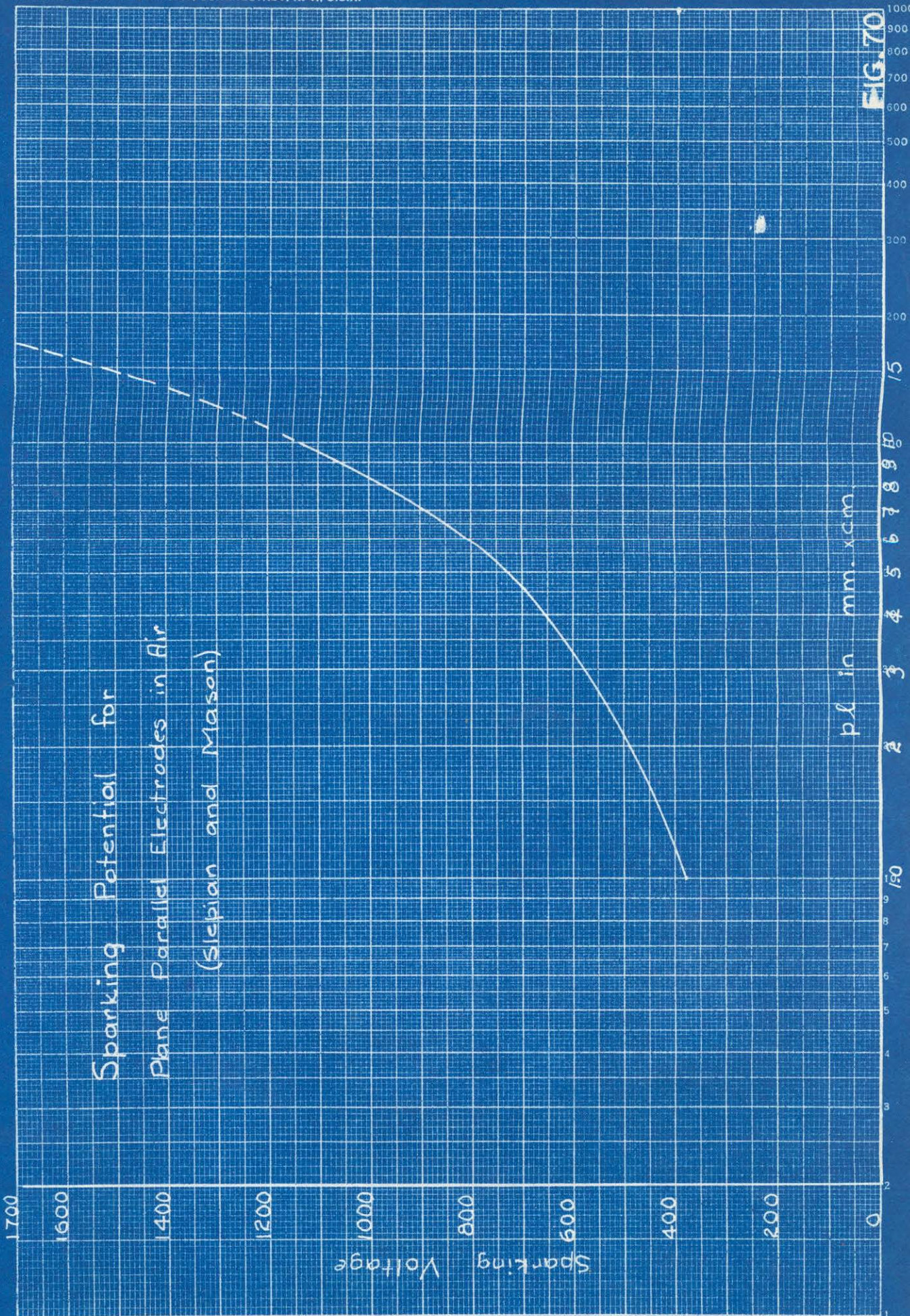


FIG. 69.





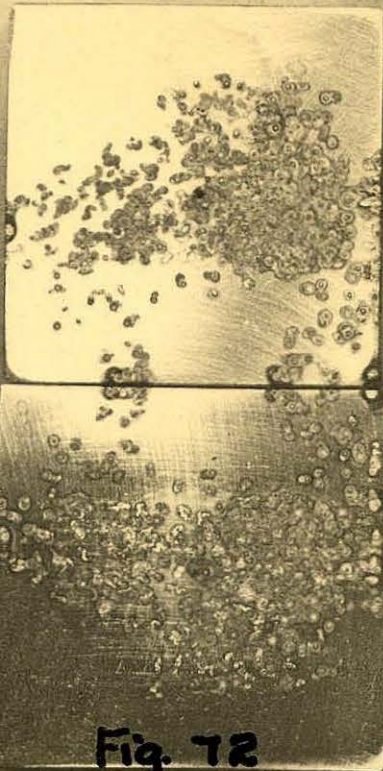


Fig. 72

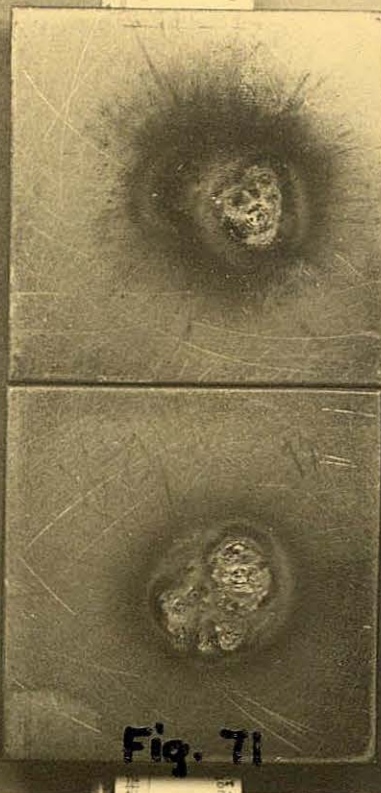


Fig. 71

Copper 50-45-1  
 $e_s = 942$  volts.  
 $t_s = 13\mu s$

Steel 50-2.05-1  
 $e_s = 394$   
 $t_s = 13\mu s$



Fig. 73

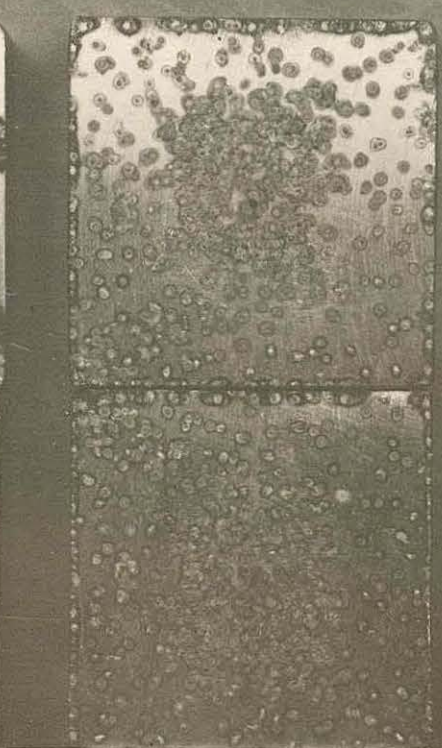


Fig. 74

Copper 50-1-1  
 $e_s = 554$   
 $t_s = 18.6$

Copper 50-2.05-1/2  
 $e_s = 843$   
 $t_s = 41$

Copper 50-1-1  
 $e_s = 1310$   
 $t_s = 140$

2 4 6 10

Fig. 75

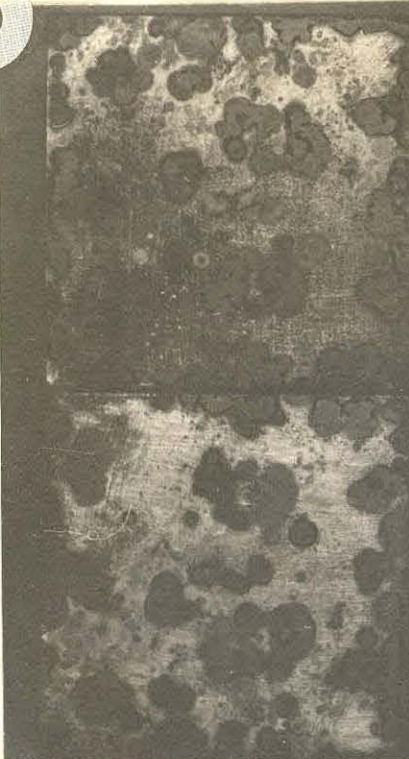


Fig. 76

Copper 50-1- $\frac{1}{4}$   
 $e_s = 684$   
 $t_s = 21.5$

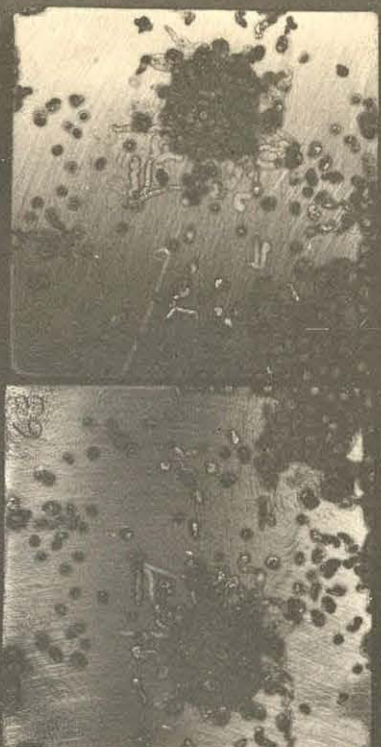


Fig. 77

Copper 50-45-1  
 $e_s = 835$   
 $t_s = 36.1$

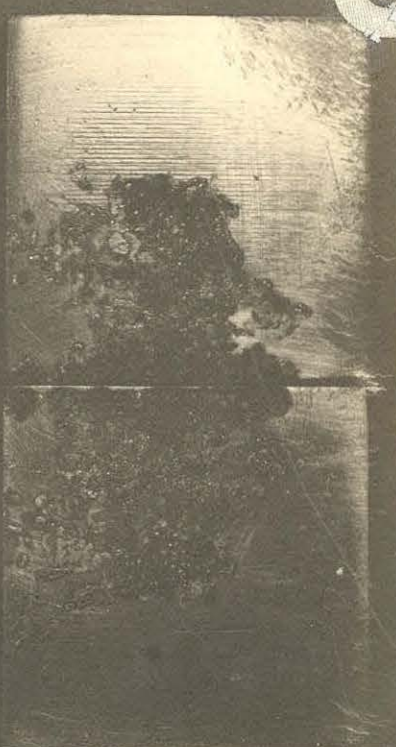


Fig. 78

Copper 25-2.05-1  
 $e_s = 655$   
 $t_s = 30$

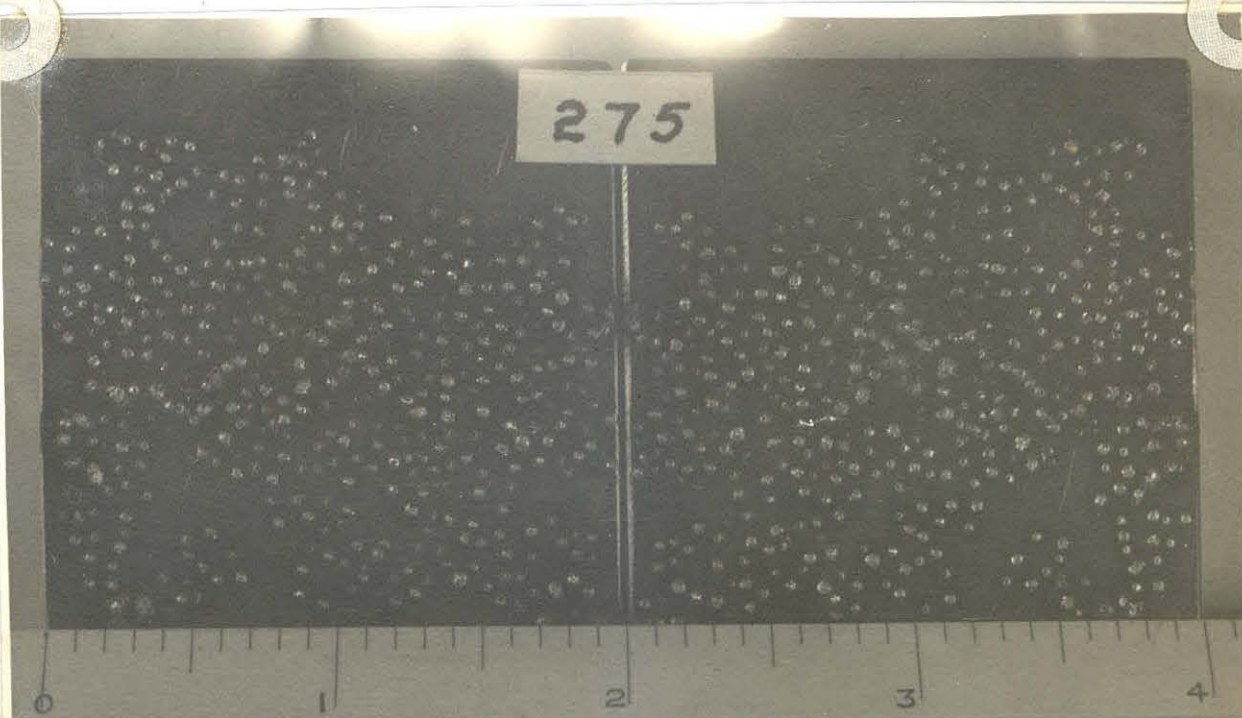


Fig. 79

Steel

25-1- $\frac{1}{2}$   
 $e_s = 468$   
 $t_s = 6.5$

189

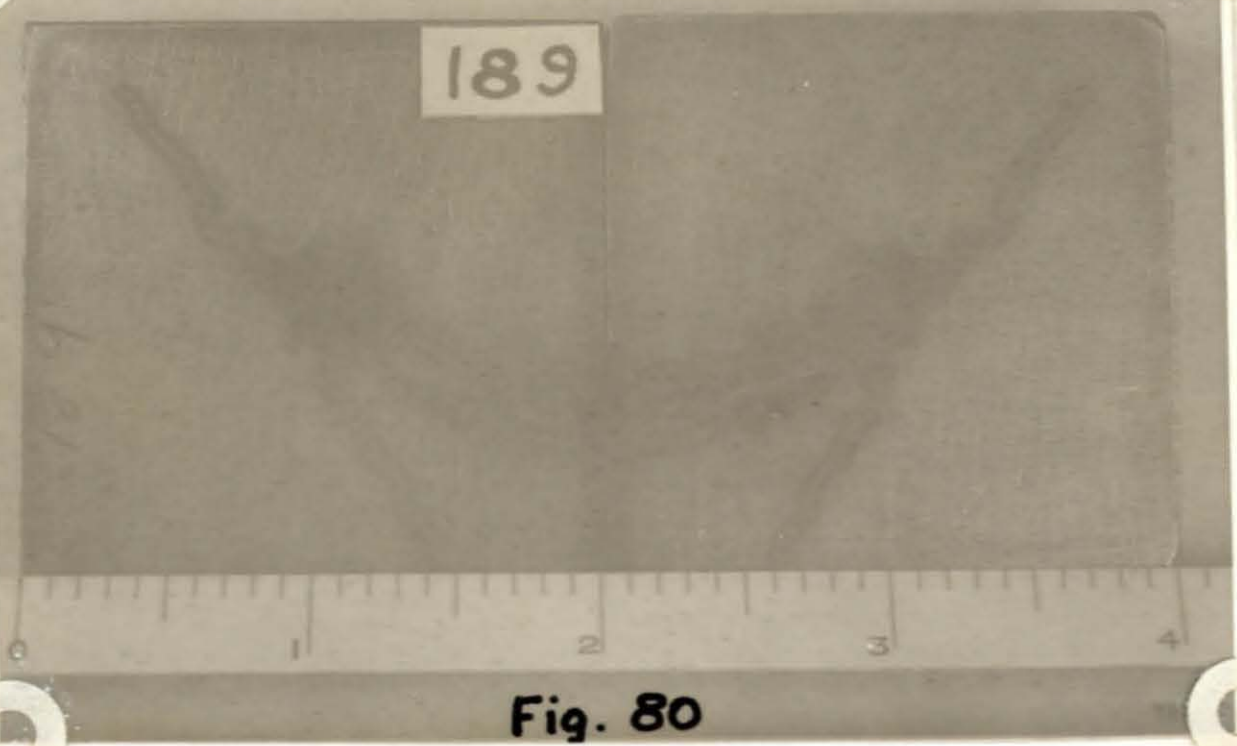


Fig. 80

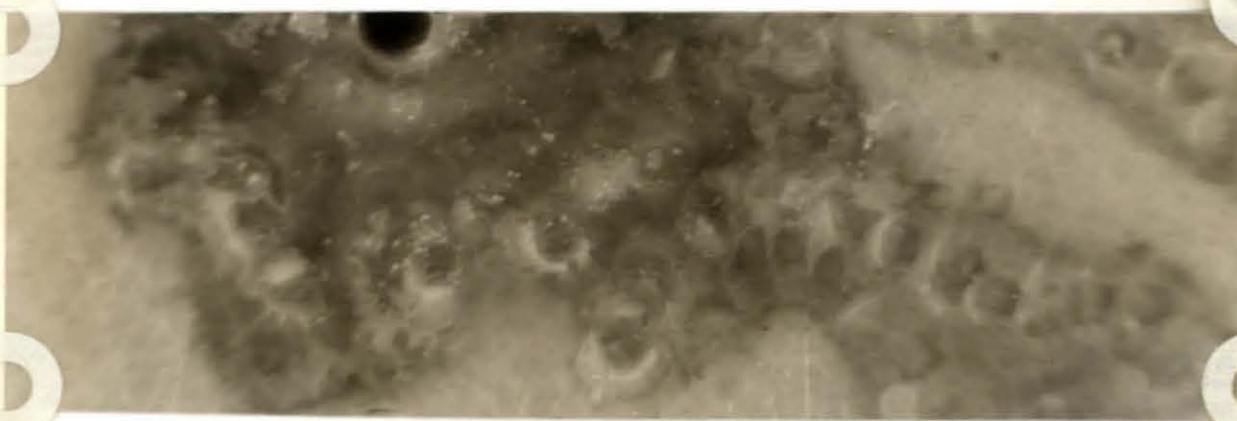


Fig. 81

steel

$$50 - 2.05 - \frac{L}{2}$$

$$e_s = 439$$

$$t_s = 77.7$$